Chapter 2
Methods: Ab Initio Downfolding and Model-Calculation Techniques

2.1 Multi-energy-scale Ab Initio Scheme for Correlated Electrons (MACE)

2.1.1 General Framework

In principle, all the low-energy phenomena such as superconductivity and magnetism arise from the following global energy scale Hamiltonian:

$$\hat{\mathcal{H}} = -\sum_I \frac{\hbar^2}{2M_I}\frac{\partial^2}{\partial \mathbf{R}_I^2} - \sum_i \frac{\hbar^2}{2m}\frac{\partial^2}{\partial \mathbf{r}_i^2} + \sum_{i<j}\frac{e^2}{|\mathbf{r}_i - \mathbf{r}_j|} - \sum_{i,I}\frac{Z_I e^2}{|\mathbf{r}_i - \mathbf{R}_I|} + \sum_{I<J}\frac{Z_I Z_J e^2}{|\mathbf{R}_I - \mathbf{R}_J|} \tag{2.1}$$

where $\mathbf{r}_i$ and $\mathbf{R}_I$ denote the position of the ith electron and Ith nucleus with the charge $-e$ and $Z_I e$, respectively. m and M_I are the mass of the electron and the Ith nucleus, respectively. $\hbar$ is the Planck constant. Therefore, we have only to analyze the Hamiltonian to understand the physical properties of materials. However, unfortunately, none of the existing analytic and numerical methods can solve it exactly, except the case where the number of degrees of freedom is very small. Even the electronic Hamiltonian derived by applying the Born-Oppenheimer approximation [1] to the Hamiltonian in Eq. (2.1)

$$\hat{\mathcal{H}} = \sum_i \left(-\frac{\hbar^2}{2m}\frac{\partial^2}{\partial \mathbf{r}_i^2} - \sum_I \frac{Z_I e^2}{|\mathbf{r}_i - \mathbf{R}_I|} \right) + \sum_{i<j}\frac{e^2}{|\mathbf{r}_i - \mathbf{r}_j|} \tag{2.2}$$

can not be solved exactly, if the number of electrons exceeds $\sim$10.

Y. Nomura, *Ab Initio Studies on Superconductivity in Alkali-Doped Fullerides*,
Springer Theses, DOI 10.1007/978-981-10-1442-0_2

Given the situation, we have to resort to some reliable approximation. The density functional theory (DFT) [2, 3] gives a very good approximation to the electronic Hamiltonian [Eq. (2.2)] in the global energy scale. It successfully reproduces the material dependence of global electronic structure reflecting e.g., the chemical composition and the atomic positions. However, the DFT fails in describing strong correlation effects such as the Mott transition [4] and thus it has a severe limitation in understanding the properties of strongly correlated materials. On the other hand, model-calculation techniques developed to analyze low-energy models are good at treating the electron correlations, while it is difficult for them to take into account the material dependence since the parameters in the model are usually determined by hand.

The above consideration leads to an idea of combining the DFT and the model calculations to study strongly correlated materials [5–7]. It can be justified by the energy hierarchy in the electronic structure [7]: Under the strong electronic correlation, the low-energy bands near the Fermi level E_F, which we call target bands, may be reconstructed intensively, while the structure of the high-energy bands will not change drastically. Furthermore, at a temperature where low-energy phenomena (e.g., superconductivity) emerge, the high-energy states are nearly "frozen", i.e., they are nearly totally occupied or empty. Then, nearly all the excitation processes occur in t-subspace, the subspace which the target bands span (For later use, we define r-subspace as the rest of the Hilbert space). Therefore, the physical properties are determined by this low-energy region.

This hierarchical structure allows us to construct the following three-stage scheme [7], which we will refer to as the multi-energy-scale ab initio scheme for correlated electrons (MACE):

1. Obtain the global energy structure by the DFT and define the low-energy subspace.
2. Trace out the high-energy degrees of freedom and derive low-energy effective Hamiltonian (downfolding).
3. Solve the derived Hamiltonian accurately by the model-calculation method.

2.1.2 Low-Energy Effective Hamiltonian

Here, we derive the form of the low-energy Hamiltonian starting from the global energy scale Hamiltonian. We consider the following type of the global energy scale Hamiltonian

$$\hat{\mathcal{H}} = \sum_{\alpha\beta} \mathcal{H}^0_{\text{el}}(\alpha, \beta)\, \hat{c}^\dagger_\alpha \hat{c}_\beta + \sum_{\alpha\beta\alpha'\beta'} \mathcal{H}_{\text{el-el}}(\alpha, \beta, \alpha', \beta')\, \hat{c}^\dagger_\alpha \hat{c}^\dagger_{\alpha'} \hat{c}_{\beta'} \hat{c}_\beta + \sum_{\alpha\beta\nu} \mathcal{H}_{\text{el-ph}}(\alpha, \beta, \nu)\, \hat{c}^\dagger_\alpha \hat{c}_\beta (\hat{b}_\nu + \hat{b}^\dagger_\nu) + \sum_{\mu\nu} \mathcal{H}^0_{\text{ph}}(\mu, \nu)\, \hat{b}^\dagger_\mu \hat{b}_\nu, \tag{2.3}$$

where $\hat{c}^\dagger$ and $\hat{c}$ ($\hat{b}^\dagger$ and $\hat{b}$) are the creation and the annihilation operators for electrons (phonons), respectively. The Hamiltonian is composed of the electron kinetic energy (first term), the Coulomb interaction (second term), the electron-phonon interaction (third term), and the phonon one-body part (fourth term). This Hamiltonian is derived from Eq. (2.1) by quantizing the nuclei motion as the phonon within the Born-Oppenheimer approximation [1] and by considering up to the linear coupling between electrons and phonons. The partition function Z in the coherent state path-integral formulation [8] is written as

$$Z = \int \mathcal{D}b^* \mathcal{D}b \mathcal{D}c^* \mathcal{D}c \; e^{-S[b^*, b, c^*, c]} \tag{2.4}$$

with b^* and b (c^* and c) denoting the set of phonon coherent state variables (Grassman variables) $\{b_\nu^*\}$ and $\{b_\nu\}$ ($\{c_\alpha^*\}$ and $\{c_\alpha\}$), respectively. Here, the action $S[b^*, b, c^*, c]$ reads

$$S[b^*, b, c^*, c] = \int \mathcal{L}[b^*, b, c^*, c] d\tau, \tag{2.5}$$

where $\mathcal{L}[b^*, b, c^*, c]$ is the Lagrangian given by

$$\mathcal{L}[b^*, b, c^*, c] = \sum_\nu b_\nu^* \partial_\tau b_\nu + \sum_\alpha c_\alpha^* \partial_\tau c_\alpha + \mathcal{H}[b^*, b, c^*, c]. \tag{2.6}$$

Now we divide the electronic degrees of freedom into high-energy and low-energy degrees of freedom, to which we will attach subscripts H and L, respectively. We integrate out the high-energy degrees of freedom, which will define the effective action for the low-energy electrons and the phonons [5, 9],

$$\frac{1}{Z_{\text{eff}}} e^{-S_{\text{eff}}[b^*, b, c_L^*, c_L]} = \frac{1}{Z} \int \mathcal{D}c_H^* \mathcal{D}c_H \; e^{-S[b^*, b, c_L^*, c_L, c_H^*, c_H]}. \tag{2.7}$$

Defining the effective Lagrangian as $\mathcal{L}_{\text{eff}} = \partial S_{\text{eff}} / \partial \tau$, we consider the following quantity

$$\tilde{\mathcal{H}}_{\text{eff}} = \mathcal{L}_{\text{eff}}[b^*, b, c_L^*, c_L] - \sum_\nu b_\nu^* \partial_\tau b_\nu - \sum_{\alpha_L} c_{\alpha_L}^* \partial_\tau c_{\alpha_L}. \tag{2.8}$$

This quantity is not static any more, i.e., it contains some frequency dependence. Furthermore, there exist higher order terms which do not exist in the original Hamiltonian in Eq. (2.3) (e.g., interaction term involving six fermion operators).

If we neglect the frequency dependence and the higher order terms, $\tilde{\mathcal{H}}_{\rm eff}$ can be expressed as the static Hamiltonian,[1] whose form is the same as that of Eq. (2.3):

$$\hat{\mathcal{H}}_{\rm eff} = \sum_{\alpha_L\beta_L} \tilde{\mathcal{H}}^0_{\rm el}(\alpha_L, \beta_L)\hat{c}^\dagger_{\alpha_L}\hat{c}_{\beta_L} + \sum_{\alpha_L\beta_L\alpha'_L\beta'_L} \tilde{\mathcal{H}}_{\text{el-el}}(\alpha_L, \beta_L, \alpha'_L, \beta'_L)\hat{c}^\dagger_{\alpha_L}\hat{c}^\dagger_{\alpha'_L}\hat{c}_{\beta'_L}\hat{c}_{\beta_L} + \sum_{\alpha_L\beta_L\nu} \tilde{\mathcal{H}}_{\text{el-ph}}(\alpha_L, \beta_L, \nu)\hat{c}^\dagger_{\alpha_L}\hat{c}_{\beta_L}(\hat{b}_\nu + \hat{b}^\dagger_\nu) + \sum_{\mu\nu} \tilde{\mathcal{H}}^0_{\rm ph}(\mu, \nu)\hat{b}^\dagger_\mu\hat{b}_\nu. \quad (2.9)$$

The $\hat{\mathcal{H}}_{\rm eff}$ Hamiltonian is defined in the low-energy subspace (t-subspace), thus, we interpret it as a low-energy effective Hamiltonian. Note that the $\tilde{\mathcal{H}}^0_{\rm el}$, $\tilde{\mathcal{H}}_{\text{el-el}}$, $\tilde{\mathcal{H}}_{\text{el-ph}}$, and $\tilde{\mathcal{H}}^0_{\rm ph}$ parameters in Eq. (2.9) differ from the bare parameters in Eq. (2.3), since the elimination of the high-energy degrees of freedom gives a renormalization of these terms. These terms will be further renormalized by the processes involving the t-subspace electrons and the phonons, which are accurately treated when the derived low-energy Hamiltonian is solved. Therefore, this scheme treats the renormalization effects in two steps: The ones originating from the high-energy electrons are implicitly included in the input parameters, and the ones from the t-subspace electrons and the phonons are explicitly considered afterward. In other words, this downfolding procedure enables to avoid the double counting of the renormalization arising from the low-energy dynamics.

In practice, derivations of the parameters in the low-energy effective model are usually done by perturbative approaches since the vertex corrections for the processes involving the high-energy electrons are usually small [7]. In the present study, the electronic one-body part of the Hamiltonian [the first term on the r.h.s. of Eq. (2.9)] is constructed by the techniques of the maximally localized Wannier function [11–13], where we neglect the self-energy correction associated with the downfolding procedure.[2] The detail of the method is given in Sect. 2.2.2. The Coulomb interaction parameters [the second term on the r.h.s. of Eq. (2.9)] are calculated as the Wannier matrix elements of the partially screened Coulomb interaction, where the partial screening is calculated through the constrained random phase approximation [15] (see Sect. 2.2.3). To derive the phonon-related part [the third and fourth terms on the r.h.s. of Eq. (2.9)], we developed a new ab initio scheme, which we call constrained density-functional perturbation theory (cDFPT) [16]. In the cDFPT, partially-renormalized electron-phonon couplings and phonon-frequencies are calculated, which is detailed in Sect. 2.2.5.

The derived Hamiltonian needs to be analyzed to study low-energy phenomena. Low-energy solvers are described in Sect. 2.3. In order to smoothly connect the derivation and analysis of the low-energy Hamiltonian, we need some interfaces. In Sect. 2.4, we explain the interfaces and overview the whole scheme.

[1] See e.g., Ref. [10] for the study in which the frequency dependence of the Coulomb interaction in $\tilde{\mathcal{H}}_{\rm eff}$ is explicitly treated.

[2] The self-energy correction gives only a quantitative change in the low-energy band structure, whose effects were studied in detail in e.g., Ref. [14].

2.2 Ab Initio Downfolding for Electron-Phonon Coupled Systems

2.2.1 Density Functional Theory

The MACE relies on band structure calculations using the density functional theory (DFT), which makes it possible to take into account material dependence. The DFT [17] is one of the most powerful methods to treat the global-energy-scale electronic Hamiltonian with treating atoms with non-relativistic Born-Oppenheimer approximation [1]

$$\hat{\mathcal{H}} = \sum_i \left(-\frac{\hbar^2}{2m}\frac{\partial^2}{\partial \mathbf{r}_i^2} - \sum_I \frac{Z_I e^2}{|\mathbf{r}_i - \mathbf{R}_I|} \right) + \sum_{i<j} \frac{e^2}{|\mathbf{r}_i - \mathbf{r}_j|}. \tag{2.10}$$

As is already mentioned, it is impossible to solve this many body problem analytically and numerically.

However, a breakthrough occurred in 1964: Hohenberg and Kohn [2] proved that, as far as the ground state has no degeneracy, the electron density of the ground state and the external potential have one-to-one correspondence. Therefore, once the ground-state electron density is known, the external potential is determined uniquely. Furthermore, we can calculate the total number of electrons by the integral of the electron density over all space. By solving the Hamiltonian with thus calculated potential and number of electrons, the ground state properties can be derived. Later, by Kohn himself [18] and Levy [19], it was proved that, even in the case where the ground states are degenerate, the one-to-one correspondence of the external potential and the ground-state electron density holds.

Hohenberg and Kohn [2] also gave a variational principle: There exists a functional of the electron density for the ground state energy

$$E_v[\rho] = E_{\text{kin}}[\rho] + \int \rho(\mathbf{r}) v(\mathbf{r}) d\mathbf{r} + E_{ee}[\rho] \tag{2.11}$$

with the electron density $\rho(\mathbf{r})$, the external potential $v(\mathbf{r})$, the kinetic energy $E_{\text{kin}}[\rho]$, the potential energy of electron-electron interaction $E_{ee}[\rho]$; it satisfies the inequality

$$E_v[\rho] \geq E_v[\rho_0], \tag{2.12}$$

where ρ_0 is the electron density of the ground state. Therefore, the electron density which gives the global minimum of the energy functional is the ground-state electron density. Note that, here, the electron density used in the minimization process has to be given by the ground-state anti-symmetric wave function for a certain external potential. This limit was also lifted by Levy [19, 20], who proved that the variational

methods can be applied to electron densities given by every possible anti-symmetric wave functions.

These developments have given a firm justification for the DFT, which uses the electron density as a basic variable and express the electronic energy in terms of the functional of the electron density. The next breakthrough was given by Kohn and Sham [3], which opened up a way for the practical DFT calculations: They introduced "*fictitious*" non-interacting system whose external potential is determined to give the same electron density as that of the true interacting system. The electron density is written as

$$\rho(\mathbf{r}) = \sum_{i=1}^{N} |\phi_i(\mathbf{r})|^2 \tag{2.13}$$

with the total number of electrons N and the spatial part of the one-particle wave function $\phi_i(\mathbf{r})$. They define the exchange correlation functional $E_{\rm xc}[\rho]$ as

$$E_{\rm xc}[\rho] = \big(E_{\rm kin}[\rho] - E_{\rm kin}^{\rm KS}[\rho]\big) + \big(E_{ee}[\rho] - E_{\rm H}[\rho]\big), \tag{2.14}$$

where $E_{\rm kin}^{\rm KS}[\rho]$ is a simple functional for the kinetic energy

$$E_{\rm kin}^{\rm KS}[\rho] = \sum_{i=1}^{N} \int \phi_i^*(\mathbf{r}) \left(-\frac{\hbar^2}{2m}\frac{\partial^2}{\partial \mathbf{r}^2}\right) \phi_i(\mathbf{r}) d\mathbf{r} \tag{2.15}$$

and $E_{\rm H}[\rho]$ is the Hartree term

$$E_{\rm H}[\rho] = \frac{e^2}{2} \int\int \frac{\rho(\mathbf{r})\rho(\mathbf{r}')}{|\mathbf{r}-\mathbf{r}'|} d\mathbf{r} d\mathbf{r}'. \tag{2.16}$$

One should care that the exchange correlation functional $E_{\rm xc}[\rho]$ also includes the difference between the true kinetic energy $E_{\rm kin}[\rho]$ and the simplified kinetic energy $E_{\rm kin}^{\rm KS}[\rho]$, on top of the real exchange correlation energy. The total energy functional is rewritten as

$$E_v[\rho] = E_{\rm kin}^{\rm KS}[\rho] + \int \rho(\mathbf{r}) v(\mathbf{r}) d\mathbf{r} + E_{\rm H}[\rho] + E_{\rm xc}[\rho]. \tag{2.17}$$

To obtain the ground-state energy, we need to minimize the energy functional $E_v[\rho]$, whose condition is

$$\frac{\delta}{\delta \phi_i^*(\mathbf{r})} \left\{ E_v[\rho] - \sum_{i,j=1}^{N} \varepsilon_{ij} \left(\int \phi_i^*(\mathbf{r}) \phi_j(\mathbf{r}) d\mathbf{r} - \delta_{ij} \right) \right\} = 0, \tag{2.18}$$

where ε_{ij} is the Lagrange parameter which ensures the orthonormality of the one-particle wave functions ϕ_i's. Equation (2.18) yields

$$\left[-\frac{\hbar^2}{2m}\frac{\partial^2}{\partial \mathbf{r}^2} + v_{\text{eff}}(\mathbf{r})\right]\phi_i(\mathbf{r}) = \sum_{j=1}^{N}\varepsilon_{ij}\phi_j(\mathbf{r}) \tag{2.19}$$

with

$$v_{\text{eff}}(\mathbf{r}) = v(\mathbf{r}) + e^2\int\frac{\rho(\mathbf{r}')}{|\mathbf{r}-\mathbf{r}'|}d\mathbf{r}' + v_{\text{xc}}(\mathbf{r}) \tag{2.20}$$

$$v_{\text{xc}}(\mathbf{r}) = \frac{\delta E_{\text{xc}}[\rho]}{\delta\rho(\mathbf{r})}. \tag{2.21}$$

Since the matrix (ε_{ij}) is Hermitian, we diagonalize Eq. (2.19) and get so called Kohn-Sham equation

$$\left[-\frac{\hbar^2}{2m}\frac{\partial^2}{\partial \mathbf{r}^2} + v_{\text{eff}}(\mathbf{r})\right]\psi_i(\mathbf{r}) = \varepsilon_i\psi_i(\mathbf{r}), \tag{2.22}$$

where the electron density is given by $\rho(\mathbf{r}) = \sum_{i=1}^{N}|\psi_i(\mathbf{r})|^2$. The electron density and the form of $v_{\text{eff}}(\mathbf{r})$ are unchanged under the transformation because the transformation is unitary. Note that, at this point, we have not yet used any approximation, i.e., the Kohn-Sham equation is exact.

In the practical calculations, since the form of $E_{\text{xc}}[\rho]$ is unknown, we need some approximation for it. One of the most frequently used approximations is the local density approximation (LDA), in which $E_{\text{xc}}[\rho]$ is approximated as

$$E_{\text{xc}}^{\text{LDA}}[\rho] = \int\rho(\mathbf{r})\varepsilon_{\text{xc}}(\rho(\mathbf{r}))d\mathbf{r}. \tag{2.23}$$

Here, $\varepsilon_{\text{xc}}(\rho(\mathbf{r}))$ is the exchange-correlation energy density per particle of the homogeneous electron gas with the constant electron density $\rho(\mathbf{r}) = \rho_{\text{const.}}$ and the compensating positively-charged jellium [21, 22]. The generalized gradient approximation (GGA) [23, 24] is also often employed, where the gradient of the electron density on top of the local density, is used to improve the exchange correlation energy.

In the following, we list the procedures of the ground state calculations based on the DFT:

1. Prepare initial density $\rho_1(\mathbf{r})$. Set $m = 1$.
2. Calculate $v_{\text{eff}}(\mathbf{r})$ from the mth density $\rho_m(\mathbf{r})$ within the LDA, the GGA, or other approximations.
3. Solve the Kohn-Sham equation [Eq. (2.22)] and obtain eigenvalues and eigenstates $\{\varepsilon_i, \psi_i(\mathbf{r})\}$.
4. Calculate new density by $\rho_{\text{new}}(\mathbf{r}) = \sum_{i=1}^{N}|\psi_i(\mathbf{r})|^2$.

5. Mix the new density with the old density and obtain $(m+1)$th density $\rho_{m+1}(\mathbf{r}) = \alpha\rho_{\text{new}}(\mathbf{r}) + (1-\alpha)\rho_m(\mathbf{r})$. α is a mixing parameter.
6. If the difference between $\rho_m(\mathbf{r})$ and $\rho_{m+1}(\mathbf{r})$ is sufficiently small below the given threshold, we regard that a converged solution for the ground state density is obtained. Otherwise, set $m = m+1$ and go back to the step 2.

2.2.2 Maximally Localized Wannier Function

In order to construct the low-energy model, it is convenient to employ localized functions as a basis. However, wave functions derived from DFT band-structure calculations are Bloch states, i.e., they are delocalized in space. Therefore, we need to transform Bloch states into Wannier states.

In general, the Wannier state can be constructed from the Bloch state by the Fourier transformation. For simplicity, let us first consider the single-orbital case. In this case, the Wannier function localized at the unit cell with the position $\mathbf{R}$, $\phi_{\mathbf{R}}$, is related with the Bloch functions $\psi_{\mathbf{k}}$'s via

$$\phi_{\mathbf{R}}(\mathbf{r}) = \frac{1}{\sqrt{N}} \sum_{\mathbf{k}} e^{-i\mathbf{k}\cdot\mathbf{R}} \psi_{\mathbf{k}}(\mathbf{r}), \tag{2.24}$$

where N is the number of the sampling-$\mathbf{k}$ points. Without loss of generality, $\psi_{\mathbf{k}}(\mathbf{r})$ can be factorized into a product of $\psi'_{\mathbf{k}}(\mathbf{r})$ and the additional phase $e^{i\theta(\mathbf{k})}$, i.e., $\psi_{\mathbf{k}}(\mathbf{r}) = e^{i\theta(\mathbf{k})}\psi'_{\mathbf{k}}(\mathbf{r})$. Here, the gauge of $\psi'_{\mathbf{k}}(\mathbf{r})$ is chosen so that $\psi'_{\mathbf{k}}(\mathbf{r}=\mathbf{0})$ is real. Since wave functions which differ only in the global phase indicate the same state, the phase at each $\mathbf{k}$ point $e^{i\theta(\mathbf{k})}$ becomes indeterminant. Then, one immediately finds that the Wannier functions are not unique due to the indeterminacy of the phases of the Bloch functions. In the multi-orbital case, the Wannier orbitals $\phi_{l\mathbf{R}}$'s are given by

$$\phi_{l\mathbf{R}}(\mathbf{r}) = \frac{1}{\sqrt{N}} \sum_{\mathbf{k}} e^{-i\mathbf{k}\cdot\mathbf{R}} \psi^{(w)}_{l\mathbf{k}}(\mathbf{r}), \tag{2.25}$$

where $\psi^{(w)}_{l\mathbf{k}}$'s are the Wannier-gauge Bloch functions, which are related with the Kohn-Sham Bloch functions $\psi_{n\mathbf{k}}$'s by unitary transformation:

$$\psi^{(w)}_{l\mathbf{k}}(\mathbf{r}) = \sum_{n} \boldsymbol{U}^{(\mathbf{k})}_{nl} \psi_{n\mathbf{k}}(\mathbf{r}). \tag{2.26}$$

In this case, nonuniqueness of the unitary matrix $\boldsymbol{U}^{(\mathbf{k})}$ allows arbitrary choices of Wannier functions. Therefore, it is difficult to obtain "optimal" set of Wannier functions.

Marzari and Vanderbilt [11] proposed a choice called maximally localized Wannier functions, which is useful in deriving a simple form of effective Hamiltonian in the later procedure. In their scheme, a set of the unitary matrix $\{\boldsymbol{U}^{(\mathbf{k})}\}$ is determined to minimize the total spatial spread of the Wannier functions $\Omega_{\rm tot}$, which is defined as

$$\Omega_{\rm tot} = \sum_l \Omega_l, \tag{2.27}$$

where

$$\Omega_l = \sqrt{\langle \phi_{l\mathbf{0}} | r^2 | \phi_{l\mathbf{0}} \rangle - \left| \langle \phi_{l\mathbf{0}} | \mathbf{r} | \phi_{l\mathbf{0}} \rangle \right|^2}. \tag{2.28}$$

With the resultant $\{\boldsymbol{U}^{(\mathbf{k})}\}$, the maximally localized Wannier orbitals (MLWO's) are constructed from the Kohn-Sham wave functions $\psi_{n\mathbf{k}}$'s via Eqs. (2.25) and (2.26). Hereafter, we adopt the set of MLWO's as the localized basis for the low-energy Hamiltonian. Then, the onsite levels and hopping integrals $\left[\boldsymbol{\mathcal{H}}_0^{(w)}(\mathbf{R})\right]_{ll'}$ are calculated as

$$\left[\boldsymbol{\mathcal{H}}_0^{(w)}(\mathbf{R})\right]_{ll'} = \langle \phi_{l\mathbf{R}} | \hat{\mathcal{H}}_{\rm KS} | \phi_{l'\mathbf{0}} \rangle = \frac{1}{N} \sum_{\mathbf{k}} \left[\sum_n \left(\boldsymbol{U}_{nl}^{(\mathbf{k})}\right)^* \varepsilon_{n\mathbf{k}} \boldsymbol{U}_{nl'}^{(\mathbf{k})} \right] e^{i\mathbf{k}\cdot\mathbf{R}}, \tag{2.29}$$

where $\hat{\mathcal{H}}_{\rm KS}$ is the Kohn-Sham Hamiltonian and the $\varepsilon_{n\mathbf{k}}$'s are the eigenvalues of $\hat{\mathcal{H}}_{\rm KS}$. With the resultant $\boldsymbol{\mathcal{H}}_0^{(w)}(\mathbf{R})$, the electronic one-body part of the low-energy Hamiltonian $\hat{\mathcal{H}}_0$ is given by

$$\hat{\mathcal{H}}_0 = \sum_{ll'} \sum_{\mathbf{R},\mathbf{R}'} \left[\boldsymbol{\mathcal{H}}_0^{(w)}(\mathbf{R} - \mathbf{R}') \right] \hat{c}_{l\mathbf{R}}^\dagger \hat{c}_{l'\mathbf{R}'} - \sum_{l\mathbf{R}} \Delta\varepsilon_l \hat{n}_{l\mathbf{R}}, \tag{2.30}$$

where the last term is a double counting correction, which is detailed in Sect. 2.4.1. Here, $\hat{c}_{l\mathbf{R}}^\dagger$ ($\hat{c}_{l\mathbf{R}}$) creates (annihilates) the lth MLWO localized at the cell $\mathbf{R}$ and $\hat{n}_{l\mathbf{R}} = \hat{c}_{l\mathbf{R}}^\dagger \hat{c}_{l\mathbf{R}}$. The choice of the MLWO allows to express the effective low-energy Hamiltonian on the real space lattice in the forms of the transfer and the interaction as short range as possible.

2.2.3 Constrained Random Phase Approximation

We estimate an effective Coulomb interaction in the t-subspace by means of the constrained random phase approximation (cRPA) developed by Aryasetiawan et al. [15]. In general, the fully screened Coulomb interaction W is given by

$$W = \epsilon^{-1} v, \tag{2.31}$$

where ϵ is the dielectric function $\epsilon = 1 - v\chi^0$ with the irreducible polarization χ^0, and v is the bare Coulomb interaction $v(\mathbf{r}, \mathbf{r}')=\frac{e^2}{|\mathbf{r}-\mathbf{r}'|}$. We consider a decomposition of the total irreducible polarization χ^0 into the one involving only the t-subspace electrons χ_t^0 and the rest χ_r^0 [15]:

$$\chi^0 = \chi_t^0 + \chi_r^0. \tag{2.32}$$

Note that χ_r^0 contains not only the processes involving only the r-subspace degrees of freedom but also the ones involving both the t-subspace electrons and the r-subspace electrons. We define the partially screened Coulomb interaction $W^{(p)}$ as

$$W^{(p)} = \left(1 - v\chi_r^0\right)^{-1} v = \epsilon_r^{-1} v. \tag{2.33}$$

It is related with the fully screened Coulomb interaction W in Eq. (2.31) by [15]

$$W = \left(1 - W^{(p)}\chi_t^0\right)^{-1} W^{(p)}, \tag{2.34}$$

which means that if the interaction $W^{(p)}$ is screened by the t-subspace electrons, it exactly reproduces the fully screened interaction. Therefore, we can interpret $W^{(p)}$ as the effective Coulomb interaction between the t-subspace electrons. The screening processes involving only the t-subspace electrons will be considered when we solve the low-energy Hamiltonian. Therefore, in order to avoid the double counting, we have to exclude the screening effects of χ_t^0 from the effective Coulomb interaction to be used in the low-energy Hamiltonian. With the above considerations, it is appropriate to use the partially screened interaction $W^{(p)}$ for the Coulomb interaction parameters, such as Hubbard U, in the low-energy Hamiltonian.

In principle, $W^{(p)}$ has some frequency dependence, however, the partially screened Coulomb interaction is often parametrized as the Wannier matrix elements of its static part $W^{(p)}(\omega = 0)$. To calculate this quantity, we need only the static component of the polarization function $\chi^0(\omega = 0)$, which will, hereafter, be denoted just by χ^0 with omitting ω index. Furthermore, we approximate χ^0 by that calculated within the RPA:

$$\chi^0(\mathbf{r}, \mathbf{r}') = 2\sum_{nm}\sum_{\mathbf{k}\mathbf{k}'} \frac{f_{n\mathbf{k}} - f_{m\mathbf{k}'}}{\varepsilon_{n\mathbf{k}} - \varepsilon_{m\mathbf{k}'}} \psi^*_{n\mathbf{k}}(\mathbf{r})\psi_{m\mathbf{k}'}(\mathbf{r})\psi^*_{m\mathbf{k}'}(\mathbf{r}')\psi_{n\mathbf{k}}(\mathbf{r}'), \tag{2.35}$$

where $\psi_{n\mathbf{k}}$ and $\epsilon_{n\mathbf{k}}$ are the Kohn-Sham eigenfunction and eigenvalue labeled by Bloch wave vector $\mathbf{k}$ and band index n, respectively. f is the Fermi-Dirac distribution function. A factor of 2 comes from the summation over spin. Within the RPA, the total irreducible polarization χ_0 is comprised of four types of transitions: (i) occupied $\leftrightarrow$ virtual, (ii) occupied $\leftrightarrow$ target, (iii) target $\leftrightarrow$ virtual, and (iv) target $\leftrightarrow$ target. Then the decomposition of χ^0 into χ_t^0 and χ_r^0 is clear, namely, χ_t^0 contains only the

contribution from the type (iv) transitions, and the rest of the transitions [type (i), (ii), (iii) processes] contributes to χ_r^0. The explicit form of χ_r^0 is

$$\chi_r^0(\mathbf{r},\mathbf{r}') = 2\sum_{nm}{}' \sum_{\mathbf{k}\mathbf{k}'} \frac{f_{n\mathbf{k}} - f_{m\mathbf{k}'}}{\varepsilon_{n\mathbf{k}} - \varepsilon_{m\mathbf{k}'}} \psi^*_{n\mathbf{k}}(\mathbf{r})\psi_{m\mathbf{k}'}(\mathbf{r})\psi^*_{m\mathbf{k}'}(\mathbf{r}')\psi_{n\mathbf{k}}(\mathbf{r}'). \tag{2.36}$$

where $\sum'$ denotes the summation with the "constraint", where the target $\leftrightarrow$ target transition processes are excluded.

In the actual calculation using the plane-wave basis set, it is advantageous to calculate χ_r^0 using the momentum-space representation [25]:

$$\chi_{r\,\mathbf{G},\mathbf{G}'}^0(\mathbf{q}) = \frac{2}{N\Omega}\sum_{nm}{}' \sum_{\mathbf{k}} \frac{f_{n\mathbf{k}} - f_{m\mathbf{k}+\mathbf{q}}}{\varepsilon_{n\mathbf{k}} - \varepsilon_{m\mathbf{k}+\mathbf{q}}} \langle\psi_{n\mathbf{k}}|e^{-i(\mathbf{q}+\mathbf{G})\cdot\mathbf{r}}|\psi_{m\mathbf{k}+\mathbf{q}}\rangle\langle\psi_{m\mathbf{k}+\mathbf{q}}|e^{i(\mathbf{q}+\mathbf{G}')\cdot\mathbf{r}'}|\psi_{n\mathbf{k}}\rangle, \tag{2.37}$$

where N is the number of sampling-$\mathbf{k}$ points in the first Brillouin zone and Ω is the volume of the unit cell. In order to avoid the singularity in the dielectric matrix ϵ_r, it is convenient to introduce the symmetric dielectric matrix $\tilde{\epsilon}_r$ defined as [25]

$$\tilde{\epsilon}_r = v^{-1/2}\epsilon_r v^{1/2} = 1 - v^{1/2}\chi_r v^{1/2}. \tag{2.38}$$

Especially, in the reciprocal space, the Coulomb matrix v becomes diagonal as $v_{\mathbf{G},\mathbf{G}'}(\mathbf{q}) = \frac{4\pi e^2}{|\mathbf{q}+\mathbf{G}|^2}\delta_{\mathbf{G},\mathbf{G}'}$, which leads to the following expression of the dielectric matrix

$$\tilde{\epsilon}_{r\,\mathbf{G},\mathbf{G}'}(\mathbf{q}) = \frac{|\mathbf{q}+\mathbf{G}|}{|\mathbf{q}+\mathbf{G}'|}\epsilon_{r\,\mathbf{G},\mathbf{G}'}(\mathbf{q}) = \delta_{\mathbf{G},\mathbf{G}'} - 4\pi e^2 \frac{1}{|\mathbf{q}+\mathbf{G}|}\chi_{r\,\mathbf{G},\mathbf{G}'}^0(\mathbf{q})\frac{1}{|\mathbf{q}+\mathbf{G}'|}. \tag{2.39}$$

This definition of $\tilde{\epsilon}_r$ avoids the divergence of the elements with $\mathbf{q}+\mathbf{G}=\mathbf{0}$ or $\mathbf{q}+\mathbf{G}'=\mathbf{0}$ (the original dielectric matrix ϵ_r has divergence at the elements with $\mathbf{q}=\mathbf{0}$, $\mathbf{G}=\mathbf{0}$, $\mathbf{G}'\neq\mathbf{0}$). Thanks to this property, the inversion matrix of $\tilde{\epsilon}_r$ can be easily calculated without employing any tricks. Then, the partially screened Coulomb interaction in (2.33) is calculated, in momentum space representation, as

$$W_{\mathbf{G},\mathbf{G}'}^{(p)}(\mathbf{q}) = 4\pi e^2 \frac{1}{|\mathbf{q}+\mathbf{G}|}\tilde{\epsilon}_{r\,\mathbf{G},\mathbf{G}'}^{-1}(\mathbf{q})\frac{1}{|\mathbf{q}+\mathbf{G}'|}. \tag{2.40}$$

2.2.4 *Density-Functional Perturbation Theory*

The density-functional perturbation theory (DFPT) [26–29] is a standard ab initio method, as well as the frozen phonon method, to calculate the phonon frequencies

and the electron-phonon couplings. The conventional DFPT gives fully renormalized quantities within the static mean-field approximation (e.g., LDA). Figure 2.1 shows the phonon dispersions calculated with the DFPT for the fcc Al, the fcc Pb, and the bcc Nb. Good agreements with the experimental dispersions show its reliability in treating the phonon dynamics. Based on it, we have developed a novel scheme, constrained DFPT [16], to calculate *partially* renormalized phonon frequencies and electron-phonon interaction to be used in the effective low-energy Hamiltonian. Before we proceed with the explanation of the constrained DFPT, we review the DFPT in this section.

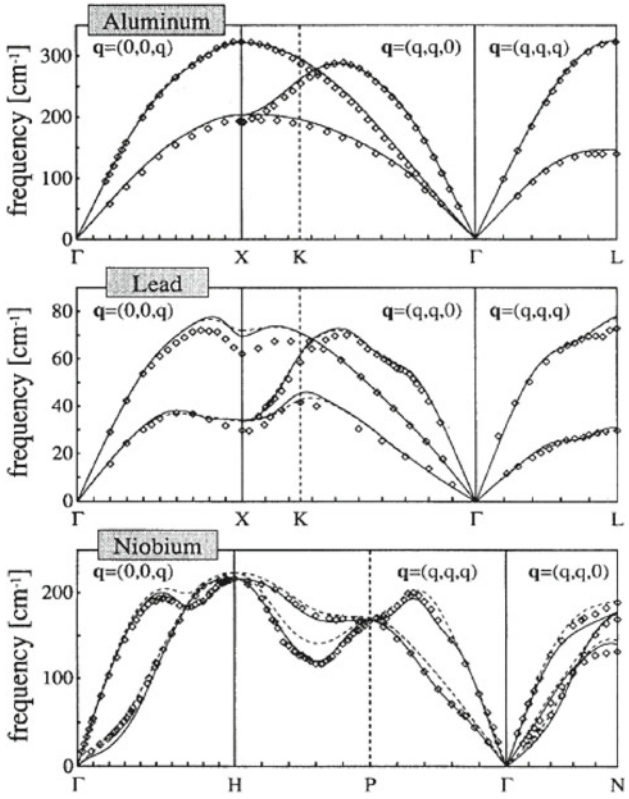

Fig. 2.1 Phonon dispersions for fcc Al, fcc Pb, and bcc Nb. The *solid* and *dashed curves* indicate the theoretically calculated phonon frequencies with the DFPT, where the difference between the *solid* and *dashed curves* comes from different smearing widths σ used in the calculation (*solid* σ = 0.3 eV, *dashed* σ = 0.7 eV). They show good agreement with the experimental data (*diamonds*). Reprinted with permission from de Gironcoli, Ref. [27]. Copyright 1995 by the American Physical Society

2.2.4.1 Lattice Dynamics

Here, we derive equations to calculate phonon frequencies [30]. We start from the time-dependent Schrödinger equation

$$i\hbar\frac{\partial\Phi\big(\{\mathbf{r}\},\{\mathbf{R}\},t\big)}{\partial t}=\left[-\sum_I\frac{\hbar^2}{2M_I}\frac{\partial^2}{\partial\mathbf{R}_I^2}-\sum_i\frac{\hbar^2}{2m}\frac{\partial^2}{\partial\mathbf{r}_i^2}+V\big(\{\mathbf{r}\},\{\mathbf{R}\}\big)\right]\Phi\big(\{\mathbf{r}\},\{\mathbf{R}\},t\big), \tag{2.41}$$

where

$$V(\{\mathbf{r}\},\{\mathbf{R}\})=\sum_{i<j}\frac{e^2}{|\mathbf{r}_i-\mathbf{r}_j|}-\sum_{i,I}\frac{Z_Ie^2}{|\mathbf{r}_i-\mathbf{R}_I|}+\sum_{I<J}\frac{Z_IZ_Je^2}{|\mathbf{R}_I-\mathbf{R}_J|} \tag{2.42}$$

with $\{\mathbf{r}\}=(\mathbf{r}_1,\ldots,\mathbf{r}_N)$ and $\{\mathbf{R}\}=(\mathbf{R}_1,\ldots,\mathbf{R}_n)$. We apply the Born-Oppenheimer approximation [1], where electrons are assumed to become equilibrium instantaneously at each lattice movement. It reflects the fact that electrons move much faster than ions. Then the wave function can be divided into lattice part Φ_n and electron part Ψ_e as

$$\Phi\big(\{\mathbf{r}\},\{\mathbf{R}\},t\big)\simeq\Phi_n\big(\{\mathbf{R}\}\big)\Psi_e\big(\{\mathbf{r}\}|\{\mathbf{R}\}\big)e^{-i\varepsilon t/\hbar}. \tag{2.43}$$

Substituting this into Eq. (2.41), we get two separate equations for electrons and ions:

$$\left[-\sum_i\frac{\hbar^2}{2m}\frac{\partial^2}{\partial\mathbf{r}_i^2}+V\big(\{\mathbf{r}\},\{\mathbf{R}\}\big)\right]\Psi_e\big(\{\mathbf{r}\}|\{\mathbf{R}\}\big)=E\big(\{\mathbf{R}\}\big)\Psi_e\big(\{\mathbf{r}\}|\{\mathbf{R}\}\big) \tag{2.44}$$

and

$$\left[-\sum_i\frac{\hbar^2}{2M_I}\frac{\partial^2}{\partial\mathbf{R}_I^2}+E\big(\{\mathbf{R}\}\big)\right]\Phi_n\big(\{\mathbf{R}\}\big)=\varepsilon\Phi_n\big(\{\mathbf{R}\}\big). \tag{2.45}$$

The ground-state energies at fixed lattice configurations $E\big(\{\mathbf{R}\}\big)$ serve as an effective potential for the lattice motion (Born-Oppenheimer energy surface). The force acting on Ith ion $\mathbf{F}_I$ is given by the derivative of the energy surface

$$\mathbf{F}_I=-\frac{\partial E\big(\{\mathbf{R}\}\big)}{\partial\mathbf{R}_I}. \tag{2.46}$$

If the ion is located at its equilibrium position, the force acting on the ion vanishes ($\mathbf{F}_I=\mathbf{0}$).

In the following, we derive the equation of motion for the lattice vibration in solids. In solids, the individual ion can be identified as the κth ion in the pth unit cell, i.e., $I = (p, \kappa)$. Let us denote the equilibrium position of the κth ion in the pth unit cell as $\mathbf{R}_{p\kappa}^{(0)} = \mathbf{R}_p + \boldsymbol{\tau}_\kappa$ with the origin of the pth unit cell $\mathbf{R}_p$ and the position of the κth ion in the unit cell $\boldsymbol{\tau}_\kappa$. Then, the position of the ion is given by

$$\mathbf{R}_{p\kappa} = \mathbf{R}_{p\kappa}^{(0)} + \mathbf{u}_{p\kappa}, \tag{2.47}$$

where $\mathbf{u}_{p\kappa}$ is the displacement from the equilibrium position. Then the kinetic energy T for the lattice vibration is written as

$$T = \frac{1}{2}\sum_{p\kappa} M_\kappa |\dot{\mathbf{u}}_{p\kappa}|^2 = \frac{1}{2}\sum_{p\kappa\alpha} M_\kappa (\dot{u}_{p\kappa}^\alpha)^2 \tag{2.48}$$

with the mass of the κth ion M_κ and the direction of the displacement $\alpha = x, y, z$. For the potential energy U, we apply the harmonic approximation

$$U = E(\{\mathbf{R}_{p\kappa}^{(0)} + \mathbf{u}_{p\kappa}\}) - E(\{|\mathbf{R}_{p\kappa}^{(0)}\}) \tag{2.49}$$

$$\simeq \frac{1}{2}\sum_{p\kappa\alpha}\sum_{p'\kappa'\alpha'}\left[\frac{\partial^2 E}{\partial R_{p\kappa}^\alpha \partial R_{p'\kappa'}^{\alpha'}}\right]_{R=R^{(0)}} u_{p\kappa}^\alpha u_{p'\kappa'}^{\alpha'}. \tag{2.50}$$

Note that the first-order terms with respect to u's vanish since the force is zero at the equilibrium position

$$\left[-\frac{\partial E(\{\mathbf{R}\})}{\partial \mathbf{R}_{p\kappa}}\right]_{R=R^{(0)}} = \mathbf{0}. \tag{2.51}$$

Substituting the expressions for T [Eq. (2.48)] and U [Eq. (2.49)] in the Lagrange equation

$$\frac{d}{dt}\frac{\partial L}{\partial \dot{u}_{p\kappa}^\alpha} - \frac{\partial L}{\partial u_{p\kappa}^\alpha} = 0 \tag{2.52}$$

with $L = T - U$, we get the equation of motion

$$M_\kappa \ddot{u}_{p\kappa}^\alpha = -\sum_{p'\kappa'\alpha'} C_{p\kappa,p'\kappa'}^{\alpha\alpha'} u_{p'\kappa'}^{\alpha'}, \tag{2.53}$$

where $C_{p\kappa,p'\kappa'}^{\alpha\alpha'}$'s are given by the elements of the Hessian matrix of the potential surface with respect to displacements and called interatomic force constants:

$$C_{p\kappa,p'\kappa'}^{\alpha\alpha'} = C_{p'\kappa',p\kappa}^{\alpha'\alpha} = \left.\frac{\partial^2 E}{\partial u_{p\kappa}^\alpha \partial u_{p'\kappa'}^{\alpha'}}\right|_{u=0}. \tag{2.54}$$

$C^{\alpha\alpha'}_{p\kappa,p'\kappa'}$ plays a role of the "spring constant" between the oscillators with indices (p, κ, α) and (p', κ', α'). Due to the translational invariance, $C^{\alpha\alpha'}_{p\kappa,p'\kappa'}$ becomes a function of the relative position $\mathbf{R}_p - \mathbf{R}_{p'}$

$$C^{\alpha\alpha'}_{p\kappa,p'\kappa'} = C^{\alpha\alpha'}_{\kappa\kappa'}(\mathbf{R}_p - \mathbf{R}_{p'}). \tag{2.55}$$

Then a solution of the equation of motion [Eq. (2.53)] will have a form:

$$\mathbf{u}_{p\kappa} = \mathbf{u}_\kappa(\mathbf{q}) \exp\bigl[i\mathbf{q}\cdot\mathbf{R}_p - i\omega(\mathbf{q})t\bigr], \tag{2.56}$$

where the displacement is labelled by a wave vector $\mathbf{q}$. Using this expression, we recast Eq. (2.53) into

$$\sum_{\kappa'\alpha'} C^{\alpha\alpha'}_{\kappa\kappa'}(\mathbf{q}) u^{\alpha'}_{\kappa'}(\mathbf{q}) = M_\kappa \omega^2(\mathbf{q}) u^\alpha_\kappa(\mathbf{q}) \tag{2.57}$$

with

$$C^{\alpha\alpha'}_{\kappa\kappa'}(\mathbf{q}) = \sum_p C^{\alpha\alpha'}_{\kappa\kappa'}(\mathbf{R}_p) \exp\bigl(-i\mathbf{q}\cdot\mathbf{R}_p\bigr). \tag{2.58}$$

By defining so called the dynamical matrix as

$$D^{\alpha\alpha'}_{\kappa\kappa'}(\mathbf{q}) \equiv \frac{1}{\sqrt{M_\kappa M_{\kappa'}}} C^{\alpha\alpha'}_{\kappa\kappa'}(\mathbf{q}) \tag{2.59}$$

and introducing a vector $\mathbf{e}_\kappa(\mathbf{q})$ such that

$$\mathbf{u}_\kappa(\mathbf{q}) \propto \frac{1}{\sqrt{M_\kappa}} \mathbf{e}_\kappa(\mathbf{q}), \tag{2.60}$$

we get the equation which is used to determine the normal modes

$$\sum_{\kappa'\alpha'} D^{\alpha\alpha'}_{\kappa\kappa'}(\mathbf{q}) e^{\alpha'}_{\kappa'}(\mathbf{q}) = \omega^2(\mathbf{q}) e^\alpha_\kappa(\mathbf{q}). \tag{2.61}$$

This equation shows that the phonon frequency $\omega(\mathbf{q})$ is given by the square root of the eigenvalues of the dynamical matrix $D^{\alpha\alpha'}_{\kappa\kappa'}(\mathbf{q})$. Since the dimension of the dynamical matrix $D^{\alpha\alpha'}_{\kappa\kappa'}(\mathbf{q})$ is $3n$ with n being the number of the atoms in the unit cell, there exist $3n$ solutions (normal modes), which we label by the index ν. The eigenvectors of the dynamical matrix satisfy the orthonormality:

$$\sum_{\kappa\alpha} e^{*\alpha}_\kappa(\mathbf{q}\nu) e^\alpha_\kappa(\mathbf{q}\nu') = \delta_{\nu\nu'}. \tag{2.62}$$

2.2.4.2 Expression for Interatomic Force Constants

Here, we derive the expression for the interatomic force constants $C^{\alpha\alpha'}_{\kappa\kappa'}(\mathbf{q})$. The Hellmann-Feynman force $\mathbf{F}_I$ is given by

$$\mathbf{F}_I = -\frac{\partial E\big(\{\mathbf{R}\}\big)}{\partial \mathbf{R}_I} = -\Big\langle \Psi_e\big(\{\mathbf{R}\}\big)\Big| \frac{\partial \hat{\mathcal{H}}_{\mathrm{BO}}\big(\{\mathbf{R}\}\big)}{\partial \mathbf{R}_I}\Big|\Psi_e\big(\{\mathbf{R}\}\big)\Big\rangle \tag{2.63}$$

$$= -\int \rho_{\{\mathbf{R}\}}(\mathbf{r})\frac{\partial V_{\mathrm{ion}}\big(\mathbf{r};\{\mathbf{R}\}\big)}{\partial \mathbf{R}_I}d\mathbf{r} - \frac{\partial E_{\mathrm{N}}\big(\{\mathbf{R}\}\big)}{\partial \mathbf{R}_I} \tag{2.64}$$

where

$$\hat{\mathcal{H}}_{\mathrm{BO}}\big(\{\mathbf{R}\}\big) = -\sum_i \frac{\hbar^2}{2m}\frac{\partial^2}{\partial \mathbf{r}_i^2} + V\big(\{\mathbf{r}\},\{\mathbf{R}\}\big), \tag{2.65}$$

$$V_{\mathrm{ion}}\big(\mathbf{r};\{\mathbf{R}\}\big) = -\sum_I \frac{Z_I e^2}{|\mathbf{r}-\mathbf{R}_I|}, \tag{2.66}$$

$$E_{\mathrm{N}}\big(\{\mathbf{R}\}\big) = \sum_{I<J}\frac{Z_I Z_J e^2}{|\mathbf{R}_I - \mathbf{R}_J|}, \tag{2.67}$$

and $\Psi_e\big(\{\mathbf{R}\}\big)$ and $\rho_{\{\mathbf{R}\}}(\mathbf{r})$ are the electronic wave function and the electron density at a fixed ionic configuration $\{\mathbf{R}\}$, respectively. Here, to derive the expression for Hellmann-Feynman force $\mathbf{F}_I$, we used the Hellmann-Feynman theorem [31, 32]:

$$\frac{\partial E_\lambda}{\partial \lambda} = \Big\langle \Psi_\lambda\Big|\frac{\partial \hat{\mathcal{H}}_\lambda}{\partial \lambda}\Big|\Psi_\lambda\Big\rangle, \tag{2.68}$$

where the Hamiltonian $\hat{\mathcal{H}}_\lambda$ depends on a parameter λ, and Ψ_λ and E_λ are the eigenstate and the eigenvalue of $\hat{\mathcal{H}}_\lambda$, respectively. The Hessian matrix, which corresponds to the matrix of interatomic force constants, is given by

$$\frac{\partial^2 E\big(\{\mathbf{R}\}\big)}{\partial \mathbf{R}_I \partial \mathbf{R}_J} = -\frac{\partial \mathbf{F}_I}{\partial \mathbf{R}_J} \tag{2.69}$$

$$= \int \frac{\partial \rho_{\{\mathbf{R}\}}(\mathbf{r})}{\partial \mathbf{R}_J}\frac{\partial V_{\mathrm{ion}}\big(\mathbf{r};\{\mathbf{R}\}\big)}{\partial \mathbf{R}_I}d\mathbf{r} + \int \rho_{\{\mathbf{R}\}}(\mathbf{r})\frac{\partial^2 V_{\mathrm{ion}}\big(\mathbf{r};\{\mathbf{R}\}\big)}{\partial \mathbf{R}_I \partial \mathbf{R}_J}d\mathbf{r} + \frac{\partial^2 E_{\mathrm{N}}\big(\{\mathbf{R}\}\big)}{\partial \mathbf{R}_I \partial \mathbf{R}_J}. \tag{2.70}$$

In solids where $I = (p\kappa)$, switching to the momentum-space representation makes the calculation simple. Considering $\partial/\partial \mathbf{R}_{p\kappa} = \partial/\partial \mathbf{u}_{p\kappa}$, we write down the expression for the interatomic force constants in the momentum space as

$$C^{\alpha\alpha'}_{\kappa\kappa'}(\mathbf{q}) = \frac{1}{N}\left[\int\left(\frac{\partial \rho(\mathbf{r})}{\partial u^\alpha_\kappa(\mathbf{q})}\right)^* \frac{\partial V_{\mathrm{ion}}(\mathbf{r})}{\partial u^{\alpha'}_{\kappa'}(\mathbf{q})}d\mathbf{r} + \int \rho(\mathbf{r})\frac{\partial^2 V_{\mathrm{ion}}(\mathbf{r})}{\partial u^{*\alpha}_\kappa(\mathbf{q})\partial u^{\alpha'}_{\kappa'}(\mathbf{q})}d\mathbf{r} + \frac{\partial^2 E_{\mathrm{N}}\big(\{\mathbf{R}\}\big)}{\partial u^{*\alpha}_\kappa(\mathbf{q})\partial u^{\alpha'}_{\kappa'}(\mathbf{q})}\right]_{u=0} \tag{2.71}$$

with N being the number of the unit cells in the Born-von Karman boundary condition. For simplicity, we omitted $\{\mathbf{R}\}$ index from $V_{\text{ion}}\left(\mathbf{r};\{\mathbf{R}\}\right)$ and $\rho_{\{\mathbf{R}\}}(\mathbf{r})$. On the r.h.s. of Eq. (2.71), the first (second) term describes the contribution from the linear (quadratic) electron-phonon coupling and the third term describes the ionic contribution. The derivation of Eq. (2.71) relies on the fact that the ionic potential is local i.e., depends on only one electronic coordination $\mathbf{r}$. However, in actual calculations using the pseudopotentials, the ionic potential usually contains non-local components, the terms which depend on two electronic coordination $\mathbf{r}$ and $\mathbf{r}'$. In Appendix A, we show how the equations are modified in the presence of the non-local components.

2.2.4.3 Linear Response (Insulating Case)

To calculate the interatomic force constants [Eq. (2.71)], or the second derivative of the electronic energy with respect to ionic displacements, we usually employ the electronic energy calculated within the LDA or the GGA. Then the second and third terms on the r.h.s. of Eq. (2.71) can be straightforwardly calculated: The equilibrium density $\rho_{\text{eq.}}(\mathbf{r})$, which is needed to calculate the second term, is given as an output of the ground state calculation within the DFT. The Coulomb interaction energy between the nuclei E_{N} in the third term is efficiently calculated by means of the Ewald summation [33]. Only the first term requires a post-process calculation: We need to calculate a linear response of the electron density to the lattice distortion.

To calculate the linear response, we assume that the system obeys the Kohn-Sham equation

$$(\mathcal{H}_{\text{SCF}} - \varepsilon_n)\psi_n(\mathbf{r}) = 0, \tag{2.72}$$

where

$$\mathcal{H}_{\text{SCF}} = -\frac{\hbar^2}{2m}\nabla^2 + V_{\text{SCF}}(\mathbf{r}) \tag{2.73}$$

$$V_{\text{SCF}}(\mathbf{r}) = V_{\text{ion}}(\mathbf{r}) + V_{\text{H}}(\mathbf{r}) + V_{\text{xc}}(\mathbf{r}) \tag{2.74}$$

with the Hartree potential $V_{\text{H}}(\mathbf{r}) = e^2 \int \rho(\mathbf{r}')/|\mathbf{r} - \mathbf{r}'|d\mathbf{r}'$, and the exchange-correlation potential $V_{\text{xc}}(\mathbf{r}) = \delta E_{\text{xc}}[\rho]/\delta\rho(\mathbf{r})$. Let us assume that a potential change due to the lattice distortion ΔV_{ion} occurs in the insulating system, in which there exists a gap between the conduction bottom and the valence top. Then the response of the system can be summarized into the self-consistent equations

$$\Delta V_{\text{SCF}}(\mathbf{r}) = \Delta V_{\text{ion}}(\mathbf{r}) + \underbrace{e^2 \int \frac{\Delta\rho(\mathbf{r}')}{|\mathbf{r} - \mathbf{r}'|}d\mathbf{r}'}_{=\Delta V_{\text{H}}(\mathbf{r})} + \underbrace{\left.\frac{dV_{\text{xc}}[\rho]}{d\rho}\right|_{\rho=\rho_{\text{eq.}}(\mathbf{r})} \Delta\rho(\mathbf{r})}_{=\Delta V_{\text{xc}}(\mathbf{r})} \tag{2.75}$$

and

$$\Delta\rho(\mathbf{r}) = 4\mathrm{Re}\sum_{v}\psi_v^*(\mathbf{r})\Delta\psi_v(\mathbf{r}) \tag{2.76}$$

$$\Delta\psi_v(\mathbf{r}) = \sum_{c}\psi_c(\mathbf{r})\frac{\langle\psi_c|\Delta V_{\mathrm{SCF}}|\psi_v\rangle}{\varepsilon_v - \varepsilon_c}. \tag{2.77}$$

Here, ψ_v and ψ_c in Eqs. (2.76) and (2.77) denote the Bloch state within the valence band and the conduction band, respectively. The factor of 2 in Eq. (2.76) comes from the sum over spin. The equations represent how the system modifies the electron charge density and screens the bare perturbation $\Delta V_{\mathrm{ion}}(\mathbf{r})$. The screenings originate from the Hartree channel ΔV_{H} and the exchange-correlation channel ΔV_{xc}, which are both related with the modulation of the electron density. The screened potential ΔV_{SCF} is related with the electron density response via Eqs. (2.76) and (2.77).

In solving Eqs. (2.75)–(2.77) self-consistently, the most time consuming part is the calculation of $\Delta\psi_v(\mathbf{r})$ via Eq. (2.77), since it requires the extensive summation over the unoccupied states. Alternatively, the same quantity can be obtained by solving the following equation [26]

$$\underbrace{\left(\mathcal{H}_{\mathrm{SCF}} + \alpha P_v - \varepsilon_v\right)}_{A}\underbrace{\left|\Delta\psi_v\right\rangle}_{\mathbf{x}} = \underbrace{-P_c\Delta V_{\mathrm{SCF}}\left|\psi_v\right\rangle}_{\mathbf{y}} \tag{2.78}$$

with the projection operators onto valence bands (conduction bands) $P_v = \sum_v \left|\psi_v\right\rangle\left\langle\psi_v\right|$ $\left(P_c = \sum_c \left|\psi_c\right\rangle\left\langle\psi_c\right|\right)$. α is a parameter to avoid null eigenvalues in the A matrix. We can prove that Eq. (2.78) indeed gives the same result as Eq. (2.77) as follows: In the Bloch basis, the A matrix is expressed as

$$A = \begin{pmatrix} \varepsilon_1+\alpha-\varepsilon_v & & & & & & \\ & \varepsilon_2+\alpha-\varepsilon_v & & & & 0 & \\ & & \ddots & & & & \\ & & & \varepsilon_{N_v}+\alpha-\varepsilon_v & & & \\ & & & & \varepsilon_{N_v+1}-\varepsilon_v & & \\ & 0 & & & & \ddots & \\ & & & & & & \varepsilon_M-\varepsilon_v \end{pmatrix} = \begin{pmatrix} A_v & 0 \\ 0 & A_c \end{pmatrix} \tag{2.79}$$

with

$$A_v = \begin{pmatrix} \varepsilon_1+\alpha-\varepsilon_v & & & 0 \\ & \varepsilon_2+\alpha-\varepsilon_v & & \\ & & \ddots & \\ 0 & & & \varepsilon_{N_v}+\alpha-\varepsilon_v \end{pmatrix} \tag{2.80}$$

and

$$A_c = \begin{pmatrix} \varepsilon_{N_v+1} - \varepsilon_v & & 0 \\ & \ddots & \\ 0 & & \varepsilon_M - \varepsilon_v \end{pmatrix}, \tag{2.81}$$

where N_v is the number of valence (occupied) states and M is the dimension of the A matrix. Note that, in the actual calculation, the A matrix is not represented in the Bloch basis, but is expressed in some basis set (e.g., plane-wave basis) to expand the wave functions. Then, M corresponds to the size of the basis set to describe the Bloch states, which should be large enough ($M \gg N_v$). In the absence of the α parameter, it is obvious that the A matrix has at least one null eigenvalue since $A_{vv} = \varepsilon_v - \varepsilon_v = 0$. α is arbitrary as far as the introduction of α gets rid of the null eigenvalue(s). Then, a simplest choice is e.g., $\alpha >$ (bandwidth of the occupied states). Since the $\mathbf{y}$ vector is written, in the Bloch representation, as

$$\mathbf{y} = \begin{pmatrix} 0 \\ \vdots \\ 0 \\ -\langle \psi_{N_v+1} | \Delta V_{\mathrm{SCF}} | \psi_v \rangle \\ \vdots \\ -\langle \psi_M | \Delta V_{\mathrm{SCF}} | \psi_v \rangle \end{pmatrix} = \begin{pmatrix} \mathbf{0} \\ \mathbf{y}_c \end{pmatrix} \begin{matrix} \} N_v \\ \} M - N_v \end{matrix}, \tag{2.82}$$

$|\Delta\psi_v\rangle$ is given by

$$|\Delta\psi_v\rangle = A^{-1}\mathbf{y} = A_c^{-1}\mathbf{y}_c = \sum_c \frac{1}{\varepsilon_v - \varepsilon_c} |\psi_c\rangle\langle\psi_c|\Delta V_{\mathrm{SCF}}|\psi_v\rangle, \tag{2.83}$$

which proves that Eqs. (2.77) and (2.78) are equivalent. Equation (2.78) requires only the information about the occupied states (note that $P_c = 1 - P_v$) and allows us to avoid the cumbersome summation over the unoccupied states, which leads to a significant reduction of the computational time.

In crystalline solids, perturbations with different wavelengths are decoupled and the self-consistent equations [Eqs. (2.75)–(2.78)] can be independently solved for each wave vector $\mathbf{q}$:

$$\begin{cases} \Delta V^{\mathbf{q}}_{\mathrm{SCF}}(\mathbf{r}) = \Delta V^{\mathbf{q}}_{\mathrm{ion}}(\mathbf{r}) + e^2 \int \frac{\Delta\rho^{\mathbf{q}}(\mathbf{r}')}{|\mathbf{r}-\mathbf{r}'|} e^{-i\mathbf{q}\cdot(\mathbf{r}-\mathbf{r}')} d\mathbf{r}' + \left.\frac{dV_{\mathrm{xc}}[\rho]}{d\rho}\right|_{\rho=\rho_{\mathrm{eq.}}(\mathbf{r})} \Delta\rho^{\mathbf{q}}(\mathbf{r}), & (2.84) \\ \Delta\rho^{\mathbf{q}}(\mathbf{r}) = 4\sum_{v\mathbf{k}} u_v^{\mathbf{k}*}(\mathbf{r}) \Delta u_v^{\mathbf{k}+\mathbf{q}}(\mathbf{r}), & (2.85) \\ \left(\mathcal{H}^{\mathbf{k}+\mathbf{q}}_{\mathrm{SCF}} + \alpha \sum_{v'} |u_{v'}^{\mathbf{k}+\mathbf{q}}\rangle\langle u_{v'}^{\mathbf{k}+\mathbf{q}}| - \varepsilon_v^{\mathbf{k}}\right) |\Delta u_v^{\mathbf{k}+\mathbf{q}}\rangle = -\left(1 - \sum_{v'} |u_{v'}^{\mathbf{k}+\mathbf{q}}\rangle\langle u_{v'}^{\mathbf{k}+\mathbf{q}}|\right) \Delta V^{\mathbf{q}}_{\mathrm{SCF}} |u_v^{\mathbf{k}}\rangle, & (2.86) \end{cases}$$

where

$$\Delta\mathcal{O}(\mathbf{r}) = \sum_{\mathbf{q}} \Delta\mathcal{O}^{\mathbf{q}}(\mathbf{r}) e^{i\mathbf{q}\cdot\mathbf{r}} \qquad \left(\mathcal{O} = \{V_{\mathrm{SCF}}, V_{\mathrm{ion}}, \rho\}\right) \tag{2.87}$$

and $u_v^{\mathbf{k}}(\mathbf{r})$ is the cell-periodic part of the Bloch wave function of the band v and the wave vector $\mathbf{k}$. In the derivation of Eq. (2.85), we utilized the relations $\mathcal{O}^{\mathbf{q}}(\mathbf{r}) = [\mathcal{O}^{-\mathbf{q}}(\mathbf{r})]^*$ (Fourier transform of the real functions) and $u_v^{\mathbf{k}}(\mathbf{r}) = [u_v^{-\mathbf{k}}(\mathbf{r})]^*$ (time reversal symmetry). It is also straightforward to verify that the solution of Eq. (2.86) is equivalent to that of the following equation:

$$\left|\Delta u_v^{\mathbf{k}+\mathbf{q}}\right\rangle = \sum_c \frac{1}{\varepsilon_v^{\mathbf{k}} - \varepsilon_c^{\mathbf{k}+\mathbf{q}}} \left|u_c^{\mathbf{k}+\mathbf{q}}\right\rangle \left\langle u_c^{\mathbf{k}+\mathbf{q}}\right| \Delta V_{\mathrm{SCF}}^{\mathbf{q}} \left|u_v^{\mathbf{k}}\right\rangle. \tag{2.88}$$

By solving Eqs. (2.84)–(2.86), we obtain the linear response of the electron density to the ionic displacements, which is to be used to calculate the first term on the r.h.s. of Eq. (2.71). As is obvious from Eqs. (2.84)–(2.86), in the DFPT methods, the wave functions calculated with the original unit cell are used, which is one of the strongest advantages of the DFPT to the other phonon-calculation methods, such as the frozen phonon method, in which we need to prepare a large supercell according to the wavelength of the phonon.

2.2.4.4 Linear Response (Metallic Case)

Next, we consider a metallic case [27]. In the DFT calculation for the metal, it is usual to introduce a smearing function $\tilde{\delta}(x)$ and the corresponding smoothed step function $\tilde{\theta}(x) = \int_{-\infty}^{x} \tilde{\delta}(x')dx'$. In the present calculation, we employ the gaussian smearing $\tilde{\delta}(x) = \exp(-x^2)/\sqrt{\pi}$. Then, the expression for the electron density response is modified as (the expression of ΔV_{SCF} remains the same)

$$\begin{aligned}\Delta\rho(\mathbf{r}) &= \sum_{n,m} \frac{\tilde{\theta}_{F,n} - \tilde{\theta}_{F,m}}{\varepsilon_n - \varepsilon_m} \psi_n^*(\mathbf{r})\psi_m(\mathbf{r}) \left\langle\psi_m\right| \Delta V_{\mathrm{SCF}} \left|\psi_n\right\rangle \\ &= 2\sum_{n,m} \frac{\tilde{\theta}_{F,n} - \tilde{\theta}_{F,m}}{\varepsilon_n - \varepsilon_m} \tilde{\theta}_{m,n} \psi_n^*(\mathbf{r})\psi_m(\mathbf{r}) \left\langle\psi_m\right| \Delta V_{\mathrm{SCF}} \left|\psi_n\right\rangle,\end{aligned} \tag{2.89}$$

where $\tilde{\theta}_{F,n}$ and $\tilde{\theta}_{m,n}$ are defined as $\tilde{\theta}_{F,n} = \tilde{\theta}\left[(\varepsilon_F - \varepsilon_n)/\sigma\right]$ and $\tilde{\theta}_{m,n} = \tilde{\theta}\left[(\varepsilon_m - \varepsilon_n)/\sigma\right]$, respectively, with the Fermi energy ε_F and a smearing width σ. If we define $\Delta\psi_n(\mathbf{r})$ as

$$\Delta\psi_n(\mathbf{r}) = \sum_m \frac{\tilde{\theta}_{F,n} - \tilde{\theta}_{F,m}}{\varepsilon_n - \varepsilon_m} \tilde{\theta}_{m,n} \psi_m(\mathbf{r}) \left\langle\psi_m\right| \Delta V_{\mathrm{SCF}} \left|\psi_n\right\rangle, \tag{2.90}$$

Equation (2.89) can be recast into

$$\Delta\rho(\mathbf{r}) = 2\sum_n \psi_n^*(\mathbf{r})\Delta\psi_n(\mathbf{r}). \tag{2.91}$$

Similarly to the insulating case, one can show that $\Delta\psi_n$'s satisfy the equation [27]

$$\underbrace{\left(\mathcal{H}_{\rm SCF} + Q - \varepsilon_n\right)}_{A}\underbrace{\left|\Delta\psi_n\right\rangle}_{\mathbf{x}} = \underbrace{-\left(\tilde{\theta}_{F,n} - P_n\right)\Delta V_{\rm SCF}\left|\psi_n\right\rangle}_{\mathbf{y}} \tag{2.92}$$

where

$$Q = \sum_m \alpha_m \left|\psi_m\right\rangle\left\langle\psi_m\right|, \quad P_n = \sum_m \beta_{n,m}\left|\psi_m\right\rangle\left\langle\psi_m\right| \tag{2.93}$$

with

$$\beta_{n,m} = \tilde{\theta}_{F,n}\tilde{\theta}_{n,m} + \tilde{\theta}_{F,m}\tilde{\theta}_{m,n} + \alpha_m\frac{\tilde{\theta}_{F,n} - \tilde{\theta}_{F,m}}{\varepsilon_n - \epsilon_m}\tilde{\theta}_{m,n}. \tag{2.94}$$

Here α_m's are parameters to avoid null eigenvalues of the A matrix, which can be set to be a constant value which is larger than [(maximum energy among partial occupied states) − (minimum energy of occupied states)] for all the partially occupied states, and zero for the totally unoccupied states. This α_m parametrization enables a calculation without any information about the totally unoccupied states. Noting that $\tilde{\theta}_{F,n} - P_n$ on the r.h.s of Eq. (2.92) is rewritten as

$$\begin{aligned}
\tilde{\theta}_{F,n} - P_n &= \sum_m \left[\tilde{\theta}_{F,n}\left(1 - \tilde{\theta}_{n,m}\right) - \tilde{\theta}_{F,m}\tilde{\theta}_{m,n} - \alpha_m\frac{\tilde{\theta}_{F,n} - \tilde{\theta}_{F,m}}{\varepsilon_n - \varepsilon_m}\tilde{\theta}_{m,n}\right]\left|\psi_m\right\rangle\left\langle\psi_m\right| \\
&= \sum_m \left[\left(\tilde{\theta}_{F,n} - \tilde{\theta}_{F,m}\right)\tilde{\theta}_{m,n} - \alpha_m\frac{\tilde{\theta}_{F,n} - \tilde{\theta}_{F,m}}{\varepsilon_n - \varepsilon_m}\tilde{\theta}_{m,n}\right]\left|\psi_m\right\rangle\left\langle\psi_m\right| \\
&= -\sum_m \left[\frac{\tilde{\theta}_{F,n} - \tilde{\theta}_{F,m}}{\varepsilon_n - \varepsilon_m}\tilde{\theta}_{m,n}\left(\varepsilon_m + \alpha_m - \varepsilon_n\right)\right]\left|\psi_m\right\rangle\left\langle\psi_m\right|
\end{aligned} \tag{2.95}$$

and that the elements of the matrix A in Eq. (2.92) are given, in the Bloch basis, by

$$A = \begin{pmatrix} \varepsilon_1+\alpha_1-\varepsilon_n & & & 0 \\ & \varepsilon_2+\alpha_2-\varepsilon_n & & \\ & & \ddots & \\ 0 & & & \varepsilon_M+\alpha_M-\varepsilon_n \end{pmatrix}, \tag{2.96}$$

we obtain the expression of $|\Delta\psi_n\rangle$:

$$|\Delta\psi_n\rangle = A^{-1}\mathbf{y} = \sum_m \frac{\tilde{\theta}_{F,n} - \tilde{\theta}_{F,m}}{\varepsilon_n - \varepsilon_m}\tilde{\theta}_{m,n}|\psi_m\rangle\langle\psi_m|\Delta V_{\mathrm{SCF}}|\psi_n\rangle, \tag{2.97}$$

which is nothing but the proof that Eq. (2.92) gives the same result as that of Eq. (2.90). Although we did not show the indices for the wave vector $\mathbf{q}$ in the above equations, linear response calculations for different wave vectors can be done individually as in the insulating case.

Only when the perturbation has periodicity with the lattice ($\mathbf{q} = \mathbf{0}$) and the number of electrons is fixed, the Fermi energy may change and $\Delta\rho$ acquires an additional term:

$$\Delta\rho(\mathbf{r}) = 2\sum_n \psi_n^*(\mathbf{r})\Delta\psi_n(\mathbf{r}) + \rho(\mathbf{r}, \varepsilon_F)\Delta\varepsilon_F \tag{2.98}$$

with

$$\rho(\mathbf{r}, \varepsilon) = \sum_n \frac{1}{\sigma}\tilde{\delta}\left(\frac{\varepsilon - \varepsilon_n}{\sigma}\right)|\psi_n(\mathbf{r})|^2. \tag{2.99}$$

The change in the Fermi energy $\Delta\varepsilon_F$ is determined by the charge neutrality condition.

2.2.4.5 Electron-Phonon Coupling

When ions move from their equilibrium position, the ionic potential changes. Then, the surrounding electrons will respond to the potential change and screen it. Electrons will feel this screened potential change and will be scattered. Within the framework of the DFT, the change is expressed as

$$\Delta V_{\mathrm{SCF}}(\mathbf{r}) = V_{\mathrm{SCF}}(\mathbf{r}; \{\mathbf{R}_{p\kappa}^{(0)} + \mathbf{u}_{p\kappa}\}) - V_{\mathrm{SCF}}(\mathbf{r}; \{\mathbf{R}_{p\kappa}^{(0)}\}) \tag{2.100}$$

$$\simeq \sum_{p\kappa} \mathbf{u}_{p\kappa} \cdot \left(\frac{\partial V_{\mathrm{SCF}}}{\partial \mathbf{R}_{p\kappa}}\right)_{R=R^{(0)}}. \tag{2.101}$$

Given that the displacement operator is written, in the second quantization formalism, as

$$\hat{\mathbf{u}}_{p\kappa} = \sum_{\mathbf{q}\nu} \sqrt{\frac{\hbar}{2M_\kappa N\omega_{\mathbf{q}\nu}}}(\hat{b}_{\mathbf{q}\nu} + \hat{b}_{-\mathbf{q}\nu}^\dagger)\mathbf{e}_\kappa(\mathbf{q}\nu)e^{i\mathbf{q}\cdot\mathbf{R}_p} \tag{2.102}$$

with $\hat{b}_{\mathbf{q}\nu}^\dagger$ and $\hat{b}_{\mathbf{q}\nu}$ being the creation and annihilation operators of the phonon with the wave vector $\mathbf{q}$ and the branch ν, respectively, the electron-phonon coupling is

expressed by the Hamiltonian

$$\hat{\mathcal{H}}_{\text{el-ph}} = \frac{1}{\sqrt{N}} \sum_{\mathbf{q}\nu} \sum_{\mathbf{k}nn'\sigma} g^{\nu}_{n'n}(\mathbf{k}, \mathbf{q}) c^{\sigma\dagger}_{n'\mathbf{k}+\mathbf{q}} c^{\sigma}_{n\mathbf{k}} (b_{\mathbf{q}\nu} + b^{\dagger}_{-\mathbf{q}\nu}). \tag{2.103}$$

Here,

$$g^{\nu}_{n'n}(\mathbf{k}, \mathbf{q}) = \sum_{\kappa\alpha} \sqrt{\frac{\hbar}{2M_\kappa \omega_{\mathbf{q}\nu}}}\, e^{\alpha}_{\kappa}(\mathbf{q}\nu) \left\langle \psi_{n'\mathbf{k}+\mathbf{q}} \left| \frac{\partial V_{\text{SCF}}(\mathbf{r})}{\partial u^{\alpha}_{\kappa}(\mathbf{q})} \right| \psi_{n\mathbf{k}} \right\rangle \tag{2.104}$$

is the electron-phonon-coupling matrix element involving the Bloch states $\psi_{n\mathbf{k}}$ and $\psi_{n'\mathbf{k}+\mathbf{q}}$ and the νth branch phonon with the wave vector $\mathbf{q}$. $c^{\sigma}_{n\mathbf{k}}$ ($c^{\sigma\dagger}_{n\mathbf{k}}$) annihilates (creates) an electron on the nth Bloch orbital with the wave vector $\mathbf{k}$ and the spin σ.

2.2.4.6 Flow of Calculation

The phonon frequencies and the electron-phonon couplings for a certain $\mathbf{q}$ vector are calculated in the following procedures. As is already mentioned, calculations for different $\mathbf{q}$ vectors can be done independently.

1. Calculate the contributions to the interatomic force constants which do not depend on the electron density response [the second and third terms on the r.h.s. of Eq. (2.71)].
2. Self-consistently solve the linear response equations [Eqs. (2.84)–(2.86) for insulating case, Eqs. (2.75), (2.91), and (2.92) for metallic case], and obtain $\partial V_{\text{SCF}}(\mathbf{r})/\partial u^{\alpha}_{\kappa}(\mathbf{q})$ and $\partial \rho(\mathbf{r})/\partial u^{\alpha}_{\kappa}(\mathbf{q})$. At the first iteration, the bare perturbation $\partial V_{\text{ion}}(\mathbf{r})/\partial u^{\alpha}_{\kappa}(\mathbf{q})$ is often employed as an initial guess for $\partial V_{\text{SCF}}(\mathbf{r})/\partial u^{\alpha}_{\kappa}(\mathbf{q})$.
3. Calculate the first term on the r.h.s. of Eq. (2.71) with the resultant $\partial \rho(\mathbf{r})/\partial u^{\alpha}_{\kappa}(\mathbf{q})$. Add it to the other contributions calculated at the step 1 and obtain the interatomic force constants.
4. Calculate the dynamical matrix [Eq. (2.59)] and diagonalize it. Phonon frequencies are given by the square root of the eigenvalues [Eq. (2.61)].
5. Calculate electron-phonon couplings via Eq. (2.104).

2.2.5 Constrained Density-Functional Perturbation Theory

2.2.5.1 Basic Idea and Practical Implementation

In this section, we show how the phonon frequencies and the electron-phonon couplings in the low-energy Hamiltonian should be parametrized. As in the case of the effective Coulomb interactions, they should be partially renormalized quantities,

which take into account the renormalization effects associated with the elimination of the high-energy degrees of freedom. In other words, we derive the parameters with avoiding the double counting of the renormalization effects which are to be taken into account in the model analysis step.

Since the present low-energy effective Hamiltonian includes the linear electron-phonon couplings that can renormalize the phonon frequencies after the model analysis, we define (ionic contribution) + (contribution from the quadratic coupling) as "bare" term, and (contribution from the linear coupling) as "renormalizing" term. Then the interatomic force constants $C^{\alpha\alpha'}_{\kappa\kappa'}(\mathbf{q})$ given in Eq. (2.71) can be divided as $C^{\alpha\alpha'}_{\kappa\kappa'}(\mathbf{q}) = {}^{\text{bare}}C^{\alpha\alpha'}_{\kappa\kappa'}(\mathbf{q}) + {}^{\text{ren.}}C^{\alpha\alpha'}_{\kappa\kappa'}(\mathbf{q})$, where ${}^{\text{bare}}C^{\alpha\alpha'}_{\kappa\kappa'}(\mathbf{q})$ gives the "bare" phonon frequencies

$$ {}^{\text{bare}}C^{\alpha\alpha'}_{\kappa\kappa'}(\mathbf{q}) = \frac{1}{N}\left[\frac{\partial^2 E_{\text{N}}(\{\mathbf{R}\})}{\partial u^{*\alpha}_{\kappa}(\mathbf{q})\partial u^{\alpha'}_{\kappa'}(\mathbf{q})} + \int \rho(\mathbf{r})\frac{\partial^2 V_{\text{ion}}(\mathbf{r})}{\partial u^{*\alpha}_{\kappa}(\mathbf{q})\partial u^{\alpha'}_{\kappa'}(\mathbf{q})}d\mathbf{r}\right], \quad (2.105) $$

and ${}^{\text{ren.}}C^{\alpha\alpha'}_{\kappa\kappa'}(\mathbf{q})$ gives the renormalization of the phonon frequencies via the linear electron-phonon coupling

$$ {}^{\text{ren.}}C^{\alpha\alpha'}_{\kappa\kappa'}(\mathbf{q}) = \frac{1}{N}\int\left(\frac{\partial\rho(\mathbf{r})}{\partial u^{\alpha}_{\kappa}(\mathbf{q})}\right)^{*}\frac{\partial V_{\text{ion}}(\mathbf{r})}{\partial u^{\alpha'}_{\kappa'}(\mathbf{q})}d\mathbf{r}. \quad (2.106) $$

The derivative of the self-consistent field potential $\partial V_{\text{SCF}}(\mathbf{r})/\partial u^{\alpha}_{\kappa}(\mathbf{q})$ in Eq. (2.104) is also decomposed into the bare contribution

$$ {}^{\text{bare}}\left[\frac{\partial V_{\text{SCF}}(\mathbf{r})}{\partial u^{\alpha}_{\kappa}(\mathbf{q})}\right] = \frac{\partial V_{\text{ion}}(\mathbf{r})}{\partial u^{\alpha}_{\kappa}(\mathbf{q})} \quad (2.107) $$

and the screening contribution

$$ {}^{\text{ren.}}\left[\frac{\partial V_{\text{SCF}}(\mathbf{r})}{\partial u^{\alpha}_{\kappa}(\mathbf{q})}\right] = \int\left(\frac{e^2}{|\mathbf{r}-\mathbf{r}'|} + \frac{dV_{\text{xc}}(\mathbf{r})}{d\rho}\delta(\mathbf{r}-\mathbf{r}')\right)\frac{\partial\rho(\mathbf{r}')}{\partial u^{\alpha}_{\kappa}(\mathbf{q})}d\mathbf{r}'. \quad (2.108) $$

We see that the origin of the renormalization of the phonon frequencies and the screening for the electron-phonon couplings is the modulation of the electron density due to the lattice motion $\partial\rho(\mathbf{r})/\partial u^{\alpha}_{\kappa}(\mathbf{q})$. The modulation calculated in the conventional DFPT scheme is the sum of contributions from all possible particle-hole excitations [Eq. (2.89)]. In the cDFPT method [16], we exclude the target ↔ target excitation processes to avoid the double counting of them, and calculate the partially renormalized phonon frequencies and electron-phonon couplings. Below, we show that the exclusion of the target ↔ target processes can be done by a slight modification in the linear response equations.

Now, we propose a practical way to impose constraint on Eqs. (2.91) and (2.92), the equations which determine the variation of the electron density. If $|\psi_n\rangle$ in Eq. (2.92) belongs to t-subspace, in order to exclude the target ↔ target polarization processes,

the r.h.s. of Eq. (2.92) should be modified as

$$\left(\mathcal{H}_{\mathrm{SCF}}+Q-\varepsilon_n\right)\left|\Delta\psi_n\right\rangle=-P_r\left(\tilde{\theta}_{F,n}-P_n\right)\Delta V_{\mathrm{SCF}}\left|\psi_n\right\rangle \tag{2.109}$$

with P_r being the projection onto the r-subspace. The very same constraint can be achieved by solving Eq. (2.92) with modified $\beta_{n,m}$'s given by

$$\beta_{n,m}=\begin{cases}\tilde{\theta}_{F,n} & \left(n,m\in t\text{-subspace}\right),\\ \tilde{\theta}_{F,n}\tilde{\theta}_{n,m}+\tilde{\theta}_{F,m}\tilde{\theta}_{m,n}+\alpha_m\frac{\tilde{\theta}_{F,n}-\tilde{\theta}_{F,m}}{\varepsilon_n-\varepsilon_m}\tilde{\theta}_{m,n} & \left(\text{the other cases}\right).\end{cases} \tag{2.110}$$

The identity can be checked as follows: When $n\in t$-subspace, both $-P_r\left(\tilde{\theta}_{F,n}-P_n\right)\Delta V_{\mathrm{SCF}}\left|\psi_n\right\rangle$ and $-\left(\tilde{\theta}_{F,n}-P_n\right)\Delta V_{\mathrm{SCF}}\left|\psi_n\right\rangle=-\left(\tilde{\theta}_{F,n}-\sum_m\beta_{n,m}\left|\psi_m\right\rangle\left\langle\psi_m\right|\right)\Delta V_{\mathrm{SCF}}\left|\psi_n\right\rangle$ with the new $\beta_{n,m}$'s give the same quantity:

$$\begin{cases}0 & \left(m\in t\text{-subspace}\right),\\ \left[\frac{\tilde{\theta}_{F,n}-\tilde{\theta}_{F,m}}{\varepsilon_n-\varepsilon_m}\tilde{\theta}_{m,n}\left(\varepsilon_m+\alpha_m-\varepsilon_n\right)\right]\left|\psi_m\right\rangle\left\langle\psi_m\right|\Delta V_{\mathrm{SCF}}\left|\psi_n\right\rangle & \left(m\in r\text{-subspace}\right).\end{cases} \tag{2.111}$$

Therefore, the r.h.s. of Eq. (2.109) is equal to that of Eq. (2.92) with the modified $\beta_{n,m}$'s, which ensures the equivalence of the two types of modifications. When we consider the practical aspect, the latter modification is much easier to implement if one has a code of the conventional DFPT. One has only to modify the part where the $\beta_{n,m}$ parameters are defined, and no modification is needed in the other parts. With the modified $\beta_{n,m}$'s and following the very same flow of calculations of the usual DFPT method, one can get the change of the electron density without target $\leftrightarrow$ target polarization processes. Then, with the resulting density response, we evaluate the partially-screened (renormalized) quantities $\omega^{(p)}$ and $g^{(p)}$.

2.2.5.2 Comparison Between cDFPT and cRPA

Here, we compare the present cDFPT with the cRPA [15]. In the cRPA to derive the effective electron-electron interactions in the model, the screening of the Coulomb interaction is decomposed into two steps [15];

$$W^{(p)}=\left(1-v\chi_r^0\right)^{-1}v \tag{2.112}$$

and

$$W^{(f)}=\left(1-W^{(p)}\chi_t^0\right)^{-1}W^{(p)}, \tag{2.113}$$

where v is the bare Coulomb interaction. Here, the total irreducible polarization χ^0 is divided into χ_t^0 and χ_r^0 with χ_t^0 being the polarization within the t-subspace and $\chi_r^0 = \chi^0 - \chi_t^0$ is the rest of the polarization. Such a decomposition holds even if v is replaced by $\tilde{v} = v + K_{\rm xc}$ with $K_{\rm xc} = \delta V_{\rm xc}/\delta\rho$ defined as the exchange-correlation kernel. Here, $V_{\rm xc}$ and ρ are the exchange-correlation potential and the electron density, respectively. Then, we obtain

$$\tilde{W}^{(p)} = \left(1 - \tilde{v}\chi_r^0\right)^{-1} \tilde{v} \tag{2.114}$$

and

$$\tilde{W}^{(f)} = \left(1 - \tilde{W}^{(p)}\chi_t^0\right)^{-1} \tilde{W}^{(p)}. \tag{2.115}$$

Now, the cDFPT to derive the phonon-related term in the low-energy Hamiltonian is formulated as follows: First, on the basis of the usual DFPT scheme [26–29], the induced electron density $\Delta\rho$ to the perturbation $\Delta V_{\rm ion}$ (bare potential) is given by[3]

$$\Delta\rho = \underbrace{\chi^0 \left(1 - \tilde{v}\chi^0\right)^{-1}}_{=\chi_{\rm LDA}} \Delta V_{\rm ion} \tag{2.116}$$

$$= \chi^0 \Delta V_{\rm SCF}, \tag{2.117}$$

where the change in the self-consistent field potential $\Delta V_{\rm SCF}$ (screened potential) is written as

$$\Delta V_{\rm SCF} = \left(1 - \tilde{v}\chi^0\right)^{-1} \Delta V_{\rm ion}. \tag{2.118}$$

Note Eqs. (2.117) and (2.118) correspond to Eqs. (2.89) and (2.75), respectively. Since the electron-phonon coupling g is given as the matrix element of the electron scattering via $\Delta V_{\rm SCF}$, the same decomposition as Eqs. (2.114) and (2.115) holds for the fully screened electron-phonon interaction; that is, $g^{(f)} = \left(1 - \tilde{v}\chi^0\right)^{-1} g^{(b)}$ is decomposed as

$$g^{(p)} = \left(1 - \tilde{v}\chi_r^0\right)^{-1} g^{(b)} \tag{2.119}$$

and

$$g^{(f)} = \left(1 - \tilde{W}^{(p)}\chi_t^0\right)^{-1} g^{(p)}. \tag{2.120}$$

[3] Strictly speaking, this expression [Eq. (2.116)] is valid only when the ionic potential $V_{\rm ion}$ is local. In practice, we utilize the pseudopotential, which has non-local part. In this case, we have to introduce three-point response functions, however, it does not change the outline presented in this section.

Therefore, the present cDFPT is formally based on the cRPA-like decomposition, but the difference is that, in the former, $\tilde{v}$ is used instead of v.

The similar idea applies to the derivation of the phonon frequencies in the low-energy effective Hamiltonian. In this case, the self-energy is decomposed. One can show that Eq. (2.106) is rewritten as

$$^{\text{ren.}}C = |g'^{(b)}|^2 \chi_{\text{LDA}}, \tag{2.121}$$

where $g'^{(b)} = \sqrt{2M\omega^{(b)}} g^{(b)}$ with the bare phonon frequency $\omega^{(b)}$. In this expression, we omitted the subscripts for simplicity. Then, we define the phonon self-energy in the DFPT scheme as

$$\Sigma = \frac{^{\text{ren.}}C}{2M\omega^{(b)}} = |g^{(b)}|^2 \chi_{\text{LDA}} \tag{2.122}$$

This self-energy can be divided into two contributions as $\Sigma = \Sigma_t + \Sigma_r$. Here, $\Sigma_r = |g^{(b)}|^2 \chi^r_{\text{LDA}}$ with $\chi^r_{\text{LDA}} = \chi^0_r \left(1 - \tilde{v}\chi^0_r\right)^{-1}$ is the phonon self-energy due to the interactions between the r-subspace electrons and the phonons. The interactions between the t-subspace electrons and the phonons through the partially-screened coupling $g^{(p)}$ give rise to the self-energy $\Sigma_t = |g^{(p)}|^2 \chi^t_{\text{LDA}}$ with $\chi^t_{\text{LDA}} = \chi^0_t \left(1 - \tilde{W}^{(p)} \chi^0_t\right)^{-1}$.[4] The decomposition of Σ into Σ_t and Σ_r is achieved by dividing the density-response contributions to $^{\text{ren.}}C$ into the target-target contribution and the others. Then, the partially-dressed phonon Green's function $D^{(p)}$ is given by

$$[D^{(p)}]^{-1} = [D^{(b)}]^{-1} - \Sigma_r, \tag{2.123}$$

where $D^{(b)}$ is the bare phonon Green's function and its pole position gives the bare phonon frequency $\omega^{(b)}$. Similarly, the pole of $D^{(p)}$ gives the effective phonon frequency $\omega^{(p)}$ in the model. If we further consider Σ_t, the fully-dressed phonon Green's function $D^{(f)}$ is derived as

$$[D^{(f)}]^{-1} = [D^{(p)}]^{-1} - \Sigma_t. \tag{2.124}$$

2.3 Analysis of Low-Energy Hamiltonian

Analyzing the derived effective low-energy Hamiltonians with accurate model-calculations techniques is of great interest. There exist a variety of methods to take into account the correlation effects beyond the static mean-field level: the dynamical mean-field theory (DMFT) [34] and its derivatives such as extended DMFT [35, 36] and cluster extensions of the DMFT [37], auxiliary field quantum Monte Carlo

[4] See Appendix B for the proof that $\Sigma_t + \Sigma_r = |g^{(p)}|^2 \chi^t_{\text{LDA}} + |g^{(b)}|^2 \chi^r_{\text{LDA}}$ is indeed identical to $\Sigma = |g^{(b)}|^2 \chi_{\text{LDA}}$.

method [38, 39], the variational Monte Carlo method (VMC) [40–44], the fluctuation exchange approximation (FLEX) [45, 46], exact diagonalization (ED), the density matrix renormalization group (DMRG) [47, 48], the functional renormalization group (fRG) [49], the path-integral renormalization group (PIRG) [50], the calculations using the thermal pure quantum (TPQ) states [51, 52], and so on. Each method has both good and bad points. For example, the ED is the most accurate method, however, the computational cost grows exponentially as the increase of the degrees of freedom in the Hamiltonian, which results in serious finite size effects. The DMFT obtains an accurate description of the local quantum fluctuations since it takes into account all the local skeleton diagrams. However, it totally neglects the spatial correlations. Since the momentum differentiation tends to be large (small) in low- (high-)dimensional systems, the DMFT is considered to become a better approximation with the increase of the dimension. The DMRG is very powerful in treating one-dimensional problems, while its application to the systems with higher dimensions is still limited. Considering these aspects, it is important to choose an appropriate solver depending on the nature of low-energy Hamiltonian.

In the case of the fcc A_3C_{60} families with the three dimensional electronic structure, a suitable low-energy Hamiltonian solver would be the DMFT since each site (=molecule) has large coordination number of 12 and the pairing symmetry of the superconductivity is s-wave (i.e., a momentum dependence is small). What makes the DMFT even more powerful in this case is that the DMFT can treat the onsite Coulomb interaction and the coupling to intramolecular phonon on the same footing. Furthermore, in order to take account of dynamics involving the off-site Coulomb interactions, we employ the extended DMFT method, for which we will give a detailed description in Sect. 2.3.2.

2.3.1 Dynamical Mean-Field Theory

2.3.1.1 Formulation

Before proceeding with the review of the extended DMFT, we start with the overview of the conventional DMFT. The basic idea of the DMFT self-consistent equations was first given by Kuramoto and Watanabe [53] for the periodic Anderson model. Here, we consider the Hubbard model in the limit of infinite dimensions $d = \infty$ [54] to describe the formulation of the DMFT.

The Hamiltonian of the single-orbital Hubbard model with only the nearest neighbor hopping t is written as

$$\hat{\mathcal{H}} = -t \sum_{\langle i,j \rangle} \sum_{\sigma} \left(\hat{c}^{\dagger}_{i\sigma} \hat{c}_{j\sigma} + \hat{c}^{\dagger}_{j\sigma} \hat{c}_{i\sigma} \right) + U \sum_{i} \hat{n}_{i\uparrow} \hat{n}_{i\downarrow}, \tag{2.125}$$

where $\hat{c}^{\dagger}_{i\sigma}$ ($\hat{c}_{i\sigma}$) creates (annihilates) the electron with the spin σ at site i, $\langle i, j\rangle$ denotes the nearest neighbor pairs, U is the Hubbard interaction, and $\hat{n}_{i\sigma} = \hat{c}^{\dagger}_{i\sigma}\hat{c}_{i\sigma}$. Metzner and Vollhardt [54] showed that, in order to avoid the divergence of the kinetic energy and keep nontrivial competition between the kinetic and the potential energies even in the limit of $d = \infty$, the hopping has to be scaled as $t \sim d^{-\frac{1}{2}}$. As a consequence of the scaling, the diagrammatic treatments become drastically simple: The diagrams with finite contributions are only the local skelton diagrams, which indicates that the self-energy is site-diagonal and momentum-independent, i.e., $\Sigma_{ij}(i\omega_n) = \Sigma(i\omega_n)\delta_{ij}$ for any Matsubara frequencies $\omega_n = (2n+1)\pi T$ [55].

Based on these considerations, Georges and Kotliar [56] noticed that the Hubbard model in infinite dimensions can be mapped onto the Anderson impurity model embedded with self-consistently determined bath sites (see also the works by, e.g., Ohkawa [57, 58] and Jarrell [59]). The single-site action of the impurity problem with the impurity-site Coulomb repulsion U is written, in the coherent state path integral formalism [8], as

$$S_{\mathrm{imp}}\left[c^*, c, \mathcal{G}_0^{-1}\right] = -\int_0^{\beta} d\tau d\tau' \sum_{\sigma} c^*_{\sigma}(\tau)\mathcal{G}_0^{-1}(\tau - \tau')c_{\sigma}(\tau') + \int_0^{\beta} d\tau\, U n_{\uparrow}(\tau) n_{\downarrow}(\tau), \tag{2.126}$$

where $c^*_{\sigma}(\tau)$ and $c_{\sigma}(\tau)$ are Grassmann variables, c^* and c denote sets of the Grassmann variables $c^* = \{c^*_{\uparrow}(\tau), c^*_{\downarrow}(\tau)\}$, $c = \{c_{\uparrow}(\tau), c_{\downarrow}(\tau)\}$, β is the inverse temperature, and $\mathcal{G}_0(\tau - \tau')$ is the "bare" Green's function obtained by integrating out the bath sites. They showed that the impurity model gives the exact self-energy for the Hubbard model in infinite dimensions provided that $\mathcal{G}_0$ satisfies the following self-consistent conditions:

$$\begin{cases} \Sigma(i\omega_n) = \left[\mathcal{G}_0(i\omega_n)\right]^{-1} - \left[G(i\omega_n)\right]^{-1}, & (2.127) \\ \left[\mathcal{G}_0(i\omega_n)\right]^{-1} = \left\{\tilde{D}\left[i\omega_n + \mu - \Sigma(i\omega_n)\right]\right\}^{-1} + \Sigma(i\omega_n). & (2.128) \end{cases}$$

Here, $G(i\omega_n)$ is the Fourier transform of the impurity-site Green's function calculated from the action S_{imp}, μ is the chemical potential, and $\tilde{D}(\zeta)$ is the Hilbert transform

$$\tilde{D}(\zeta) = \int_{-\infty}^{\infty} d\varepsilon \frac{D(\varepsilon)}{\zeta - \varepsilon} = \frac{1}{N_{\mathbf{k}}} \sum_{\mathbf{k}} \frac{1}{\zeta - \varepsilon_{\mathbf{k}}} \tag{2.129}$$

with the noninteracting density of states of the $d = \infty$ tight-binding model $D(\varepsilon)$, the eigenenergy of the noninteracting Hamiltonian $\varepsilon_{\mathbf{k}}$ and the number of $\mathbf{k}$ points $N_{\mathbf{k}}$. Since the single-site Anderson impurity model can be solved by numerically exact methods, such as the quantum Monte Carlo method, we can simulate the exact solution for the Hubbard model in infinite dimensions through the mapping.

2.3.1.2 Mott Transition: DMFT Description

One of the most remarkable successes of the DMFT is the unified description of the Mott metal-insulator transition [4, 64] in infinite dimensions. Historically, the Mott transition had been considered to occur due to the opening/closure of the gap between the upper and lower Hubbard bands (Hubbard's scenario [65]), or due to the divergence of the quasiparticle effective mass (Brinkman-Rice's scenario [66]). The DMFT calculation suggested that, at zero temperature $T = 0$, the transition from a paramagnetic metal to a paramagnetic insulator is characterized by the continuous disappearance of the quasiparticle weight Z [60] (see Fig. 2.2), which is consistent with Brinkman-Rice picture [66]. In the metal side, there exists a low-energy coherence peak understood as the Kondo resonance peak and its weight ($=Z$) gradually decreases as U increases. The rest of the spectral weight ($=1 - Z$) is transferred to the incoherent part and form the upper and lower Hubbard bands (Hubbard picture). Thus the spectral functions have three-peak structure (Fig. 2.2, $U < U_c$). In the insulating side, the coherence peak disappears and the spectrum consists of two broad peaks of the upper and lower Hubbard bands (Fig. 2.2, $U > U_c$). While the metallic

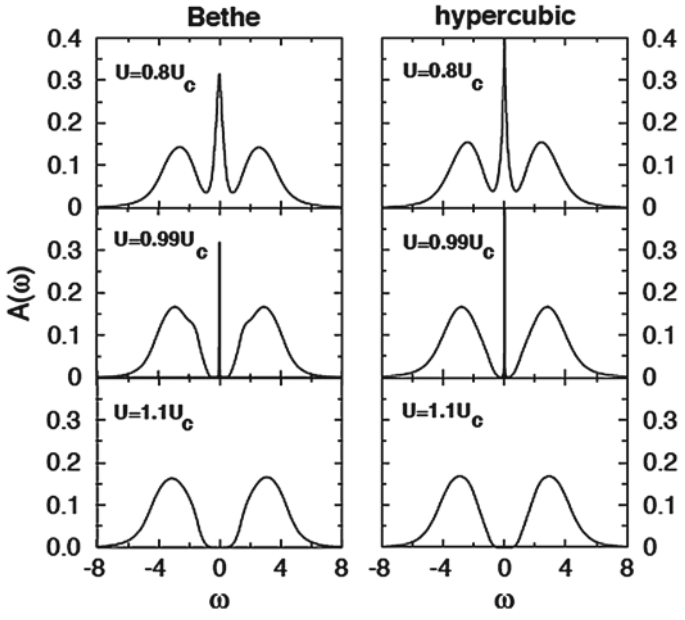

Fig. 2.2 DMFT + NRG results for spectral functions near Mott transition at $T = 0$ for half-filled single-orbital Hubbard model. The calculations were done for both the Bethe and hypercubic lattices. Effective bandwidth $W = 4\left[\int d\varepsilon D(\varepsilon)\varepsilon^2\right]^{\frac{1}{2}}$ was set to be $W = 4$ for both cases. The Mott transition occurs at $U_c = 1.47W$ and $U_c = 1.45W$ for the Bethe and the hypercubic lattices, respectively. Reprinted with permission from Bulla, Ref. [60]. Copyright 1999 by the American Physical Society

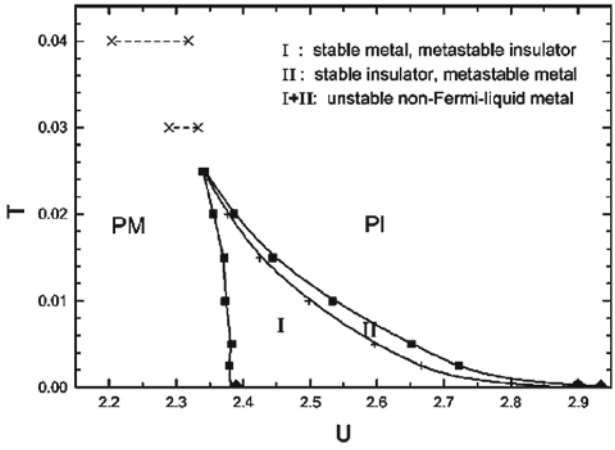

Fig. 2.3 DMFT + ED results for phase diagram of half-filled single-orbital Hubbard model defined on infinite-dimensional Bethe lattice. PM and PI denote the paramagnetic metal and the paramagnetic insulator, respectively. Symmetry-broken phases are not considered. The bandwidth W is set to be $W = 2$. The *squares* (■) and *crosses* (+) indicate the boundaries of the coexistence region $U_{c1}(T)$, $U_{c2}(T)$, and the first-order transition line $U_c(T)$, respectively. Above the critical temperature T^*, the metal-insulator transition becomes crossover. The crossover region is depicted as *dashed lines* between × symbols. At $T = 0$, the results obtained by the projective self-consistent approach [61] (circle, located at $U \sim 2.9$) and the DMFT + NRG [60, 62] (*diamonds*) are shown. Reprinted with permission from Tong et al., Ref. [63]. Copyright 2001 by the American Physical Society

state is stable below U_c ($U_c \sim 1.5W$) at $T = 0$,[5] the metastable insulating solution exists in the finite region $U_{c1} < U < U_c$ ($U_{c1} \sim 1.2W$), i.e., the metallic and insulation solutions coexist in the range $U_{c1} < U < U_c$. The coexistence is also observed at finite temperature in the range $U_{c1}(T) < U < U_{c2}(T)$ (see Fig. 2.3 for the $T - U$ phase diagram [63]). The region $U_{c2}(T) - U_{c1}(T)$ gradually shrinks as the increase of the temperature and eventually $U_{c1}(T)$ and $U_{c2}(T)$ merge at the critical end point. The metal-insulator transition becomes crossover above the critical temperature T^*. Below T^*, the Mott transition is of the first order. The first order transition line $U_c(T)$ is located in the range $U_{c1}(T) < U < U_{c2}(T)$ at $0 < T < T^*$ and it finally coincides with U_{c2} at $T = 0$, i.e., $U_{c2}(T = 0) = U_c(T = 0)$ [63].

2.3.1.3 Flow of Calculation

The above-described DMFT procedure in the infinite dimensions can also be applied to the Hubbard model in finite dimensions: One just replaces the density of states of the infinite dimensional lattice to that of finite dimensional system which one wish to

[5] If we allow the long range magnetic order, the antiferromagnetically ordered phase occupies the wide region in the T-U phase diagram at $T = 0$.

analyze. In this case, the DMFT becomes an approximation in which the self-energy is assumed to be local. Furthermore, the extension to the multi-orbital Hubbard model is also straightforward. Below, we describe the DMFT self-consistent scheme for the multi-orbital Hubbard model in finite dimensions (Bold symbols denote matrices with respect to orbital indices).

1. Prepare an initial self-energy $\mathbf{\Sigma}(i\omega_n)$.
2. Calculate the onsite Green's function using $\mathbf{\Sigma}(i\omega_n)$

$$\mathbf{G}_{\rm loc}(i\omega_n) = \frac{1}{N_{\mathbf{k}}} \sum_{\mathbf{k}} \Big[(i\omega_n + \mu)\mathbf{1} - \boldsymbol{\mathcal{H}}_0(\mathbf{k}) - \mathbf{\Sigma}(i\omega_n) \Big]^{-1}. \tag{2.130}$$

   Here, $N_{\mathbf{k}}$ is the number of $\mathbf{k}$ point in the Brillouin zone, and $\boldsymbol{\mathcal{H}}_0(\mathbf{k})$ is the matrix of the one-body part of the Hamiltonian.
3. Calculate $\boldsymbol{\mathcal{G}}_0(i\omega_n)$ via $\boldsymbol{\mathcal{G}}_0(i\omega_n) = \big[\mathbf{G}^{-1}_{\rm loc}(i\omega_n) + \mathbf{\Sigma}(i\omega_n)\big]^{-1}$.
4. Calculate the Green's function of the impurity problem $\mathbf{G}_{\rm imp}(i\omega_n)$ from the action

$$\begin{aligned} S_{\rm imp}\big[c^*, c, \boldsymbol{\mathcal{G}}_0^{-1}\big] = &- \int_0^\beta d\tau d\tau' \sum_{lm\sigma} c^*_{l\sigma}(\tau) \big[\boldsymbol{\mathcal{G}}_0^{-1}(\tau - \tau')\big]_{lm} c_{m\sigma}(\tau') \\ &+ \int_0^\beta d\tau \sum_{lmno} \sum_{\sigma\sigma'} U_{lmno} c^*_{l\sigma}(\tau) c^*_{m\sigma'}(\tau) c_{n\sigma'}(\tau) c_{o\sigma}(\tau). \end{aligned} \tag{2.131}$$

5. Calculate a new self-energy $\mathbf{\Sigma}_{\rm new}(i\omega_n)$ via $\mathbf{\Sigma}_{\rm new}(i\omega_n) = \boldsymbol{\mathcal{G}}_0^{-1}(i\omega_n) - \mathbf{G}^{-1}_{\rm imp}(i\omega_n)$.
6. Go back to the step 2 with $\mathbf{\Sigma}(i\omega_n) = \mathbf{\Sigma}_{\rm new}(i\omega_n)$ until the new self-energy $\mathbf{\Sigma}_{\rm new}(i\omega_n)$ converges to the old one, $\mathbf{\Sigma}(i\omega_n)$. Note that the equality $\mathbf{G}_{\rm loc}(i\omega_n) = \mathbf{G}_{\rm imp}(i\omega_n)$ holds when the convergence is achieved.

2.3.2 *Extended Dynamical Mean-Field Theory*

2.3.2.1 Formulation

The extended DMFT takes into account the effects of the dynamical screening of the non-local interactions beyond the original DMFT [35, 36, 67–70]. In order to understand the essence of the formulation of the extended DMFT, let us consider the single-orbital extended Hubbard model for simplicity. The extension to the multi-orbital case is again straightforward. The grand canonical Hamiltonian is given by

$$\hat{\mathcal{H}} = -\sum_{ij\sigma} t_{ij} \hat{c}^\dagger_{i\sigma} \hat{c}_{j\sigma} + \sum_i U \hat{n}_{i\uparrow} \hat{n}_{i\downarrow} + \frac{1}{2} \sum_{ij} V_{ij} \hat{N}_i \hat{N}_j - \mu \sum_i \hat{N}_i. \tag{2.132}$$

Here, V_{ij} denotes the non-local Coulomb interaction and $\hat{N}_i = \hat{n}_{i\uparrow} + \hat{n}_{1\downarrow}$. By defining $\hat{\tilde{\mathcal{O}}} = \hat{\mathcal{O}} - \langle \hat{\mathcal{O}} \rangle$, the Hamiltonian is rewritten, except a trivial constant shift, as

$$\hat{\mathcal{H}} = -\sum_{ij\sigma} t_{ij} \hat{c}^{\dagger}_{i\sigma} \hat{c}_{j\sigma} + \sum_{i} U \hat{\tilde{n}}_{i\uparrow} \hat{\tilde{n}}_{i\downarrow} + \frac{1}{2} \sum_{ij} V_{ij} \hat{\tilde{N}}_i \hat{\tilde{N}}_j - \sum_{i} \tilde{\mu}_{i\sigma} \hat{N}_i, \quad (2.133)$$

where $\tilde{\mu}_{i\sigma} = \mu - U\langle \hat{n}_{i\bar{\sigma}} \rangle - \sum_j V_{ij} \langle \hat{N}_i \rangle$ is a shifted effective chemical potential. If we assume a half-filled homogeneous system without spin polarization, i.e., $\langle n_{i\uparrow} \rangle = \langle n_{i\downarrow} \rangle = 1/2$ for every site, the Hamiltonian is further recast into

$$\hat{\mathcal{H}} = -\sum_{ij\sigma} t_{ij} \hat{c}^{\dagger}_{i\sigma} \hat{c}_{j\sigma} + \sum_{i} U \hat{\tilde{n}}_{i\uparrow} \hat{\tilde{n}}_{i\downarrow} + \frac{1}{2} \sum_{ij} V_{ij} \hat{\tilde{N}}_i \hat{\tilde{N}}_j - \tilde{\mu} \sum_{i} \hat{N}_i, \quad (2.134)$$

with $\tilde{\mu} = \mu - U/2 - \sum_j V_{0j}$. The action of the lattice problem in the coherent-state path integral formalism [8] is given by

$$S[c^*_i, c_i] = \int_0^\beta d\tau \left\{ \sum_{i\sigma} c^*_{i\sigma}(\tau) \left[\frac{\partial}{\partial \tau} - \tilde{\mu} \right] c_{i\sigma}(\tau) + \mathcal{H}[c^*_i, c_i] \right\} \quad (2.135)$$

$$= \int_0^\beta d\tau \left\{ -\sum_{ij\sigma} c^*_{i\sigma}(\tau) \left[\tilde{G}_0^{-1} \right]_{ij} c_{j\sigma}(\tau) + U \sum_i \tilde{n}_{i\uparrow}(\tau) \tilde{n}_{i\downarrow}(\tau) + \frac{1}{2} \sum_{ij} V_{ij} \tilde{N}_i(\tau) \tilde{N}_j(\tau) \right\}, \quad (2.136)$$

where $c^*_{i\sigma}$ and $c_{i\sigma}$ denote the Grassmann variables corresponding to the creation operator $\hat{c}^{\dagger}_{i\sigma}$ and the annihilation operator $\hat{c}_{i\sigma}$, respectively, $c^*_i = \{c^*_{i\sigma}(\tau)\}$, $c_i = \{c_{i\sigma}(\tau)\}$, $\left[\tilde{G}_0^{-1}\right]_{ij} = (-\partial_\tau + \tilde{\mu})\ \delta_{ij} + t_{ij}$, $\tilde{n}_{i\sigma} = c^*_{i\sigma} c_{i\sigma} - 1/2$, and $\tilde{N}_i = \tilde{n}_{i\uparrow} + \tilde{n}_{i\downarrow}$. From the action, the partition function $Z = \mathrm{Tr}\, e^{-\beta \hat{\mathcal{H}}}$ is calculated as

$$Z = \int \prod_{i\sigma} \mathcal{D}[c^*_{i\sigma}(\tau)] \mathcal{D}[c_{i\sigma}(\tau)]\ e^{-S[c^*_i, c_i]}. \quad (2.137)$$

Now, we apply the Hubbard-Stratonovich transformation [71, 72] to decouple the nonlocal interaction part[6]

[6]There is another formulation of the extended DMFT, in which the Hubbard-Stratonovich transformation is applied to both the local and non-local interactions [69, 70].

$$\frac{1}{2}\sum_{ij} V_{ij}\tilde{N}_i(\tau)\tilde{N}_j(\tau) = \frac{1}{2}\sum_{ij}\tilde{N}_i(\tau)[V-\lambda I]_{ij}\tilde{N}_j(\tau) + \frac{1}{2}\lambda\tilde{N}_i(\tau)\tilde{N}_i(\tau)$$
$$= -\frac{1}{2}\sum_{ij}\tilde{N}_i(\tau)[\lambda I - V]_{ij}\tilde{N}_j(\tau) + \lambda\tilde{n}_{i\uparrow}(\tau)\tilde{n}_{i\downarrow}(\tau) + \frac{\lambda}{4} \tag{2.138}$$

where we define a matrix V with the elements $[V]_{ij} = V_{ij}$ and introduce a shift $-\lambda I$ ($\lambda > 0$) with the identity matrix I to make the matrix $\lambda I - V$ positive definite. The Hubbard-Stratonovich transformation is based on the following identity:

$$\exp\left(\frac{1}{2}\sum_{i,j=1}^{M} x_i A_{ij} x_j\right) = \int_{-\infty}^{\infty} \frac{dy_1 \ldots dy_M}{\sqrt{(2\pi)^M \det A}} \exp\left(-\frac{1}{2}\sum_{i,j=1}^{M} y_i \left[A^{-1}\right]_{ij} y_j \mp \sum_{i=1}^{M} x_i y_i\right) \tag{2.139}$$

with a real symmetric positive-definite $M \times M$ matrix A and real variables $\{x_i, y_i\}$. Hereafter, we will choose $-$ sign for $\mp\sum_{i=1}^{M} x_i y_i$ term. By identifying A with $V' \equiv \lambda I - V$, x_i with $\tilde{N}_i(\tau)$, and y_i with an auxiliary boson field $\phi_i'(\tau)$ at each time slice,[7] the partition function is recast, with neglecting a trivial constant factor coming from $\lambda/4$ term in Eq. (2.138), as

$$Z = \int \prod_{i\sigma} \mathcal{D}\left[c_{i\sigma}^*(\tau)\right]\mathcal{D}\left[c_{i\sigma}(\tau)\right]\mathcal{D}\left[\phi_i'(\tau)\right] e^{-S'\left[c_i^*,\, c_i,\, \phi_i'\right]} \tag{2.140}$$

where the new action S' is given by

$$S'\left[c_i^*, c_i, \phi_i'\right] = \int_0^\beta d\tau \left\{-\sum_{ij\sigma} c_{i\sigma}^*(\tau)[\tilde{G}_0^{-1}]_{ij} c_{j\sigma}(\tau) + (U+\lambda)\sum_i \tilde{n}_{i\uparrow}(\tau)\tilde{n}_{i\downarrow}(\tau)\right.$$
$$\left. + \sum_i \phi_i'(\tau)\tilde{N}_i(\tau) + \frac{1}{2}\sum_{ij}\phi_i'(\tau)[V'^{-1}]_{ij}\phi_j'(\tau)\right\} \tag{2.141}$$

with ϕ_i' denoting a set of the auxiliary boson fields $\phi_i' = \left\{\phi_i'(\tau)\right\}$. The impurity site action can be constructed by taking one site (0th site) and integrating out all the other sites in Eq. (2.141) and taking the limit of $d = \infty$. In the limit of $d \to \infty$, the hopping term should be scaled as $t_{ij} \sim d^{-||i-j||/2}$ with $||i-j||$ being a "distance" between site i and site j, which takes some integer number (e.g., if sites i and j are the nearest neighbor, $||i-j|| = 1$). As for the Coulomb interaction part, to avoid the divergence of the Hartree contribution from V_{ij} terms, V_{ij} has to be scaled as

[7] In the coherent-state path integral formalism, the coherent states, the eigenstates of the annihilation operators, are used as the basis. Since the eigenvalues of the boson operators, which are constructed to be Hermitian, are real numbers, we can treat the operators as if they were just real numbers in this formalism.

$V_{ij} \sim d^{-||i-j||}$ [55]. In this case, it was shown that, among all the diagrams involving the non-local Coulomb interactions, only the Hartree-type diagrams survive at $d = \infty$, i.e., the off-site Coulomb interactions become static and trivial. However, if we only consider the dynamical part of the density (the difference from the thermal average) and the homogeneous systems, we can introduce another scaling, namely $V_{ij} \sim d^{-||i-j||/2}$ [36]. The new scaling, which is employed in the extended DMFT, allows us to take into account the dynamical screening effects coming from the non-local Coulomb interactions by absorbing the static Hartree contributions into the chemical potential. Then, the impurity model action within the extended DMFT formalism is given by (we omit the site index 0 for simplicity)

$$\begin{aligned} S'_{\mathrm{imp}}\left[c^*, c, \phi', \mathcal{G}_0^{-1}, {\mathcal{D}'_0}^{-1}\right] = & -\int_0^\beta d\tau d\tau' \sum_\sigma c_\sigma^*(\tau)\mathcal{G}_0^{-1}(\tau-\tau')c_\sigma(\tau') \\ & + \int_0^\beta d\tau\,(U+\lambda)\tilde{n}_\uparrow(\tau)\tilde{n}_\downarrow(\tau) + \int_0^\beta d\tau\,\phi'(\tau)\tilde{N}(\tau) \\ & - \frac{1}{2}\int_0^\beta d\tau d\tau' \phi'(\tau){\mathcal{D}'_0}^{-1}(\tau-\tau')\phi'(\tau') \end{aligned} \tag{2.142}$$

with self-consistent conditions:

$$\begin{cases} \Sigma(i\omega_n) = \mathcal{G}_0^{-1}(i\omega_n) - G^{-1}(i\omega_n), & (2.143) \\ \mathcal{G}_0^{-1}(i\omega_n) = \left\{ \dfrac{1}{N_{\mathbf{k}}} \displaystyle\sum_{\mathbf{k}} \frac{1}{i\omega_n + \tilde{\mu} - \varepsilon_{\mathbf{k}} - \Sigma(i\omega_n)} \right\}^{-1} + \Sigma(i\omega_n) & (2.144) \end{cases}$$

and

$$\begin{cases} \Pi'(i\nu_n) = {\mathcal{D}'_0}^{-1}(i\nu_n) - {D'}^{-1}(i\nu_n), & (2.145) \\ {\mathcal{D}'_0}^{-1}(i\nu_n) = \left\{ -\dfrac{1}{N_{\mathbf{k}}} \displaystyle\sum_{\mathbf{k}} \frac{1}{{V'_{\mathbf{k}}}^{-1} + \Pi'(i\nu_n)} \right\}^{-1} + \Pi'(i\nu_n). & (2.146) \end{cases}$$

Here, $G(i\omega_n)$ and $D'(i\nu_n)$ are the Fourier transform of the impurity site Green's function of the electrons $G(\tau-\tau') = -\langle \mathcal{T}\hat{c}(\tau)\hat{c}^\dagger(\tau')\rangle_{S'_{\mathrm{imp}}}$ and the auxiliary bosons $D'(\tau-\tau') = -\langle \mathcal{T}\hat{\phi}'(\tau)\hat{\phi}'(\tau')\rangle_{S'_{\mathrm{imp}}}$, respectively. $\varepsilon_{\mathbf{k}}$ and $V'_{\mathbf{k}}$ are the Fourier transform of $-t_{ij}$ and $\lambda - V_{ij}$, respectively. In this formulation, the effects of the off-site interactions are partially taken into account through the processes which start and end at the site 0. However, the processes which end at a site different from the initial site are neglected. Then, the self-energy obtained by the extended DMFT calculation is local as in the case of the DMFT.

In the following, we show that λ, which was originally introduced to decouple the non-local Coulomb interaction terms, is not necessary any more. Performing the integral over the bosonic field in the equation (we assume that the matrix $(-{\mathcal{D}'_0}^{-1})$ is positive definite, for which we will give a proof below)

$$Z_{\rm imp} = \int \prod_{\sigma} \mathcal{D}\big[c^*_\sigma(\tau)\big]\mathcal{D}\big[c_\sigma(\tau)\big]\mathcal{D}\big[\phi'(\tau)\big] \exp\Big(-S'_{\rm imp}\big[c^*, c, \phi', \mathcal{G}_0^{-1}, {\mathcal{D}'_0}^{-1}\big]\Big), \tag{2.147}$$

one gets

$$Z_{\rm imp} = \left\{ \int \prod_{\sigma} \mathcal{D}\big[c^*_\sigma(\tau)\big]\mathcal{D}\big[c_\sigma(\tau)\big] \exp\Big(-S'_{\rm imp}\big[c^*, c, \mathcal{G}_0^{-1}, \mathcal{D}'_0\big]\Big) \right\} \times (\text{const.}) \tag{2.148}$$

with

$$\begin{aligned} S'_{\rm imp}\big[c^*, c, \mathcal{G}_0^{-1}, \mathcal{D}'_0\big] = &- \int_0^\beta d\tau d\tau' \sum_\sigma c^*_\sigma(\tau)\mathcal{G}_0^{-1}(\tau-\tau')c_\sigma(\tau') + \int_0^\beta d\tau\, (U+\lambda)\tilde{n}_\uparrow(\tau)\tilde{n}_\downarrow(\tau) \\ &+ \frac{1}{2}\int_0^\beta d\tau d\tau' \tilde{N}(\tau)\mathcal{D}'_0(\tau-\tau')\tilde{N}(\tau'). \end{aligned} \tag{2.149}$$

Here, we note that the eigenvalues of the $\mathcal{D}'_0$ matrix $\big\{\mathcal{D}'_0(i\nu_n)\big\}$ satisfy the condition $\mathcal{D}'_0(i\nu_n) < -\lambda$, which can be shown as follows: $\mathcal{D}'_0(i\nu_n)$ calculated via Eq. (2.146) satisfies the inequality $\mathcal{D}'_0(i\nu_n) < -\lambda$ when $-\frac{1}{\max\{V'_k\}} < \Pi'(i\nu_n) < 0$. Generally, the auxiliary-boson self-energy $\Pi'(i\nu_n)$ in Eqs. (2.145) and (2.146) is negative. Within the extended DMFT, $|\Pi'(i\nu_n)| > \frac{1}{\max\{V'_k\}}$ is the criteria for instability towards charge ordering. Therefore, if the non-local Coulomb interaction is not strong enough to give the instability, we can expect $-\frac{1}{\max\{V'_k\}} < \Pi'(i\nu_n) < 0$ and thus $\mathcal{D}'_0(i\nu_n) < -\lambda$. This fact allows us to introduce a new Weiss function $\mathcal{D}_0(i\nu_n) = \mathcal{D}'_0(i\nu_n) + \lambda$. We rewrite Eq. (2.149) with $\mathcal{D}_0$ with neglecting a trivial constant shift:

$$\begin{aligned} S_{\rm imp}\big[c^*, c, \mathcal{G}_0^{-1}, \mathcal{D}_0\big] = &- \int_0^\beta d\tau d\tau' \sum_\sigma c^*_\sigma(\tau)\mathcal{G}_0^{-1}(\tau-\tau')c_\sigma(\tau') + \int_0^\beta d\tau\, U\tilde{n}_\uparrow(\tau)\tilde{n}_\downarrow(\tau) \\ &+ \frac{1}{2}\int_0^\beta d\tau d\tau' \tilde{N}(\tau)\mathcal{D}_0(\tau-\tau')\tilde{N}(\tau'). \end{aligned} \tag{2.150}$$

Since the $(-\mathcal{D}_0)$ matrix is positive-definite, we can apply the Hubbard-Stratonovich decomposition [71, 72] to $\frac{1}{2}\int_0^\beta d\tau d\tau' \tilde{N}(\tau)\mathcal{D}_0(\tau-\tau')\tilde{N}(\tau')$ term, which yields the modified impurity-site action:

$$\begin{aligned} S_{\rm imp}\big[c^*, c, \phi, \mathcal{G}_0^{-1}, \mathcal{D}_0^{-1}\big] = &- \int_0^\beta d\tau d\tau' \sum_\sigma c^*_\sigma(\tau)\mathcal{G}_0^{-1}(\tau-\tau')c_\sigma(\tau') + \int_0^\beta d\tau\, U\tilde{n}_\uparrow(\tau)\tilde{n}_\downarrow(\tau) \\ &+ \int_0^\beta d\tau\, \phi(\tau)\tilde{N}(\tau) - \frac{1}{2}\int_0^\beta d\tau d\tau' \phi(\tau)\mathcal{D}_0^{-1}(\tau-\tau')\phi(\tau'), \end{aligned} \tag{2.151}$$

where we introduce a set of new auxiliary boson fields $\{\phi(\tau)\}$. The old and new actions give the same electronic self-energy and Green's function, since the actions after the integral over the boson fields agree with each other except a trivial constant shift. On the other hand, the quantities related to the auxiliary boson fields, which are irrelevant to the physical observables, may change [67]. The new self-consistent conditions for the bosonic part read

$$\begin{cases} \Pi(i\nu_n) = \mathcal{D}_0^{-1}(i\nu_n) - D^{-1}(i\nu_n), & (2.152) \\ \mathcal{D}_0^{-1}(i\nu_n) = \left\{ \dfrac{1}{N_{\mathbf{k}}} \displaystyle\sum_{\mathbf{k}} \frac{1}{{V_{\mathbf{k}}}^{-1} - \Pi(i\nu_n)} \right\}^{-1} + \Pi(i\nu_n). & (2.153) \end{cases}$$

Here, $D(i\nu_n)$ is the impurity site Green's function of the auxiliary bosons on the Matsubara axis, and $V_{\mathbf{k}}$ is the Fourier transform of V_{ij}. The self-consistent equations for the electrons [Eqs. (2.145) and (2.146)] are unchanged. Note that, now the λ parameter completely disappears from the formulas of the extended DMFT.

Finally, we briefly comment on how effective Coulomb interaction between the impurity-site electrons is modified due to the presence of non-local Coulomb interactions. The expression in Eq. (2.150) allows us to interpret $U + \mathcal{D}_0(i\nu_n)$ as the effective Coulomb interaction between the impurity-site electrons. The Weiss function $\mathcal{D}_0(i\nu_n)$ generally takes negative value. In high-frequency limit, it approaches zero since $\Pi(i\nu_n) \to 0$ as $|\nu_n| \to \infty$. It means that the non-local Coulomb interaction brings about dynamical screening of the onsite Coulomb interaction: the electrons feel a screened Coulomb interaction at low-frequencies, while they feel the bare Coulomb interaction ($=U$) in the high-frequency limit.

2.3.2.2 Flow of Extended DMFT Calculation

Here, we describe the self-consistent procedure of the extended DMFT in the case of multi-orbital Hubbard model with the Hamiltonian,

$$\hat{\mathcal{H}} = \underbrace{-\sum_{ijlm\sigma} t_{il,jm} \hat{c}_{il}^{\sigma\dagger} \hat{c}_{jm}^{\sigma}}_{=\hat{\mathcal{H}}_0} + \sum_{i\sigma\sigma'} \sum_{lmno} U_{lmno} \hat{c}_{il}^{\sigma\dagger} \hat{c}_{im}^{\sigma'\dagger} \hat{c}_{in}^{\sigma'} \hat{c}_{io}^{\sigma} + \frac{1}{2} \sum_{ij} V_{ij} \hat{\tilde{N}}_i \hat{\tilde{N}}_j - \mu \sum_i \hat{N}_i, \tag{2.154}$$

where l, m, n, and o denote orbital indices, $\hat{N}_i = \sum_l \hat{n}_{il} = \sum_{l\sigma} \hat{c}_{il}^{\sigma\dagger} \hat{c}_{il}^{\sigma}$. Since the orbital dependence of the off-site Coulomb interactions is usually small, we ignore it. Then, the auxiliary boson will couple to the total density of each site. In the following, the bold symbols denote matrices with respect to orbital indices.

1. Prepare initial self-energies, $\mathbf{\Sigma}(i\omega_n)$ and $\Pi(i\nu_n)$.
2. Calculate the onsite Green's function, $\mathbf{G}_{\mathrm{loc}}(i\omega_n)$ and $D_{\mathrm{loc}}(i\nu_n)$, via

$$\mathbf{G}_{\rm loc}(i\omega_n) = \frac{1}{N_{\mathbf{k}}}\sum_{\mathbf{k}}\Big[\big(i\omega_n+\mu\big)\mathbf{1} - \boldsymbol{\mathcal{H}}_0(\mathbf{k}) - \boldsymbol{\Sigma}(i\omega_n)\Big]^{-1} \tag{2.155}$$

with the $\boldsymbol{\mathcal{H}}_0(\mathbf{k})$ is the Fourier transform of the one-body part of the Hamiltonian and

$$D_{\rm loc}(i\nu_n) = \frac{1}{N_{\mathbf{q}}}\sum_{\mathbf{q}}\frac{1}{V_{\mathbf{q}}^{-1} - \Pi(i\nu_n)}, \tag{2.156}$$

respectively.

3. Compute the Weiss functions, $\boldsymbol{\mathcal{G}}_0(i\omega_n)$ and $\mathcal{D}_0(i\nu_n)$, via

$$\boldsymbol{\mathcal{G}}_0^{-1}(i\omega_n) = \mathbf{G}_{\rm loc}^{-1}(i\omega_n) + \boldsymbol{\Sigma}(i\omega_n) \tag{2.157}$$

and

$$\mathcal{D}_0^{-1}(i\nu_n) = D_{\rm loc}^{-1}(i\nu_n) + \Pi(i\nu_n), \tag{2.158}$$

respectively.

4. Solve the impurity problem with the action

$$\begin{aligned} S_{\rm imp}\big[c^*, c, \boldsymbol{\mathcal{G}}_0^{-1}, \mathcal{D}_0\big] = &-\int_0^\beta d\tau d\tau' \sum_{lm\sigma} c_{l\sigma}^*(\tau)\big[\boldsymbol{\mathcal{G}}_0^{-1}(\tau-\tau')\big]_{lm} c_{m\sigma}(\tau') \\ &+ \int_0^\beta d\tau \sum_{lmno}\sum_{\sigma\sigma'} U_{lmno} c_{l\sigma}^*(\tau) c_{m\sigma'}^*(\tau) c_{n\sigma'}(\tau) c_{o\sigma}(\tau) \\ &+ \frac{1}{2}\int_0^\beta d\tau d\tau' \tilde{N}(\tau)\mathcal{D}_0(\tau-\tau')\tilde{N}(\tau') \end{aligned} \tag{2.159}$$

and obtain $\mathbf{G}_{\rm imp}(i\omega_n)$. $D_{\rm imp}(i\nu_n)$ is given by

$$D_{\rm imp}(i\nu_n) = \mathcal{D}_0(i\nu_n) + \mathcal{D}_0(i\nu_n)\chi_{\rm imp}(i\nu_n)\mathcal{D}_0(i\nu_n), \tag{2.160}$$

where $\chi_{\rm imp}(i\nu_n)$ is the Fourier transform of the impurity-site charge-charge correlation function $\chi_{\rm imp}(\tau) = -\langle \mathcal{T}\hat{\tilde{N}}(\tau)\hat{\tilde{N}}(0)\rangle_{S_{\rm imp}}$.

5. Calculate new self-energies $\boldsymbol{\Sigma}_{\rm new}(i\omega_n)$ and $\Pi_{\rm new}(i\nu_n)$ via

$$\boldsymbol{\Sigma}_{\rm new}(i\omega_n) = \boldsymbol{\mathcal{G}}_0^{-1}(i\omega_n) - \mathbf{G}_{\rm imp}^{-1}(i\omega_n) \tag{2.161}$$

and

$$\Pi_{\rm new}(i\nu_n) = \mathcal{D}_0^{-1}(i\nu_n) - D_{\rm imp}^{-1}(i\nu_n), \tag{2.162}$$

respectively.

6. Iterate the procedures 2–5 until the self-energies are converged. When the convergence is achieved, the lattice onsite Green's functions and impurity site Green's functions become identical, i.e., $\mathbf{G}_{\rm loc}(i\omega_n) = \mathbf{G}_{\rm imp}(i\omega_n)$, and $D_{\rm loc}(i\nu_n) = D_{\rm imp}(i\nu_n)$.

2.3.3 *Impurity Solver: Continuous-Time Quantum Monte Carlo Method*

To perform the extended DMFT calculation, we need a solver for the impurity model. In the present study, we employ the continuous-time quantum Monte Carlo (CT-QMC) method [73]. It is free from the discretization error which exists in the Hirsch-Fye algorithm [74] and enables a numerically exact analysis. There are several types of formulation of CT-QMC to study the impurity model. The CT-INT [75, 76] and CT-AUX [77] algorithms are based on the weak-coupling expansion of the partition function. On the other hand, the CT-HYB [78] method relies on the strong coupling expansion. Thus, the computational cost of the CT-INT or the CT-AUX (CT-HYB) becomes more expensive as the increase (decrease) of correlation strength [73]. In the case of the alkali-doped fullerides, which are in the strongly correlated regime, we find that the CT-HYB method is much more efficient than the CT-INT method. Therefore we adopt the CT-HYB method, whose details are given in the following.

2.3.3.1 Multi-orbital Impurity Model with Phonon Degrees of Freedom

The Hamiltonian of the spin-unpolarized multi-orbital Anderson impurity model with SU(2)-symmetric Coulomb interactions is given by

$$\hat{\mathcal{H}} = \hat{\mathcal{H}}_{\rm bath} + \hat{\mathcal{H}}_{\rm loc} + \hat{\mathcal{H}}_{\rm hyb}. \tag{2.163}$$

Here, $\hat{\mathcal{H}}_{\rm bath}$ describes non-interacting bath sites

$$\hat{\mathcal{H}}_{\rm bath} = \sum_{p\sigma} \varepsilon_p \hat{a}^\dagger_{p\sigma} \hat{a}_{p\sigma}, \tag{2.164}$$

where ε_p is the bath site energy, and $\hat{a}^\dagger_{p\sigma}$ and $\hat{a}_{p\sigma}$ are the creation and annihilation operators for the pth bath-site electron with the spin σ, respectively. $\hat{\mathcal{H}}_{\rm loc}$ is composed of the interaction terms and the one-body part (impurity-site energy and chemical potential terms)

$$\hat{\mathcal{H}}_{\mathrm{loc}} = \sum_{l} U \left(\hat{n}_{l\uparrow} - \frac{1}{2}\right)\left(\hat{n}_{l\downarrow} - \frac{1}{2}\right) + \sum_{l<m,\sigma} U' \left(\hat{n}_{l\sigma} - \frac{1}{2}\right)\left(\hat{n}_{m\bar{\sigma}} - \frac{1}{2}\right) + \sum_{l<m,\sigma} \left(U' - J_{\mathrm{H}}\right)\left(\hat{n}_{l\sigma} - \frac{1}{2}\right)\left(\hat{n}_{m\sigma} - \frac{1}{2}\right) + \sum_{l\neq m} J_{\mathrm{H}} \hat{c}^{\dagger}_{l\uparrow}\hat{c}_{m\uparrow}\hat{c}^{\dagger}_{m\downarrow}\hat{c}_{l\downarrow} + \sum_{l\neq m} J_{\mathrm{H}} \hat{c}^{\dagger}_{l\uparrow}\hat{c}_{m\uparrow}\hat{c}^{\dagger}_{l\downarrow}\hat{c}_{m\downarrow} + \sum_{l\sigma} E_l \hat{c}^{\dagger}_{l\sigma}\hat{c}_{l\sigma} - \mu\hat{N}, \tag{2.165}$$

where U, U', and J_{H} are the intraorbital Coulomb repulsion, the interorbital Coulomb repulsion, and the Hund's coupling, respectively. E_l is the impurity-site level of l-th orbital and $\hat{N} = \sum_{l\sigma} \hat{c}^{\dagger}_{l\sigma}\hat{c}_{l\sigma}$. If the orbitals are degenerate as in the case of alkali-doped fullerides, one can set $E_1 = E_2 = \cdots = E_{N_{\mathrm{orb}}} = 0$ with N_{orb} being the number of electrons, since the impurity site energy can be absorbed into the chemical potential term. Thus, in the arguments below, we omit $\sum_{l\sigma} E_l \hat{c}^{\dagger}_{l\sigma}\hat{c}_{l\sigma}$ term. $\hat{\mathcal{H}}_{\mathrm{hyb}}$ hybridizes the bath-site and the impurity-site electrons

$$\hat{\mathcal{H}}_{\mathrm{hyb}} = \hat{\mathcal{H}}'_{\mathrm{hyb}} + \hat{\mathcal{H}}'^{\dagger}_{\mathrm{hyb}}, \tag{2.166}$$

where

$$\hat{\mathcal{H}}'_{\mathrm{hyb}} = \sum_{pl\sigma} V_{pl} \hat{a}^{\dagger}_{p\sigma}\hat{c}_{l\sigma} \tag{2.167}$$

with the amplitude of the hybridization V_{pl}. Given $\mathcal{H}_{\mathrm{bath}}$ and $\mathcal{H}_{\mathrm{hyb}}$, the hybridization function matrix $\boldsymbol{\Gamma}(i\omega_n)$ is calculated as

$$\left[\boldsymbol{\Gamma}(i\omega_n)\right]_{lm} = \Gamma_{lm}(i\omega_n) = \sum_{p} \frac{V^*_{pl} V_{pm}}{i\omega_n - \varepsilon_p}. \tag{2.168}$$

$\boldsymbol{\Gamma}(i\omega_n)$ is related with the Weiss function $\boldsymbol{\mathcal{G}}_0(i\omega_n)$ as

$$\boldsymbol{\mathcal{G}}_0(i\omega_n) = \left[(i\omega_n + \mu)\mathbf{1} - \boldsymbol{\Gamma}(i\omega_n)\right]^{-1}, \tag{2.169}$$

or

$$\boldsymbol{\Gamma}(i\omega_n) = (i\omega_n + \mu)\mathbf{1} - \boldsymbol{\mathcal{G}}_0^{-1}(i\omega_n). \tag{2.170}$$

The bath parameters V_{pl} and ε_p are determined self-consistently so as to reproduce $\boldsymbol{\mathcal{G}}_0$ at each self-consistent loop.

We furthermore take into account "phonon" degrees of freedom. In this case, the "phonons" denote both the real phonons and the auxiliary bosons introduced in the extended DMFT. Then $\hat{\mathcal{H}}_{\mathrm{loc}}$ acquires additional terms, namely, the electron-"phonon"

interactions and "phonon" one-body term[8]

$$\hat{\mathcal{H}}_{\rm loc}^{\rm phonon} = \sum_{l\nu} g_l^{\nu}\left(\hat{n}_{l\uparrow}+\hat{n}_{l\downarrow}-1\right)\left(\hat{b}_{\nu}^{\dagger}+\hat{b}_{\nu}\right) + \sum_{l<m,\sigma\nu} \lambda_{lm}^{\nu}\left(\hat{c}_{l\sigma}^{\dagger}\hat{c}_{m\sigma}+\hat{c}_{m\sigma}^{\dagger}\hat{c}_{l\sigma}\right)\left(\hat{B}_{\nu}^{\dagger}+\hat{B}_{\nu}\right) + \sum_{\nu}\omega_{\nu}\hat{b}_{\nu}^{\dagger}\hat{b}_{\nu} + \sum_{\nu}\Omega_{\nu}\hat{B}_{\nu}^{\dagger}\hat{B}_{\nu}, \tag{2.171}$$

where $\hat{b}_{\nu}^{\dagger}$ ($\hat{b}_{\nu}$) creates (annihilates) "phonons" which couple to the density of the orbitals, and $\hat{B}_{\nu}^{\dagger}$ ($\hat{B}_{\nu}$) creates (annihilates) phonons which give non-density-type couplings.[9] As we will show in the following, the density-type electron-"phonon" couplings can be efficiently treated [79, 80] by employing the Lang-Firsov transformation [81]. However, when we employ this efficient method for the density-type electron-"phonon" coupling term, the non-density-type electron-phonon coupling and the non-density-type Coulomb interactions, such as the spin-flip and pair-hopping terms, have to be treated via perturbation expansion [82]. This is because the Lang-Firsov transformation can be usefully applied only when the local Hamiltonian consists of density-density-type Coulomb interactions and density-type electron-phonon couplings. In the alkali-doped fullerides, the magnitudes of the positive exchange interaction (Coulomb interaction) and the negative exchange interaction mediated by phonons are comparable. We found that, in such a situation, the perturbative expansion of the both interactions gives a severe negative sign problem, for which we have not come up with a solution. Since the alkali-doped fullerides have rather high phonon frequencies up to ∼0.2 eV, as a starting point, we take into account the phonons which give non-density-type couplings in the anti-adiabatic limit, i.e., $\Omega_{\nu}\to\infty$ with keeping the ratio $(\lambda_{lm}^{\nu})^2/\Omega_{\nu}$ fixed. It results in instantaneous phonon-mediated interactions $(J_{\rm ph})_{lm} = -\sum_{\nu} 2(\lambda_{lm}^{\nu})^2/\Omega_{\nu}$, which do not cause the serious negative sign problem. The investigation of the effect coming from the finiteness of the phonon frequency remains as a future issue (see Sect. 5.2). The resulting Hamiltonian reads

$$\hat{\mathcal{H}}_{\rm loc}^{\rm phonon} = \sum_{l\nu} g_l^{\nu}\left(\hat{n}_{l\uparrow}+\hat{n}_{l\downarrow}-1\right)\left(\hat{b}_{\nu}^{\dagger}+\hat{b}_{\nu}\right) + \sum_{\nu}\omega_{\nu}\hat{b}_{\nu}^{\dagger}\hat{b}_{\nu} - \sum_{l<m,\sigma} J_{\rm ph}\hat{n}_{l\sigma}\hat{n}_{m\sigma} + \sum_{l\neq m} J_{\rm ph}\hat{c}_{l\uparrow}^{\dagger}\hat{c}_{m\uparrow}\hat{c}_{m\downarrow}^{\dagger}\hat{c}_{l\downarrow} + \sum_{l\neq m} J_{\rm ph}\hat{c}_{l\uparrow}^{\dagger}\hat{c}_{m\uparrow}\hat{c}_{l\downarrow}^{\dagger}\hat{c}_{m\downarrow}. \tag{2.172}$$

[8] Since we consider the low-energy Hamiltonian, the Coulomb interaction in Eq. (2.165) and the electron-phonon couplings in Eq. (2.171) should be partially screened quantities. Then, they have some frequency dependence reflecting the frequency dependence of the polarization [see Eqs. (2.114) and (2.119)]. In this section we assume them to be static since we expect this assumption is a good approximation in the case of the alkali-doped fullerides (see Appendix in Chap. 3.).

[9] The non-local Coulomb interactions with the form $V_{ij}\hat{N}_i\hat{N}_j$ only give the density-type coupling. Therefore, $\hat{B}_{\nu}^{\dagger}$ and $\hat{B}_{\nu}$ can be identified with the real-phonon operators.

Here, we assume that $J_{\rm ph}$ has no orbital-dependence, which holds for the fcc A_3C_{60} systems. With the electron contribution in Eq. (2.165) and the phonon contribution in Eq. (2.172), the local Hamiltonian to be solved by the quantum Monte Carlo method is given by

$$\hat{\mathcal{H}}_{\rm loc} = \hat{\mathcal{H}}^0_{\rm loc} + \hat{\mathcal{H}}'_{\rm loc}, \tag{2.173}$$

where $\hat{\mathcal{H}}^0_{\rm loc}$ is composed of the density-density type Coulomb interactions, the density-type electron-"phonon" coupling, the "phonon" one-body part, and the chemical potential term

$$\begin{aligned}\hat{\mathcal{H}}^0_{\rm loc} = &\sum_l U\left(\hat{n}_{l\uparrow}-\frac{1}{2}\right)\left(\hat{n}_{l\downarrow}-\frac{1}{2}\right) + \sum_{l<m,\sigma} U'\left(\hat{n}_{l\sigma}-\frac{1}{2}\right)\left(\hat{n}_{m\bar{\sigma}}-\frac{1}{2}\right)\\ &+ \sum_{l<m,\sigma}\left(U'-J_{\rm eff}\right)\left(\hat{n}_{l\sigma}-\frac{1}{2}\right)\left(\hat{n}_{m\sigma}-\frac{1}{2}\right) + \sum_{l\nu} g^\nu_l\left(\hat{n}_{l\uparrow}+\hat{n}_{l\downarrow}-1\right)\left(\hat{b}^\dagger_\nu+\hat{b}_\nu\right)\\ &+ \sum_\nu \omega_\nu \hat{b}^\dagger_\nu \hat{b}_\nu - \mu\hat{N}\end{aligned} \tag{2.174}$$

with $J_{\rm eff} \equiv J_{\rm H} + J_{\rm ph}$, and $\hat{\mathcal{H}}'_{\rm loc}$ consists of the spin-flip term $\hat{\mathcal{H}}^{\rm s.f.}_{\rm loc}$ and the pair-hopping term $\hat{\mathcal{H}}^{\rm p.h.}_{\rm loc}$

$$\hat{\mathcal{H}}'_{\rm loc} = \hat{\mathcal{H}}^{\rm s.f.}_{\rm loc} + \hat{\mathcal{H}}^{\rm p.h.}_{\rm loc} = \sum_{l\neq m} J_{\rm eff} \underbrace{\hat{c}^\dagger_{l\uparrow}\hat{c}_{m\uparrow}\hat{c}^\dagger_{m\downarrow}\hat{c}_{l\downarrow}}_{=\left[\hat{\mathcal{O}}_{\rm s.f.}\right]_{lm}} + \sum_{l\neq m} J_{\rm eff} \underbrace{\hat{c}^\dagger_{l\uparrow}\hat{c}_{m\uparrow}\hat{c}^\dagger_{l\downarrow}\hat{c}_{m\downarrow}}_{=\left[\hat{\mathcal{O}}_{\rm p.h.}\right]_{lm}}. \tag{2.175}$$

Here, the magnitudes of the spin-flip and pair-hopping interactions are the same. This equality always holds within the present model-derivation techniques treating only the charge response function. When we consider the spin and orbital degrees of freedom explicitly in the downfolding procedure, the values for the spin-flip and the pair-hopping interactions can be slightly different from each other, which might affect the superconducting instability at a quantitative level. It would be interesting to formulate a new downfolding scheme in this direction (see also Sect. 5.2).

2.3.3.2 Strong-Coupling Expansion of Partition Function

The CT-HYB relies on the perturbation expansion of $\hat{\mathcal{H}}_{\rm hyb}$. When we employ the efficient method to treat the density-type electron-"phonon" coupling, we also perform the perturbation expansion of $\hat{\mathcal{H}}'_{\rm loc}$. Now, we define the unperturbed Hamiltonian $\hat{\mathcal{H}}_0$ as $\hat{\mathcal{H}}_0 = \hat{\mathcal{H}}^0_{\rm loc} + \hat{\mathcal{H}}_{\rm bath}$. Then, the perturbation expansion of $\hat{\mathcal{H}}_{\rm hyb}$ and $\hat{\mathcal{H}}'_{\rm loc}$ leads to the following expression for the partition function:

$$
\begin{aligned}
Z = & \sum_{k_h=0}^{\infty}\sum_{k_s=0}^{\infty}\sum_{k_p=0}^{\infty}(-J_{\mathrm{eff}})^{k_s+k_p}\int_0^\beta d\tau_1\cdots\int_{\tau_{k_h-1}}^\beta d\tau_{k_h}\int_0^\beta d\tau_1'\cdots\int_{\tau_{k_h-1}'}^\beta d\tau_{k_h}'\int_0^\beta d\tau_1''\cdots\int_{\tau_{k_s-1}''}^\beta d\tau_{k_s}'' \\
& \times\int_0^\beta d\tau_1'''\cdots\int_{\tau_{k_p-1}'''}^\beta d\tau_{k_p}'''\ \mathrm{Tr}\Big[\,\mathcal{T}e^{-\beta\hat{\mathcal{H}}_0}\,\hat{\mathcal{H}}_{\mathrm{hyb}}'^{\dagger}(\tau_{k_h})\hat{\mathcal{H}}_{\mathrm{hyb}}'(\tau_{k_h}')\cdots\hat{\mathcal{H}}_{\mathrm{hyb}}'^{\dagger}(\tau_1)\hat{\mathcal{H}}_{\mathrm{hyb}}'(\tau_1') \\
& \qquad\qquad\times\ \hat{\mathcal{O}}_{\mathrm{s.f.}}(\tau_{k_s}'')\cdots\hat{\mathcal{O}}_{\mathrm{s.f.}}(\tau_1'')\,\hat{\mathcal{O}}_{\mathrm{p.h.}}(\tau_{k_p}''')\cdots\hat{\mathcal{O}}_{\mathrm{p.h.}}(\tau_1''')\,\Big] \\
= & \sum_{k_h=0}^{\infty}\sum_{k_s=0}^{\infty}\sum_{k_p=0}^{\infty}(-J_{\mathrm{eff}})^{k_s+k_p}\int_0^\beta d\tau_1\cdots\int_{\tau_{k_h-1}}^\beta d\tau_{k_h}\int_0^\beta d\tau_1'\cdots\int_{\tau_{k_h-1}'}^\beta d\tau_{k_h}'\int_0^\beta d\tau_1''\cdots\int_{\tau_{k_s-1}''}^\beta d\tau_{k_s}'' \\
& \times\int_0^\beta d\tau_1'''\cdots\int_{\tau_{k_p-1}'''}^\beta d\tau_{k_p}'''\sum_{p_1,p_1',\ldots,p_{k_h},p_{k_h}'}\sum_{l_1,l_1',\ldots,l_{k_h},l_{k_h}'}\sum_{\sigma_1,\ldots,\sigma_{k_h}}\sum_{l_1'',\ldots,l_{k_s}''}\sum_{m_1'',\ldots,m_{k_s}''}\sum_{l_1''',\ldots,l_{k_p}'''}\sum_{m_1''',\ldots,m_{k_p}'''} \\
& \times V_{p_1l_1}^*V_{p_1'l_1'}\cdots V_{p_{k_h}l_{k_h}}^*V_{p_{k_h}'l_{k_h}'}\,\mathrm{Tr}_a\Big[\,\mathcal{T}e^{-\beta\hat{\mathcal{H}}_{\mathrm{bath}}}\,\hat{a}_{p_{k_h}\sigma_{k_h}}(\tau_{k_h})\hat{a}_{p_{k_h}'\sigma_{k_h}}^{\dagger}(\tau_{k_h}')\cdots\hat{a}_{p_1\sigma_1}(\tau_1)\hat{a}_{p_1'\sigma_1}^{\dagger}(\tau_1')\,\Big] \\
& \times \mathrm{Tr}_b\mathrm{Tr}_c\Big[\,\mathcal{T}e^{-\beta\hat{\mathcal{H}}_{\mathrm{loc}}^0}\,\hat{c}_{l_{k_h}\sigma_{k_h}}^{\dagger}(\tau_{k_h})\hat{c}_{l_{k_h}'\sigma_{k_h}}(\tau_{k_h}')\cdots\hat{c}_{l_1\sigma_1}^{\dagger}(\tau_1)\hat{c}_{l_1'\sigma_1}(\tau_1')[\hat{\mathcal{O}}_{\mathrm{s.f.}}]_{l_{k_s}''m_{k_s}''}(\tau_{k_s}'')\cdots \\
& \times [\hat{\mathcal{O}}_{\mathrm{s.f.}}]_{l_1''m_1''}(\tau_1'')\,[\hat{\mathcal{O}}_{\mathrm{p.h.}}]_{l_{k_p}'''m_{k_p}'''}(\tau_{k_p}''')\cdots[\hat{\mathcal{O}}_{\mathrm{p.h.}}]_{l_1'''m_1'''}(\tau_1''')\,\Big], \qquad (2.176)
\end{aligned}
$$

where we have defined the trace over the bath-site electronic, impurity-site electronic, and impurity-site bosonic degrees of freedom as Tr_a, Tr_c, and Tr_b, respectively. To get non-zero contribution to Z, the orders of the expansion in terms of $\hat{\mathcal{H}}_{\mathrm{hyb}}'^{\dagger}$ and $\hat{\mathcal{H}}_{\mathrm{hyb}}'$ have to be the same, thus we only consider such cases in Eq. (2.176). Since bath-site electrons are noninteracting, we can easily perform the trace over bath-site degrees of freedom Tr_a, whose result is

$$
\begin{aligned}
& \frac{1}{Z_{\mathrm{bath}}}\Bigg\{\sum_{p_1,p_1',\ldots,p_{k_\sigma},p_{k_\sigma}'}V_{p_1l_1}^*V_{p_1'l_1'}\cdots V_{p_{k_\sigma}l_{k_\sigma}}^*V_{p_{k_\sigma}'l_{k_\sigma}'}\,\mathrm{Tr}_a\Big[\,\mathcal{T}e^{-\beta\hat{\mathcal{H}}_{\mathrm{bath}}} \\
& \times\ \hat{a}_{p_{k_\sigma}\sigma}(\tau_{k_\sigma})\hat{a}_{p_{k_\sigma}'\sigma}^{\dagger}(\tau_{k_\sigma}')\cdots\hat{a}_{p_1\sigma}(\tau_1)\hat{a}_{p_1'\sigma}^{\dagger}(\tau_1')\,\Big]\Bigg\} = \det A^{(\sigma)}\big[C_{\mathrm{hyb}}^{\sigma}(k_\sigma)\big] \qquad (2.177)
\end{aligned}
$$

for $\sigma=\uparrow,\downarrow$. Here, we have defined a configuration of the expansion in powers of $\hat{\mathcal{H}}_{\mathrm{hyb}}$ as

$$
C_{\mathrm{hyb}}^{\sigma}(k_\sigma)=\big\{(l_1,l_1',\tau_1,\tau_1'),(l_2,l_2',\tau_2,\tau_2'),\ldots,(l_{k_\sigma},l_{k_\sigma}',\tau_{k_\sigma},\tau_{k_\sigma}')\big\}. \qquad (2.178)
$$

Z_{bath} is the bath-site partition function

$$
Z_{\mathrm{bath}}=\mathrm{Tr}_a e^{-\beta\hat{\mathcal{H}}_{\mathrm{bath}}}=\prod_{\sigma}\prod_{p}(1+e^{-\beta\varepsilon_p}), \qquad (2.179)
$$

and $A^{(\sigma)}\left[C^{\sigma}_{\mathrm{hyb}}(k_\sigma)\right]$ is a $k_\sigma \times k_\sigma$ matrix with elements $A^{(\sigma)}_{ij}\left[C^{\sigma}_{\mathrm{hyb}}(k_\sigma)\right] = \Gamma_{l_i l'_j}(\tau_i - \tau'_j)$:

$$A^{(\sigma)}\left[C^{\sigma}_{\mathrm{hyb}}(k_\sigma)\right] = \begin{pmatrix} \Gamma_{l_1 l'_1}(\tau_1 - \tau'_1) & \Gamma_{l_1 l'_2}(\tau_1 - \tau'_2) & \cdots & \Gamma_{l_1 l'_{k_\sigma}}(\tau_1 - \tau'_{k_\sigma}) \\ \Gamma_{l_2 l'_1}(\tau_2 - \tau'_1) & \Gamma_{l_2 l'_2}(\tau_2 - \tau'_2) & \cdots & \Gamma_{l_2 l'_{k_\sigma}}(\tau_2 - \tau'_{k_\sigma}) \\ \vdots & \vdots & \ddots & \vdots \\ \Gamma_{l_{k_\sigma} l'_1}(\tau_{k_\sigma} - \tau'_1) & \Gamma_{l_{k_\sigma} l'_2}(\tau_{k_\sigma} - \tau'_2) & \cdots & \Gamma_{l_{k_\sigma} l'_{k_\sigma}}(\tau_{k_\sigma} - \tau'_{k_\sigma}) \end{pmatrix}. \tag{2.180}$$

Furthermore, if we consider a solution where the orbitals are degenerate, the Green's function becomes diagonal with respect to the orbitals and the orbital dependence vanishes, i.e., $\left[\mathbf{G}(i\omega_n)\right]_{ij} = G(i\omega_n)\delta_{ij}$. Similarly, the off-diagonal elements and the orbital dependence of other quantities such as the self-energy $\mathbf{\Sigma}(i\omega_n)$, the Weiss function $\boldsymbol{\mathcal{G}}_0$, and the hybridization function $\mathbf{\Gamma}(i\omega_n)$ vanish. Then the $A^{(\sigma)}\left[C^{\sigma}_{\mathrm{hyb}}(k_\sigma)\right]$ matrix becomes block-diagonal with respect to orbital indices. In this case, the partition function in Eq. (2.176) is simplified to

$$\begin{aligned} Z = Z_{\mathrm{bath}} & \left\{ \prod_{l\sigma} \sum_{k_{l\sigma}=0}^{\infty} \int_0^\beta d\tau_1^{(l\sigma)} \cdots \int_{\tau_{k_{l\sigma}-1}}^\beta d\tau_{k_{l\sigma}}^{(l\sigma)} \int_0^\beta d\tau_1'^{(l\sigma)} \cdots \int_{\tau'_{k_{l\sigma}-1}}^\beta d\tau_{k_{l\sigma}}'^{(l\sigma)} \right\} \\ & \times \sum_{k_s=0}^{\infty} \sum_{k_p=0}^{\infty} \int_0^\beta d\tau_1'' \cdots \int_{\tau''_{k_s-1}}^\beta d\tau''_{k_s} \int_0^\beta d\tau_1''' \cdots \int_{\tau'''_{k_p-1}}^\beta d\tau'''_{k_p} \\ & \times \sum_{l''_1,\ldots,l''_{k_s}} \sum_{m''_1,\ldots,m''_{k_s}} \sum_{l'''_1,\ldots,l'''_{k_p}} \sum_{m'''_1,\ldots,m'''_{k_p}} \left\{ \prod_{l\sigma} \det A^{(l\sigma)}\left[C^{l\sigma}_{\mathrm{hyb}}(k_{l\sigma})\right] \right\} \\ & \times (-J_{\mathrm{eff}})^{k_s+k_p} \mathrm{Tr}_b \mathrm{Tr}_c \Bigg[\mathcal{T} e^{-\beta \hat{\mathcal{H}}^0_{\mathrm{loc}}} \left\{ \prod_{l\sigma} \hat{c}^\dagger_{l\sigma}\left(\tau_{k_{l\sigma}}^{(l\sigma)}\right) \hat{c}_{l\sigma}\left(\tau_{k_{l\sigma}}'^{(l\sigma)}\right) \cdots \hat{c}^\dagger_{l\sigma}\left(\tau_1^{(l\sigma)}\right) \hat{c}_{l\sigma}\left(\tau_1'^{(l\sigma)}\right) \right\} \\ & \times \left[\hat{\mathcal{O}}_{\mathrm{s.f.}}\right]_{l''_{k_s} m''_{k_s}}(\tau''_{k_s}) \cdots \left[\hat{\mathcal{O}}_{\mathrm{s.f.}}\right]_{l''_1 m''_1}(\tau''_1) \left[\hat{\mathcal{O}}_{\mathrm{p.h.}}\right]_{l'''_{k_p} m'''_{k_p}}(\tau'''_{k_p}) \cdots \left[\hat{\mathcal{O}}_{\mathrm{p.h.}}\right]_{l'''_1 m'''_1}(\tau'''_1) \Bigg], \end{aligned} \tag{2.181}$$

where we have defined a new configuration

$$C^{l\sigma}_{\mathrm{hyb}}(k_{l\sigma}) = \left\{ \left(\tau_1^{(l\sigma)}, \tau_1'^{(l\sigma)}\right), \left(\tau_2^{(l\sigma)}, \tau_2'^{(l\sigma)}\right), \ldots, \left(\tau_{k_{l\sigma}}^{(l\sigma)}, \tau_{k_{l\sigma}}'^{(l\sigma)}\right) \right\}. \tag{2.182}$$

Now, we define a total configuration $C\left(\{k_{l\sigma}\}, k_s, k_p\right)$ as

$$C\left(\{k_{l\sigma}\}, k_s, k_p\right) = \left\{ \left\{ C^{l\sigma}_{\mathrm{hyb}}(k_{l\sigma}) \right\}, C_{\mathrm{s.f.}}(k_s), C_{\mathrm{p.h.}}(k_p) \right\} \tag{2.183}$$

with the configuration related with the spin-flip term

$$C_{\mathrm{s.f.}}(k_s) = \left\{ (l''_1, m''_1, \tau''_1), (l''_2, m''_2, \tau''_2), \ldots, (l''_{k_s}, m''_{k_s}, \tau''_{k_s}) \right\} \tag{2.184}$$

and the configuration related with the pair-hopping term

$$C_{\text{p.h.}}(k_p) = \left\{(l_1''', m_1''', \tau_1'''), (l_2''', m_2''', \tau_2'''), \ldots, (l_{k_p}''', m_{k_p}''', \tau_{k_p}''')\right\}. \tag{2.185}$$

We also define a weight related to Tr_b and Tr_c traces as

$$\begin{aligned}\mathcal{W}_{\text{loc}}\Big[C\big(\{k_{l\sigma}\}, k_s, k_p\big)\Big] = (-J_{\text{eff}})^{k_s+k_p}\text{Tr}_b\text{Tr}_c\Bigg[\mathcal{T}e^{-\beta\hat{\mathcal{H}}^0_{\text{loc}}}\Bigg\{\prod_{l\sigma}\hat{c}^\dagger_{l\sigma}\big(\tau^{(l\sigma)}_{k_{l\sigma}}\big)\hat{c}_{l\sigma}\big(\tau'^{(l\sigma)}_{k_{l\sigma}}\big)\cdots \\ \times\ \hat{c}^\dagger_{l\sigma}\big(\tau^{(l\sigma)}_1\big)\hat{c}_{l\sigma}\big(\tau'^{(l\sigma)}_1\big)\Bigg\} \\ \times\ \big[\hat{\mathcal{O}}_{\text{s.f.}}\big]_{l''_{k_s}m''_{k_s}}(\tau''_{k_s})\cdots\big[\hat{\mathcal{O}}_{\text{s.f.}}\big]_{l''_1m''_1}(\tau''_1) \\ \times\ \big[\hat{\mathcal{O}}_{\text{p.h.}}\big]_{l'''_{k_p}m'''_{k_p}}(\tau'''_{k_p})\cdots\big[\hat{\mathcal{O}}_{\text{p.h.}}\big]_{l'''_1m'''_1}(\tau'''_1)\Bigg].\end{aligned} \tag{2.186}$$

Then the partition function in Eq. (2.181) is recast into

$$\begin{aligned}\frac{Z}{Z_{\text{bath}}} = &\left\{\prod_{l\sigma}\sum_{k_{l\sigma}=0}^{\infty}\int_0^\beta d\tau_1^{(l\sigma)}\cdots\int_{\tau_{k_{l\sigma}-1}}^\beta d\tau_{k_{l\sigma}}^{(l\sigma)}\int_0^\beta d\tau_1'^{(l\sigma)}\cdots\int_{\tau'_{k_{l\sigma}-1}}^\beta d\tau_{k_{l\sigma}}'^{(l\sigma)}\right\} \\ &\times\sum_{k_s=0}^{\infty}\sum_{k_p=0}^{\infty}\int_0^\beta d\tau_1''\cdots\int_{\tau''_{k_s-1}}^\beta d\tau''_{k_s}\int_0^\beta d\tau_1'''\cdots\int_{\tau'''_{k_p-1}}^\beta d\tau'''_{k_p}\left\{\prod_{l\sigma}\det A^{(l\sigma)}\big[C^{l\sigma}_{\text{hyb}}(k_{l\sigma})\big]\right\} \\ &\times\sum_{l''_1,\ldots,l''_{k_s}}\sum_{m''_1,\ldots,m''_{k_s}}\sum_{l'''_1,\ldots,l'''_{k_p}}\sum_{m'''_1,\ldots,m'''_{k_p}}\mathcal{W}_{\text{loc}}\big[C\big(\{k_{l\sigma}\}, k_s, k_p\big)\big].\end{aligned} \tag{2.187}$$

This expression allows us to interpret $\mathcal{W}_{\text{tot}}\big[C\big(\{k_{l\sigma}\}, k_s, k_p\big)\big]$ given by

$$\begin{aligned}\mathcal{W}_{\text{tot}}\Big[C\big(\{k_{l\sigma}\}, k_s, k_p\big)\Big] = &\left\{\prod_{l\sigma}\det A^{(l\sigma)}\big[C^{l\sigma}_{\text{hyb}}(k_{l\sigma})\big]\prod_{i=1}^{k_{l\sigma}}d\tau_i^{(l\sigma)}d\tau_i'^{(l\sigma)}\right\} \\ &\times\mathcal{W}_{\text{loc}}\Big[C\big(\{k_{l\sigma}\}, k_s, k_p\big)\Big]\prod_{i''}^{k_s}d\tau_{i''}''\prod_{i'''}^{k_p}d\tau_{i'''}'''\end{aligned} \tag{2.188}$$

as the weight for the configuration $C\big(\{k_{l\sigma}\}, k_s, k_p\big)$. Based on the weight, we perform the Monte Carlo simulations using the Metropolis-Hastings algorithm [83, 84].

2.3.3.3 Calculation Details to Evaluate $\mathcal{W}_{\rm loc}\big[C\big(\{k_{l\sigma}\},k_s,k_p\big)\big]$

In order to calculate $\mathcal{W}_{\rm loc}\big[C\big(\{k_{l\sigma}\},k_s,k_p\big)\big]$, we apply the Lang-Firsov transformation [81]. Defining $\hat{X}_\nu=(\hat{b}_\nu^\dagger+\hat{b}_\nu)/\sqrt{2}$, $\hat{P}_\nu=-i(\hat{b}_\nu^\dagger-\hat{b}_\nu)/\sqrt{2}$, and $\hat{X}_l^{(0)\nu}=\sqrt{2}g_l^\nu/\omega_\nu$ $(n_{l\uparrow}+n_{l\downarrow}-1)$, we rewrite the electron-"phonon" interaction terms and "phonon" one-body terms as

$$\sum_{l\nu} g_l^\nu\big(\hat{n}_{l\uparrow}+\hat{n}_{l\downarrow}-1\big)\big(\hat{b}_\nu^\dagger+\hat{b}_\nu\big)+\sum_\nu \omega_\nu \hat{b}_\nu^\dagger\hat{b}_\nu=\sum_{l\nu}\omega_\nu \hat{X}_l^{(0)\nu}\hat{X}_\nu+\sum_\nu\frac{\omega_\nu}{2}\big(\hat{X}_\nu^2+\hat{P}_\nu^2\big). \tag{2.189}$$

The Lang-Firsov transformation [81]

$$^{\rm LF}\hat{\mathcal{O}}=\exp\left(\sum_{l\nu} i\hat{P}_\nu\hat{X}_l^{(0)\nu}\right)\hat{\mathcal{O}}\exp\left(-\sum_{l\nu} i\hat{P}_\nu\hat{X}_l^{(0)\nu}\right) \tag{2.190}$$

transforms the operators as

$$\begin{cases} ^{\rm LF}\hat{X}_\nu=\hat{X}_\nu-\sum_l \hat{X}_l^{(0)\nu}, & (2.191)\\ ^{\rm LF}\hat{P}_\nu=\hat{P}_\nu, & (2.192)\\ ^{\rm LF}\hat{c}_{l\sigma}^\dagger\equiv\hat{d}_{l\sigma}^\dagger=\exp\left[\sum_\nu\frac{g_l^\nu}{\omega_\nu}\left(\hat{b}_\nu^\dagger-\hat{b}_\nu\right)\right]\hat{c}_{l\sigma}^\dagger, & (2.193)\\ ^{\rm LF}\hat{c}_{l\sigma}\equiv\hat{d}_{l\sigma}=\exp\left[-\sum_\nu\frac{g_l^\nu}{\omega_\nu}\left(\hat{b}_\nu^\dagger-\hat{b}_\nu\right)\right]\hat{c}_{l\sigma}, & (2.194)\\ ^{\rm LF}\hat{n}_{l\sigma}=\hat{d}_{l\sigma}^\dagger\hat{d}_{l\sigma}=\hat{c}_{l\sigma}^\dagger\hat{c}_{l\sigma}=\hat{n}_{l\sigma}. & (2.195)\end{cases}$$

$\hat{d}_{l\sigma}^\dagger$ and $\hat{d}_{l\sigma}$ can be understood as the polaron operators [81], where the electronic operators ($\hat{c}_{l\sigma}^\dagger$ and $\hat{c}_{l\sigma}$) are dressed by the "phonon" factors $\Big(\hat{F}_l^s=\exp\Big[s\sum_\nu\frac{g_l^\nu}{\omega_\nu}\left(\hat{b}_\nu^\dagger-\hat{b}_\nu\right)\Big]$, $s=\pm1\Big)$. The Lang-Firsov transformation applied to $\hat{\mathcal{H}}_{\rm loc}^0$ leads to [79, 80]

$$\begin{aligned}^{\rm LF}\hat{\mathcal{H}}_{\rm loc}^0=&\sum_l U\left(\hat{n}_{l\uparrow}-\frac{1}{2}\right)\left(\hat{n}_{l\downarrow}-\frac{1}{2}\right)+\sum_{l<m,\sigma}U'\left(\hat{n}_{l\sigma}-\frac{1}{2}\right)\left(\hat{n}_{m\bar{\sigma}}-\frac{1}{2}\right)\\&+\sum_{l<m,\sigma}\left(U'-J_{\rm eff}\right)\left(\hat{n}_{l\sigma}-\frac{1}{2}\right)\left(\hat{n}_{m\sigma}-\frac{1}{2}\right)+\sum_{l\nu}\omega_\nu\hat{X}_l^{(0)\nu}\left(\hat{X}_\nu-\sum_{l'}\hat{X}_{l'}^{(0)\nu}\right)\\&+\sum_\nu\frac{\omega_\nu}{2}\left[\left(\hat{X}_\nu-\sum_l\hat{X}_{l'}^{(0)\nu}\right)^2+\hat{P}_\nu^2\right]-\mu\hat{N}\end{aligned}$$

$$= \sum_{l} U_{\mathrm{eff}} \left(\hat{n}_{l\uparrow} - \frac{1}{2}\right)\left(\hat{n}_{l\downarrow} - \frac{1}{2}\right) + \sum_{l<m,\sigma} U'_{\mathrm{eff}} \left(\hat{n}_{l\sigma} - \frac{1}{2}\right)\left(\hat{n}_{m\bar{\sigma}} - \frac{1}{2}\right)$$
$$+ \sum_{l<m,\sigma} \left(U'_{\mathrm{eff}} - J_{\mathrm{eff}}\right)\left(\hat{n}_{l\sigma} - \frac{1}{2}\right)\left(\hat{n}_{m\sigma} - \frac{1}{2}\right) + \sum_{\nu} \omega_\nu \hat{b}^\dagger_\nu \hat{b}_\nu - \mu_{\mathrm{eff}} \hat{N} + (\text{const.}). \tag{2.196}$$

A remarkable feature of the Hamiltonian after the Lang-Firsov transformation ${}^{\mathrm{LF}}\hat{\mathcal{H}}^0_{\mathrm{loc}}$ is that there are no explicit electron-"phonon" interaction terms any more, i.e., the electrons and the "phonons" are decoupled [79, 80]. The forms of the density-density type electron interaction terms are unchanged, however, the interaction strengths are modified as $U \to U_{\mathrm{eff}} = U + U_{\text{"ph"}} = U - \sum_\nu 2(g^\nu_l)^2/\omega_\nu$, and $U' \to U'_{\mathrm{eff}} = U' + U'_{\text{"ph"}} = U' - \sum_\nu 2 g^\nu_l g^\nu_m/\omega_\nu$ $(l \neq m)$. Here, we omitted the orbital indices because orbital dependences vanish in the alkali-doped fullerides. The chemical potential is also shifted as $\mu \to \mu_{\mathrm{eff}} = \mu + U_{\text{"ph"}}/2 + (N_{\mathrm{orb}} - 1)U'_{\text{"ph"}}$. For later use, we define the bosonic part of the Hamiltonian as $\hat{\mathcal{H}}^b_{\mathrm{LF}} = \sum_\nu \omega_\nu \hat{b}^\dagger_\nu \hat{b}_\nu$ and electronic part as $\hat{\mathcal{H}}^c_{\mathrm{LF}} = {}^{\mathrm{LF}}\hat{\mathcal{H}}^0_{\mathrm{loc}} - \hat{\mathcal{H}}^b_{\mathrm{LF}} - (\text{const.})$ (we ignore the constant term since it is completely irrelevant).

Since the trace does not change through the Lang-Firsov transformation, which is unitary, $\mathcal{W}_{\mathrm{loc}}\left[C\left(\{k_{l\sigma}\}, k_s, k_p\right)\right]$ can be calculated with the Hamiltonian after the transformation

$$\mathcal{W}_{\mathrm{loc}}\left[C\left(\{k_{l\sigma}\}, k_s, k_p\right)\right] = (-J_{\mathrm{eff}})^{k_s+k_p} \mathrm{Tr}_b \mathrm{Tr}_c \Bigg[\mathcal{T} e^{-\beta\left({}^{\mathrm{LF}}\hat{\mathcal{H}}^0_{\mathrm{loc}}\right)} \Bigg\{ \prod_{l\sigma} \hat{d}^\dagger_{l\sigma}\left(\tau^{(l\sigma)}_{k_{l\sigma}}\right) \hat{d}_{l\sigma}\left(\tau^{\prime(l\sigma)}_{k_{l\sigma}}\right) \cdots$$
$$\times \hat{d}^\dagger_{l\sigma}\left(\tau^{(l\sigma)}_1\right) \hat{d}_{l\sigma}\left(\tau^{\prime(l\sigma)}_1\right) \Bigg\} \left[{}^{\mathrm{LF}}\hat{\mathcal{O}}_{\mathrm{s.f.}}\right]_{l''_{k_s} m''_{k_s}} (\tau''_{k_s}) \cdots \left[{}^{\mathrm{LF}}\hat{\mathcal{O}}_{\mathrm{s.f.}}\right]_{l''_1 m''_1} (\tau''_1)$$
$$\times \left[{}^{\mathrm{LF}}\hat{\mathcal{O}}_{\mathrm{p.h.}}\right]_{l'''_{k_p} m'''_{k_p}} (\tau'''_{k_p}) \cdots \left[{}^{\mathrm{LF}}\hat{\mathcal{O}}_{\mathrm{p.h.}}\right]_{l'''_1 m'''_1} (\tau'''_1) \Bigg] \tag{2.197}$$

with $\left[{}^{\mathrm{LF}}\hat{\mathcal{O}}^{\mathrm{s.f.}}\right]_{lm} = \hat{d}^\dagger_{l\uparrow}\hat{d}_{m\uparrow}\hat{d}^\dagger_{m\downarrow}\hat{d}_{l\downarrow}$ and $\left[{}^{\mathrm{LF}}\hat{\mathcal{O}}_{\mathrm{p.h.}}\right]_{lm} = \hat{d}^\dagger_{l\uparrow}\hat{d}_{m\uparrow}\hat{d}^\dagger_{l\downarrow}\hat{d}_{m\downarrow}$. Since ${}^{\mathrm{LF}}\hat{\mathcal{H}}^0_{\mathrm{loc}}$ has no explicit electron-"phonon" coupling term, Tr_b and Tr_c can be performed individually, i.e., $\mathcal{W}_{\mathrm{loc}}\left[C\left(\{k_{l\sigma}\}, k_s, k_p\right)\right] = \mathcal{W}_b\left[C\left(\{k_{l\sigma}\}, k_s, k_p\right)\right] \times \mathcal{W}_c\left[C\left(\{k_{l\sigma}\}, k_s, k_p\right)\right]$.

Here, the "phonon" contribution $\mathcal{W}_b\left[C\left(\{k_{l\sigma}\}, k_s, k_p\right)\right]$ is given by

$$\mathcal{W}_b\left[C\left(\{k_{l\sigma}\}, k_s, k_p\right)\right] = \mathrm{Tr}_b \Bigg[\mathcal{T} e^{-\beta\hat{\mathcal{H}}^b_{\mathrm{LF}}} \Bigg\{ \prod_{l\sigma} \hat{F}^{+1}_l\left(\tau^{(l\sigma)}_{k_{l\sigma}}\right) \hat{F}^{-1}_l\left(\tau^{\prime(l\sigma)}_{k_{l\sigma}}\right) \cdots$$
$$\times \hat{F}^{+1}_l\left(\tau^{(l\sigma)}_1\right) \hat{F}^{-1}_l\left(\tau^{\prime(l\sigma)}_1\right) \Bigg\} \left[\hat{F}_{\mathrm{s.f.}}\right]_{l''_{k_s} m''_{k_s}} (\tau''_{k_s}) \cdots \left[\hat{F}_{\mathrm{s.f.}}\right]_{l''_1 m''_1} (\tau''_1)$$
$$\times \left[\hat{F}_{\mathrm{p.h.}}\right]_{l'''_{k_p} m'''_{k_p}} (\tau'''_{k_p}) \cdots \left[\hat{F}_{\mathrm{p.h.}}\right]_{l'''_1 m'''_1} (\tau'''_1) \Bigg], \tag{2.198}$$

where

$$\begin{cases} \left[\hat{F}_{\text{s.f.}}\right]_{lm}(\tau) = \hat{F}_l^{+1}(\tau+3\epsilon)\hat{F}_m^{-1}(\tau+2\epsilon)\hat{F}_m^{+1}(\tau+\epsilon)\hat{F}_l^{-1}(\tau) & (2.199) \\ \left[\hat{F}_{\text{p.h.}}\right]_{lm}(\tau) = \hat{F}_l^{+1}(\tau+3\epsilon)\hat{F}_m^{-1}(\tau+2\epsilon)\hat{F}_l^{+1}(\tau+\epsilon)\hat{F}_m^{-1}(\tau). & (2.200) \end{cases}$$

with an infinitesimal real number ϵ to define the time order within $\left[\hat{F}_{\text{s.f.}}\right]_{lm}(\tau)$ and $\left[\hat{F}_{\text{p.h.}}\right]_{lm}(\tau)$. The time ordering results in

$$\mathcal{W}_b\Big[C\big(\{k_{l\sigma}\},k_s,k_p\big)\Big] = \text{Tr}_b\Big[e^{-\beta\hat{\mathcal{H}}^b_{\text{LF}}}\hat{F}^{\tilde{s}_{k_t}}_{\tilde{l}_{k_t}}(\tilde{\tau}_{k_t})\cdots\hat{F}^{\tilde{s}_1}_{\tilde{l}_1}(\tilde{\tau}_1)\Big], \tag{2.201}$$

where k_t is the total number of the $\hat{F}$ operators $k_t = \sum_{l\sigma} 2k_{l\sigma} + 4k_s + 4k_p$, the imaginary times in Eq. (2.198) are arranged to obey the time order $0 \le \tilde{\tau}_1 < \cdots < \tilde{\tau}_{k_t} < \beta$, and $\tilde{l}_i$'s ($\tilde{s}_i$'s) are the corresponding orbital indices (signs of the phonon factors). The weight has an analytic form and thus can be easily calculated as [79, 80]

$$\mathcal{W}_b\Big[C\big(\{k_{l\sigma}\},k_s,k_p\big)\Big] = \exp\left[\sum_{k_t\ge i>j\ge 1}\tilde{s}_i\tilde{s}_j K_{\tilde{l}_i\tilde{l}_j}(\tilde{\tau}_i-\tilde{\tau}_j)\right] \tag{2.202}$$

with $K_{ll'}(\tau)$ being a function defined in the region $\tau \in [0,\beta]$:

$$\begin{cases} K_{ll'}(\tau) = K'_{ll'}(\tau) - K'_{ll}(0) & (2.203) \\ K'_{ll'}(\tau) = -\dfrac{g^\nu_l g^\nu_{l'}}{\omega_\nu^2}\dfrac{\cosh\big[(\tau-\beta/2)\omega_\nu\big]}{\sinh[\beta\omega_\nu/2]}. & (2.204) \end{cases}$$

The electronic contribution $\mathcal{W}_c\big[C\big(\{k_{l\sigma}\},k_s,k_p\big)\big]$ to the weight $\mathcal{W}_{\text{loc}}\big[C\big(\{k_{l\sigma}\},k_s,k_p\big)\big]$ is given by

$$\begin{aligned} \mathcal{W}_c\Big[C\big(\{k_{l\sigma}\},k_s,k_p\big)\Big] &= \text{Tr}_c\Big[\mathcal{T}e^{-\beta\hat{\mathcal{H}}^c_{\text{LF}}}\Big\{\prod_{l\sigma}\hat{c}^\dagger_{l\sigma}(\tau^{(l\sigma)}_{k_{l\sigma}})\hat{c}_{l\sigma}(\tau^{\prime(l\sigma)}_{k_{l\sigma}})\cdots\hat{c}^\dagger_{l\sigma}(\tau^{(l\sigma)}_1)\hat{c}_{l\sigma}(\tau^{\prime(l\sigma)}_1)\Big\} \\ &\quad\times\Big[\hat{\mathcal{O}}_{\text{s.f.}}\Big]_{l''_{k_s}m''_{k_s}}(\tau''_{k_s})\cdots\Big[\hat{\mathcal{O}}_{\text{s.f.}}\Big]_{l''_1m''_1}(\tau''_1) \\ &\quad\times\Big[\hat{\mathcal{O}}_{\text{p.h.}}\Big]_{l'''_{k_p}m'''_{k_p}}(\tau'''_{k_p})\cdots\Big[\hat{\mathcal{O}}_{\text{p.h.}}\Big]_{l'''_1m'''_1}(\tau'''_1)\Big]\times(-J_{\text{eff}})^{k_s+k_p} \\ &= (-J_{\text{eff}})^{k_s+k_p}s_{\mathcal{T}}\,\text{Tr}_c\Big[e^{-\beta\hat{\mathcal{H}}^c_{\text{LF}}}\hat{\mathcal{O}}_{k'_t}(\tilde{\tau}_{k'_t})\cdots\hat{\mathcal{O}}_1(\tilde{\tau}_1)\Big], \end{aligned} \tag{2.205}$$

where $\hat{\mathcal{O}}_i$'s take $\hat{c}^\dagger$, $\hat{c}$, $\hat{\mathcal{O}}_{\text{s.f.}}$ or $\hat{\mathcal{O}}_{\text{p.h.}}$ with appropriate orbital/spin indices, $k'_t = \sum_{l\sigma}2k_{l\sigma} + k_s + k_p$, $s_{\mathcal{T}}$ is a sign coming from the permutations of fermion operators to arrange them in the time order. The trace over fermion degrees of freedom Tr_c can be performed by using the matrix representation of the operators $[\mathcal{O}]_{ij} = \langle i|\hat{\mathcal{O}}|j\rangle$

with $|i\rangle$ and $|j\rangle$ being the eigenstates of the $\hat{\mathcal{H}}^c_{\rm LF}$ Hamiltonian, which is evaluated as

$$\mathrm{Tr}_c\left[e^{-\beta\hat{\mathcal{H}}^c_{\rm LF}}\hat{\mathcal{O}}_{k'_t}(\tilde{\tau}_{k'_t})\cdots\hat{\mathcal{O}}_1(\tilde{\tau}_1)\right] = \mathrm{Tr}\Big[H(\beta-\tilde{\tau}_{k'_t})\mathcal{O}_{k'_t}H(\tilde{\tau}_{k'_t}-\tilde{\tau}_{k'_t-1})\mathcal{O}_{k'_t-1}\cdots\mathcal{O}_1H(\tilde{\tau}_1)\Big], \tag{2.206}$$

where the elements of the $H(\tau)$ matrix are given by $\big[H(\tau)\big]_{ij} = \exp(-E_i\tau)\delta_{ij}$ with E_i's being the eigenvalues of the $\hat{\mathcal{H}}^c_{\rm LF}$ Hamiltonian [85]. The calculation of the trace can be more efficiently performed if one makes use of the conserved quantities of $\hat{\mathcal{H}}^c_{\rm LF}$ [86]. In the case of the multi-orbital Anderson impurity model, by employing the conserved-number set of total number of electrons N, z component of the total spin S_z, and the "**PS**" vector defined as $\mathbf{PS} = \big[(n_{1\uparrow}-n_{1\downarrow})^2,\ldots,(n_{N_{\rm orb}\uparrow}-n_{N_{\rm orb}\downarrow})^2\big]$, the $\mathcal{H}^c_{\rm LF}$ matrix can be block diagonalized, whose size is drastically reduced from the original size of $4^{N_{\rm orb}}$ [87]. For example, the maximum (average) block sizes are reduced to 3 (1.45), 10 (2.90), and 35 (6.92) for $N_{\rm orb} = 3$, 5, 7, respectively (the original matrix sizes are 64, 1024, and 16384, respectively) [87]. We label the blocks by α ($\alpha = 1,\ldots,N_b$ with N_b being the number of the blocks), and the αth block size is denoted as M_α. An operator $\hat{\mathcal{O}}$ acted on the states in the $\alpha_{\rm in}$th block will connect them with the states in some block, which we will denote as $\alpha_{\rm out}$th block. Then, the $\mathcal{O}$ matrix can be expressed as an $M_{\alpha_{\rm out}}\times M_{\alpha_{\rm in}}$ matrix whose elements are given by $[\mathcal{O}]_{ij} = \langle i;\alpha_{\rm out}|\hat{\mathcal{O}}|j;\alpha_{\rm in}\rangle$. We find that $\alpha_{\rm in}\neq\alpha_{\rm out}$ for $\hat{\mathcal{O}} = \hat{c}^\dagger, \hat{c}$, and $\alpha_{\rm in} = \alpha_{\rm out}$ for $\hat{\mathcal{O}} = \hat{\mathcal{O}}_{\rm s.f.}, \hat{\mathcal{O}}_{\rm p.h.}$. Now, Tr[...] can be evaluated as $\sum_\alpha \mathrm{Tr}_\alpha[\ldots]$ with Tr_α being the trace of the αth block [86, 87]. Note that, while the sequence of the matrix operations starts from the αth block and ends with the αth block, in between them, it may pass through other blocks. Since the cost of matrix operation is $O(N^3)$, the reduction of the matrix size drastically speeds up the trace calculations.

As we will show later, in the update of the configuration employed in the present study, the expansion order of the spin-flip or pair-hopping terms (k_s or k_p) is changed by one. However, if we consider e.g., a configuration where $k_{l\sigma} = 0$ for all $(l\sigma)$ channels (i.e., no hybridization vertices) and $k_s = 1$, one can easily show that the weight for the configuration is zero since the matrix representation of $\hat{\mathcal{O}}_{\rm s.f.}$ has only off-diagonal elements, which do not contribute to the trace. Therefore, if one employs the single-vertex update ($k_s \to k_s \pm 1$), the transition from $k_s = 0$ configuration to $k_s = 2$ is impossible since it has to go through $k_s = 1$ configuration, which means that the single-vertex update violates the ergodicity. The very same problem holds for pair-hopping term. To solve the problems, we introduce an auxiliary spin $s_a = \pm 1$ to add diagonal elements to the $\mathcal{O}_{\rm s.f.}$ and $\mathcal{O}_{\rm p.h.}$ matrices as

$$[\mathcal{O}_{\rm s.f.}]_{ij} \to [\mathcal{O}'_{\rm s.f.}(s_a)]_{ij} = [\mathcal{O}_{\rm s.f.}]_{ij} + s_a\gamma\delta_{ij} \tag{2.207}$$

and

$$[\mathcal{O}_{\rm p.h.}]_{ij} \to [\mathcal{O}'_{\rm p.h.}(s_a)]_{ij} = [\mathcal{O}_{\rm p.h.}]_{ij} + s_a\gamma\delta_{ij}, \tag{2.208}$$

respectively.[10] Here γ is a positive real number, for which we typically use $\gamma \sim 0.01$. If the magnitude of $J_{\rm eff}$ is very small as in the case of C_{60} superconductors, to increase the acceptance ratio, we use a slightly larger value $\gamma \sim 0.03$. Since $\mathcal{O}_{\rm s.f.} = \frac{1}{2}\sum_{s_a} \mathcal{O}'_{\rm s.f.}(s_a)$ and $\frac{1}{2}\mathcal{O}_{\rm p.h.} = \sum_{s_a} \mathcal{O}'_{\rm p.h.}(s_a)$, we can reproduce the original weight by sampling both $s_a = \pm 1$. With this trick, the $k_s = 1$ configuration or $k_p = 1$ configuration has a non-zero weight, which makes the single-vertex update to satisfy the ergodicity condition.[11] Note that the real weight for $k_s = 1$ configuration or $k_p = 1$ configuration is still zero, since (weight with $s_a = +1$) = $-$(weight with $s_a = -1$).

Based on the above considerations, we enlarge the configuration space to include the auxiliary Ising-type spins and redefine the configurations as

$$\begin{cases} C_{\rm s.f.}(k_s) \to C'_{\rm s.f.}(k_s) = \left\{(l''_1, m''_1, \tau''_1, s''_1), (l''_2, m''_2, \tau''_2, s''_2), \ldots, (l''_{k_s}, m''_{k_s}, \tau''_{k_s}, s''_{k_s})\right\} \\ C_{\rm p.h.}(k_p) \to C'_{\rm p.h.}(k_p) = \left\{(l'''_1, m'''_1, \tau'''_1, s'''_1), (l'''_2, m'''_2, \tau'''_2, s'''_2), \ldots, (l'''_{k_p}, m'''_{k_p}, \tau'''_{k_p}, s'''_{k_p})\right\}, \\ C\left(\{k_{l\sigma}\}, k_s, k_p\right) \to C'\left(\{k_{l\sigma}\}, k_s, k_p\right) = \left\{\left\{C^{l\sigma}_{\rm hyb}(k_{l\sigma})\right\}, C'_{\rm s.f.}(k_s), C'_{\rm p.h.}(k_p)\right\}, \end{cases} \quad (2.209)$$

where s''_i's and s'''_i's are the auxiliary spins. Then the weight for the $C'\left(\{k_{l\sigma}\}, k_s, k_p\right)$ configuration is given by

$$\begin{aligned} \mathcal{W}_{\rm tot}\left[C'\left(\{k_{l\sigma}\}, k_s, k_p\right)\right] = & \left\{\prod_{l\sigma} \det A^{(l\sigma)}\left[C^{l\sigma}_{\rm hyb}(k_{l\sigma})\right] \prod_{i=1}^{k_{l\sigma}} d\tau_i^{(l\sigma)} d\tau_i'^{(l\sigma)}\right\} \\ & \times \mathcal{W}_b\left[C'\left(\{k_{l\sigma}\}, k_s, k_p\right)\right] \mathcal{W}'_c\left[C'\left(\{k_{l\sigma}\}, k_s, k_p\right)\right] \prod_{i''}^{k_s} d\tau''_{i''} \prod_{i'''}^{k_p} d\tau'''_{i'''}, \end{aligned} \quad (2.210)$$

where $\det A^{(l\sigma)}$ and $\mathcal{W}_b$ are not affected by the introduction of auxiliary spins, while the method to compute the electronic contribution $\mathcal{W}'_c$ is modified as

$$\begin{aligned} \mathcal{W}'_c\left[C'\left(\{k_{l\sigma}\}, k_s, k_p\right)\right] &= \left(-\frac{J_{\rm eff}}{2}\right)^{k_s+k_p} s_{\mathcal{T}} {\rm Tr}\left[H(\beta - \tilde{\tau}_{k'_t}) \mathcal{O}_{k'_t} H(\tilde{\tau}_{k'_t} - \tilde{\tau}_{k'_t - 1}) \mathcal{O}_{k'_t - 1} \cdots \mathcal{O}_1 H(\tilde{\tau}_1)\right] \\ &= \left(-\frac{J_{\rm eff}}{2}\right)^{k_s+k_p} s_{\mathcal{T}} \sum_{\alpha=1}^{N_b} \sum_{i=1}^{M_\alpha} \\ &\quad \times \underbrace{\left[H(\beta - \tilde{\tau}_{k'_t}) \mathcal{O}_{k'_t} H(\tilde{\tau}_{k'_t} - \tilde{\tau}_{k'_t - 1}) \mathcal{O}_{k'_t - 1} \cdots \mathcal{O}_1 H(\tilde{\tau}_1)\right]_{i\alpha, i\alpha}}_{w_{i\alpha}} \end{aligned} \quad (2.211)$$

[10] In practice, the $\mathcal{O}_{\rm s.f.}$ and $\mathcal{O}_{\rm p.h.}$ matrices have non-zero off-diagonal elements for a limited blocks (the diagonal elements are always zero). Then, it is enough to introduce the constant shift matrices $s_a \gamma I$ to the block-diagonalized matrices which have nonzero off-diagonal elements, where I is the identity matrix.

[11] An alternative solution is e.g., to introduce the n-vertices update, where $k_s \to k_s \pm n$ or $k_p \to k_p \pm n$ [82].

where $\mathcal{O}$ takes $c^\dagger$, c, $\mathcal{O}'_{\text{s.f.}}$, and $\mathcal{O}'_{\text{p.h.}}$ with proper orbital, spin, and auxiliary spin indices. The partition function is then written as

$$\frac{Z}{Z_{\text{bath}}} = \sum_{\text{configurations}}{}' \mathcal{W}_{\text{tot}}\Big[C'\big(\{k_{l\sigma}\}, k_s, k_p\big)\Big], \tag{2.212}$$

where the "summation" over all possible configurations $\sum'$ denotes the sum over the expansion order $\big(\{k_{l\sigma}\}, k_s, k_p\big)$, the integral over τ's, and the sum over orbital, spin, and auxiliary spin indices.

2.3.3.4 Update Scheme

In the Metropolis-Hastings algorithm [83, 84], we perform the importance sampling over every possible configurations with the weights $\mathcal{W}_{\text{tot}}$'s in Eq. (2.210). We employ the following updates for the simulations of the normal state [73, 82, 85, 88]:

1. Add a pair of $(l\sigma)$ component of the hybridization vertices at random times τ and τ' in the range $\tau, \tau' \in \big[0, \beta\big)$, i.e., increase the expansion order of $(l\sigma)$ component by one $k_{l\sigma} \to k_{l\sigma} + 1$.
2. Remove a randomly-chosen pair from the existing $(l\sigma)$-component hybridization vertices in $\big[0, \beta\big)$, i.e., decrease the expansion order of $(l\sigma)$ component by one $k_{l\sigma} \to k_{l\sigma} - 1$.
3. Add a pair of $(l\sigma)$ component of the hybridization vertices at random times τ and τ' in a range shorter than that of the update 1. The range is set to be $[\tau_0, \tau_0 + \Delta\tau\big)$ with a random time $\tau_0 \in \big[0, \beta\big)$ and the interval $\Delta\tau$ $(0 < \Delta\tau < \beta)$.
4. Remove a randomly-chosen pair from the existing $(l\sigma)$-component hybridization vertices in a limited range $\big[\tau_0, \tau_0 + \Delta\tau\big)$ with a random time $\tau_0 \in \big[0, \beta\big)$ and the interval $\Delta\tau$ $(0 < \Delta\tau < \beta)$.
5. Add one spin-flip or pair-hopping vertex with randomly-chosen orbital and auxiliary spin indices at a random time τ $(0 \le \tau < \beta)$, i.e., $k_s \to k_s + 1$ or $k_p \to k_p + 1$.
6. Remove, randomly, one of the existing spin-flip or pair-hopping vertices vertices in $[0, \beta\big)$, i.e., $k_s \to k_s - 1$ or $k_p \to k_p - 1$.
7. Shift the imaginary time of one of the existing hybridization vertices (the expansion orders do not change). We use a random number to determine the magnitude of the time shift (see below for the detail).

The updates 1, 2, 5, and 6 are necessary to ensure the ergodicity. The updates 3, 4, and 7 are introduced to improve the acceptance rates and the efficiency of the simulation. Note that updates 1–4 have to be done for all $(l\sigma)$ channels. τ_0 in updates 3 and 4 is randomly chosen at each steps, while we fix the value of $\Delta\tau$ in the simulation. We typically use $\Delta\tau/\beta \sim 0.05$.

In the Metropolis-Hasting algorithm [83, 84], the acceptance rate is determined to satisfy the detailed balance condition:

$$P(C'_{\rm old} \to C'_{\rm new}) = \min\Big[R(C'_{\rm old}, C'_{\rm new}), 1\Big]. \tag{2.213}$$

$$R(C'_{\rm old}, C'_{\rm new}) = \frac{\mathcal{W}_{\rm tot}(C'_{\rm new})P_0(C'_{\rm new} \to C'_{\rm old})}{\mathcal{W}_{\rm tot}(C'_{\rm old})P_0(C'_{\rm old} \to C'_{\rm new})} \tag{2.214}$$

with $P_0(C'_{\rm old} \to C'_{\rm new})$ being a proposal probability for the transition from an old configuration $C'_{\rm old}$ to a new configuration $C'_{\rm new}$. Here, we omitted the $(\{k_{l\sigma}\}, k_s, k_p)$ indices from the configuration $C'\big(\{k_{l\sigma}\}, k_s, k_p\big)$ for simplicity. In the simulations, at each proposal, we calculate the acceptance rate in Eq. (2.213) and compare it with a random number r between 0 and 1 generated by the Mersenne Twister [89]. If r is smaller than the acceptance rate, the proposal is accepted and the configuration is changed into the new configuration. Below, we list the ratio $R(C'_{\rm old}, C'_{\rm new})$ for the above mentioned updates.

For the update 1, the proposal probabilities are given by $P_0(C'_{\rm old} \to C'_{\rm new}) = (d\tau)^2/\beta^2$ and $P_0(C'_{\rm new} \to C'_{\rm old}) = 1/(k_{l\sigma}+1)^2$. Then the $R(C'_{\rm old}, C'_{\rm new})$ ratio is given by [85]

$$\text{update 1}: R(C'_{\rm old}, C'_{\rm new}) = \frac{\beta^2}{(k_{l\sigma}+1)^2} \frac{\mathcal{W}_b(C'_{\rm new})\mathcal{W}'_c(C'_{\rm new}) \det A^{(l\sigma)}(C'_{\rm new})}{\mathcal{W}_b(C'_{\rm old})\mathcal{W}'_c(C'_{\rm old}) \det A^{(l\sigma)}(C'_{\rm old})}, \tag{2.215}$$

where the determinant ratio is efficiently calculated by the Sherman-Morrison formula [90, 91] with $\mathcal{O}(k^2_{l\sigma})$ operations. Similarly, the ratio for the update 2 is [85]

$$\text{update 2}: R(C'_{\rm old}, C'_{\rm new}) = \frac{k^2_{l\sigma}}{\beta^2} \frac{\mathcal{W}_b(C'_{\rm new})\mathcal{W}'_c(C'_{\rm new}) \det A^{(l\sigma)}(C'_{\rm new})}{\mathcal{W}_b(C'_{\rm old})\mathcal{W}'_c(C'_{\rm old}) \det A^{(l\sigma)}(C'_{\rm old})}. \tag{2.216}$$

To compute the acceptance rate of the updates 3 and 4, we have to count the number of the existing $(l\sigma)$-component hybridization vertices in $[\tau_0, \tau_0 + \Delta\tau)$, which is denoted by $k'_{l\sigma}$. Then, the ratios for the updates 3 and 4 are given by [88]

$$\text{update 3}: \quad R(C'_{\rm old}, C'_{\rm new}) = \frac{(\Delta\tau)^2}{(k'_{l\sigma}+1)^2} \frac{\mathcal{W}_b(C'_{\rm new})\mathcal{W}'_c(C'_{\rm new}) \det A^{(l\sigma)}(C'_{\rm new})}{\mathcal{W}_b(C'_{\rm old})\mathcal{W}'_c(C'_{\rm old}) \det A^{(l\sigma)}(C'_{\rm old})} \tag{2.217}$$

$$\text{update 4}: \quad R(C'_{\rm old}, C'_{\rm new}) = \frac{k'^2_{l\sigma}}{(\Delta\tau)^2} \frac{\mathcal{W}_b(C'_{\rm new})\mathcal{W}'_c(C'_{\rm new}) \det A^{(l\sigma)}(C'_{\rm new})}{\mathcal{W}_b(C'_{\rm old})\mathcal{W}'_c(C'_{\rm old}) \det A^{(l\sigma)}(C'_{\rm old})}. \tag{2.218}$$

At the update 5, we first randomly choose either the spin-flip term or the pair-hopping term, and randomly determine orbital components l, m $(l < m)$ and the orientation of the auxiliary spin s_a. Then we pick a random time from$[0, \beta)$. $P_0(C'_{\rm old} \to$

$C'_{\rm new}$) for the update 5 is hence given by $P_0(C'_{\rm old} \to C'_{\rm new}) = 1/2 \times 1/N_{\rm orb}(N_{\rm orb} - 1) \times 1/2 \times d\tau/\beta = d\tau/[4N_{\rm orb}(N_{\rm orb} - 1)\beta]$. $P_0(C'_{\rm new} \to C'_{\rm old})$ is simply a probability to pick one of $(k_s + k_p + 1)$ vertices $P_0(C'_{\rm new} \to C'_{\rm old}) = 1/(k_s + k_p + 1)$. The proposal probabilities for the update 6 can be derived in a similar way. Thus we obtain the ratios for the updates 5 and 6 as

$$\text{update 5}: \quad R(C'_{\rm old}, C'_{\rm new}) = \frac{4N_{\rm orb}(N_{\rm orb} - 1)\beta}{k_s + k_p + 1} \frac{\mathcal{W}_b(C'_{\rm new})\mathcal{W}'_c(C'_{\rm new})}{\mathcal{W}_b(C'_{\rm old})\mathcal{W}'_c(C'_{\rm old})}, \tag{2.219}$$

$$\text{update 6}: \quad R(C'_{\rm old}, C'_{\rm new}) = \frac{k_s + k_p}{4N_{\rm orb}(N_{\rm orb} - 1)\beta} \frac{\mathcal{W}_b(C'_{\rm new})\mathcal{W}'_c(C'_{\rm new})}{\mathcal{W}_b(C'_{\rm old})\mathcal{W}'_c(C'_{\rm old})}. \tag{2.220}$$

Note that the determinant ratio of A matrix disappears since the spin-flip and pair-hopping terms contain no bath-site electron operators.

In the update 7, we randomly choose a channel from $(l\sigma) = (1\uparrow)$ to $(N_{\rm orb}\downarrow)$. Let us assume that the $(l\sigma)$ channel is chosen. Since there exists $2k_{l\sigma}$ vertices in the $(l\sigma)$ channel, we choose one of them by a probability $1/2k_{l\sigma}$. We set the magnitude of the time shift by $\delta\tau = \beta/2 \times \left[\tanh(2ra - a)/\tanh(a) + 1\right]$, where r is a random number chosen from [0, 1). We always set a positive real constant a to be $a = 2.5$, while in principle, a can be tuned case by case to improve the acceptance rate. This formula generates small shift ($\delta\tau \sim 0$ or $\delta\tau \sim \beta$)[12] with a large probability, which helps to improve the acceptance rate. Since, in this case, the equality $P_0(C'_{\rm old} \to C'_{\rm new}) = P_0(C'_{\rm new} \to C'_{\rm old})$ holds, the $R(C'_{\rm old}, C'_{\rm new})$ ratio for the update 7 is given by

$$\text{update 7}: R(C'_{\rm old}, C'_{\rm new}) = \frac{\mathcal{W}_b(C'_{\rm new})\mathcal{W}'_c(C'_{\rm new}) \det A^{(l\sigma)}(C'_{\rm new})}{\mathcal{W}_b(C'_{\rm old})\mathcal{W}'_c(C'_{\rm old}) \det A^{(l\sigma)}(C'_{\rm old})}. \tag{2.221}$$

While in the above argument, we implicitly assume that the $R(C'_{\rm old}, C'_{\rm new})$ ratio is positive or zero, it sometimes becomes negative. In this case, we use the absolute value $|R(C'_{\rm old}, C'_{\rm new})|$ to calculate the acceptance rates. Correspondingly, it produces negative signs in the Monte Carlo simulations. We found that a large value of γ in Eqs. (2.207) and (2.208) produces a larger amount of negative signs. In the case of the simulations of the low-energy models for the alkali-doped fullerides using $\gamma \sim 0.03$, the average sign is ∼0.5.

2.3.3.5 Measurements

In order to cycle the self-consistent loop, we have to measure, at least, the impurity-site Green's function $\mathbf{G}_{\rm imp}$ and the charge-charge correlation function $\chi_{\rm imp}$. The diagonal part of the Green's function with the spin σ $[\mathbf{G}^{\sigma}_{\rm imp}]_{ll}$ $(l = 1, \ldots N_{\rm orb})$ is efficiently estimated by using the inverse matrix of $A^{(l\sigma)}$ $(\equiv B^{(l\sigma)})$ as [73, 78]

[12] $\delta\tau \sim \beta$ corresponds to the shift in minus direction by the amount $\beta - \delta\tau \sim 0$.

$$\left[\mathbf{G}^{\sigma}_{\mathrm{imp}}(\tau)\right]_{ll} = \frac{1}{\beta}\left\langle \sum_{i,j=1}^{k_{l\sigma}} \left[B^{(l\sigma)}\right]_{ji} \tilde{\delta}(\tau, \tau_j'^{(l\sigma)} - \tau_i^{(l\sigma)}) \right\rangle_{\mathrm{MC}}, \tag{2.222}$$

where $\langle \ldots \rangle_{\mathrm{MC}}$ indicates the Monte-Carlo average, and $\tilde{\delta}(\tau, \tau_j' - \tau_i)$ is defined as

$$\tilde{\delta}(\tau, \tau') = \begin{cases} \delta(\tau - \tau'), & (\tau' > 0) \\ -\delta(\tau - \tau' - \beta). & (\tau' < 0) \end{cases} \tag{2.223}$$

Note that the expansion order $k_{l\sigma}$ may change measurement by measurement. The off-diagonal elements of the Green's function vanish in the case where the off-diagonal hybridization functions are zero. In the simulation of the paramagnetic phase, we often take average over the spin at each self-consistent cycle.

As for the charge-charge correlation function χ_{imp}, since the operators for total number of electrons $\hat{N}$ commute with the $\mathcal{H}^c_{\mathrm{LF}}$ Hamiltonian, there exists an efficient way to directly measure χ_{imp} on the Matsubara axis [86]. First, let us define a "probability" of the $|i;\alpha\rangle$ state (ith eigenstate of $\mathcal{H}^c_{\mathrm{LF}}$ in block α), using $w_{i\alpha}$ in Eq. (2.211), as [86]

$$p_{i\alpha} = \frac{w_{i\alpha}}{\sum_{\alpha=1}^{N_b}\sum_{i=1}^{M_\alpha} w_{i\alpha}}. \tag{2.224}$$

With $p_{i\alpha}$'s, the expectation value of the static part of the correlation function $\chi_{\mathrm{imp}}(0)$ is computed as [86]

$$\chi_{\mathrm{imp}}(0) = \frac{1}{\beta}\left\langle \sum_{\alpha=1}^{N_b}\sum_{i=1}^{M_\alpha} p_{i\alpha}\left(\sum_{k=0}^{k_t'} N_{\alpha_k}(\tilde{\tau}_{k+1} - \tilde{\tau}_k)\right)^2 \right\rangle_{\mathrm{MC}} - \beta N_{\mathrm{av}}^2, \tag{2.225}$$

where $\tilde{\tau}_k$'s ($1 \le k \le k_t'$) are the same as those in Eq. (2.211). On top of that, we define $\tilde{\tau}_{k_t'+1}$ and $\tilde{\tau}_0$ as $\tilde{\tau}_{k_t'+1} = \beta$ and $\tilde{\tau}_0 = 0$. N_{α_k} is the number of electrons of the eigenstates in α_kth block with α_k identifying the trace of the blocks which are passed through during the matrix operation. N_{av} is the average occupation at the impurity site, which is given by

$$N_{\mathrm{av}} = \left\langle \sum_{\alpha=1}^{N_b}\sum_{i=1}^{M_\alpha} p_{i\alpha}\left(\sum_{k=0}^{k_t'} N_{\alpha_k}\frac{\tilde{\tau}_{k+1} - \tilde{\tau}_k}{\beta}\right) \right\rangle_{\mathrm{MC}}. \tag{2.226}$$

Similarly, the dynamical part of the correlation function $\chi_{\mathrm{imp}}(i\nu_n)$ ($\nu_n \neq 0$) can be estimated as [86]

$$\chi_{\mathrm{imp}}(i\nu_n) = \frac{1}{\beta}\left\langle \sum_{\alpha=1}^{N_b}\sum_{i=1}^{M_\alpha} p_{i\alpha}\left|\sum_{k=0}^{k_t'} N_{\alpha_k}\frac{e^{i\nu_n\tilde{\tau}_{k+1}} - e^{i\nu_n\tilde{\tau}_k}}{i\nu_n}\right|^2 \right\rangle_{\mathrm{MC}}. \tag{2.227}$$

2.3.3.6 Flow of Calculation

1. Choose an update from above listed seven types of updates.
2. Compute the acceptance rate $P(C'_{\text{old}} \to C'_{\text{new}})$ in Eq. (2.213) for the chosen update.
3. Generate a uniform random number r between 0 and 1 with the Mersenne Twister [89].
4. If $r < P(C'_{\text{old}} \to C'_{\text{new}})$, move to a new configuration. Otherwise, leave the old configuration.
5. Once every $N_{\text{meas.}}$ times, perform measurements of the impurity-site Green's function $\mathbf{G}_{\text{imp}}$, the charge-charge correlation function χ_{imp}, and so on. A simplest choice of $N_{\text{meas.}}$ is $N_{\text{meas.}} \geq (\sum_{l\sigma} k_{l\sigma} + k_s + k_p)/(\text{average acceptance rate})$.
6. Go back to step 1.

Before starting the measurements, we typically take "warm-up" steps, where we repeat steps 1–4 for $\sim 100 N_{\text{meas.}}$ times to thermalize. If the thermalization is slow, you need longer "warm-up" iterations.

2.3.4 *Simulation of Superconducting State Within Extend DMFT*

The schemes described above refer to the simulation of normal paramagnetic phases. If we want to treat an s-wave superconducting phase, we need some modifications in the schemes [92]. To this end, we introduce the Nambu spinor as

$$\Psi_{\mathbf{k}} = \begin{pmatrix} \hat{c}^{\uparrow}_{\mathbf{k}1} \\ \vdots \\ \hat{c}^{\uparrow}_{\mathbf{k}N_{\text{orb}}} \\ \hat{c}^{\downarrow\dagger}_{-\mathbf{k}1} \\ \vdots \\ \hat{c}^{\downarrow\dagger}_{-\mathbf{k}N_{\text{orb}}} \end{pmatrix}. \tag{2.228}$$

The Green's function is defined as

$$\tilde{\mathbf{G}}_{\mathbf{k}}(\tau) = -\langle \mathcal{T} \Psi_{\mathbf{k}}(\tau) \Psi^{\dagger}_{\mathbf{k}}(0) \rangle \tag{2.229}$$

$$= \begin{pmatrix} \mathbf{G}_{\mathbf{k}}(\tau) & \mathbf{F}_{\mathbf{k}}(\tau) \\ \mathbf{F}^{\dagger}_{\mathbf{k}}(\tau) & -\mathbf{G}_{-\mathbf{k}}(-\tau) \end{pmatrix}, \tag{2.230}$$

where $\mathbf{F}_{\mathbf{k}}(\tau)$ is a matrix of the anomalous Green's function with elements $[\mathbf{F}_{\mathbf{k}}(\tau)]_{lm} = -\langle \mathcal{T} \hat{c}^{\uparrow}_{\mathbf{k}l}(\tau) \hat{c}^{\downarrow}_{-\mathbf{k}m}(0) \rangle$. Here, we assume that the up-spin and down-spin normal Green's function are identical. Following the notations in Sects. 2.3.1, 2.3.2, and 2.3.3.2, the

bold symbols without the tilde symbol denote matrices with respect to orbital indices. The bold symbols with the tilde symbol denote matrices in the Nambu representation.

Correspondingly, the Weiss function, the self-energy, and the hybridization function, are also expressed in the Nambu representation. The self-energy has a form

$$\tilde{\boldsymbol{\Sigma}}(i\omega_n) = \begin{pmatrix} \boldsymbol{\Sigma}_{\mathrm{N}}(i\omega_n) & \boldsymbol{\Sigma}_{\mathrm{A}}(i\omega_n) \\ \boldsymbol{\Sigma}_{\mathrm{A}}^{\dagger}(-i\omega_n) & -\boldsymbol{\Sigma}_{\mathrm{N}}^{*}(i\omega_n) \end{pmatrix}, \tag{2.231}$$

where $\boldsymbol{\Sigma}_{\mathrm{N}}(i\omega_n)$ [$\boldsymbol{\Sigma}_{\mathrm{A}}(i\omega_n)$] is the normal [anomalous] self-energy. We consider the singlet even-frequency intra-orbital pairing, which will be most favored in the presence of a negative pair-hopping interaction, and assume the orbital degeneracy. In this case, the anomalous self-energy is written as $[\boldsymbol{\Sigma}_{\mathrm{A}}(i\omega_n)]_{ij} = \Sigma_{\mathrm{A}}(i\omega_n)\delta_{ij}$, where $\Sigma_{\mathrm{A}}(i\omega_n)$ takes a real number[13] and satisfies the equality $\Sigma_{\mathrm{A}}(i\omega_n) = \Sigma_{\mathrm{A}}(-i\omega_n)$. Therefore, $\boldsymbol{\Sigma}_{\mathrm{A}}^{\dagger}(-i\omega_n) = \boldsymbol{\Sigma}_{\mathrm{A}}(i\omega_n)$. It leads to the expression of the self-energy

$$\tilde{\boldsymbol{\Sigma}}(i\omega_n) = \begin{pmatrix} \boldsymbol{\Sigma}_{\mathrm{N}}(i\omega_n) & \boldsymbol{\Sigma}_{\mathrm{A}}(i\omega_n) \\ \boldsymbol{\Sigma}_{\mathrm{A}}(i\omega_n) & -\boldsymbol{\Sigma}_{\mathrm{N}}^{*}(i\omega_n) \end{pmatrix}. \tag{2.232}$$

The hybridization function is obtained by

$$\tilde{\boldsymbol{\Gamma}}(i\omega_n) = \begin{pmatrix} (i\omega_n + \mu)\mathbf{1} & 0 \\ 0 & (i\omega_n - \mu)\mathbf{1} \end{pmatrix} - \tilde{\boldsymbol{\mathcal{G}}}_0^{-1}(i\omega_n). \tag{2.233}$$

Below, we will show how the introduction of anomalous part modifies the CT-HYB scheme. As for the impurity-site action in Eq. (2.159), only the Weiss function part is modified, i.e.,

$$-\int_0^\beta d\tau d\tau' \sum_{lm\sigma} c_{l\sigma}^*(\tau)\left[\boldsymbol{\mathcal{G}}_0^{-1}(\tau-\tau')\right]_{lm} c_{m\sigma}(\tau') \;\rightarrow\; -\int_0^\beta d\tau d\tau' \Psi^\dagger(\tau)\tilde{\boldsymbol{\mathcal{G}}}_0^{-1}(\tau-\tau')\Psi(\tau'), \tag{2.234}$$

which corresponds to a modification of the expression of $\hat{\mathcal{H}}_{\mathrm{bath}}$ in Eq. (2.164) to include the anomalous part as

$$\hat{\mathcal{H}}_{\mathrm{bath}} = \sum_{p\sigma} \varepsilon_p \hat{a}_{p\sigma}^\dagger \hat{a}_{p\sigma} + \sum_p \left(\Delta_p \hat{a}_{p\uparrow}^\dagger \hat{a}_{p\downarrow}^\dagger + \mathrm{H.c.}\right). \tag{2.235}$$

The self-consistent equations (2.155), (2.157), and (2.161) in the flow of the extended DMFT calculation described in Sect. 2.3.2 are modified to

[13] We choose a gauge so that the anomalous self-energy is real.

$$\tilde{\mathbf{G}}_{\rm loc}(i\omega_n) = \frac{1}{N_k}\sum_{k}\begin{pmatrix} (i\omega_n+\mu)\mathbf{1} - \boldsymbol{\mathcal{H}}_0(\mathbf{k}) - \boldsymbol{\Sigma}_{\rm N}(i\omega_n) & -\boldsymbol{\Sigma}_{\rm A}(i\omega_n) \\ -\boldsymbol{\Sigma}_{\rm A}(i\omega_n) & (i\omega_n-\mu)\mathbf{1} + \boldsymbol{\mathcal{H}}_0(\mathbf{k}) + \boldsymbol{\Sigma}_{\rm N}^*(i\omega_n) \end{pmatrix}^{-1}, \tag{2.236}$$

$$\tilde{\boldsymbol{\mathcal{G}}}_0^{-1}(i\omega_n) = \tilde{\mathbf{G}}_{\rm loc}^{-1}(i\omega_n) + \tilde{\boldsymbol{\Sigma}}(i\omega_n) \tag{2.237}$$

and

$$\tilde{\boldsymbol{\Sigma}}_{\rm new}(i\omega_n) = \tilde{\boldsymbol{\mathcal{G}}}_0^{-1}(i\omega_n) - \tilde{\mathbf{G}}_{\rm imp}^{-1}(i\omega_n), \tag{2.238}$$

respectively. In Eq. (2.236), we assumed that the matrix elements of $\boldsymbol{\mathcal{H}}_0(\mathbf{k})$ are real and the up-spin and down-spin electrons are degenerate, which holds in the alkali-doped fullerides with the time-reversal and space-inversion symmetries.

As for the QMC part in Sect. 2.3.3.2, the existence of anomalous part of the hybridization function, the $A^{(l\uparrow)}$ and $A^{(l\downarrow)}$ matrices are not independent any more [79, 93, 94]. Therefore, we need to redefine the configuration as

$$\tilde{C}(\{k_l\}, k_s, k_p) = \left\{ \left\{ \tilde{C}^l_{\rm hyb}(k_l) \right\}, C'_{\rm s.f.}(k_s), C'_{\rm p.h.}(k_p) \right\} \tag{2.239}$$

where the definitions of $C'_{\rm s.f.}(k_s)$ and $C'_{\rm p.h.}(k_p)$ are the same as Eq. (2.209), and $\tilde{C}^l_{\rm hyb}(k_l)$ is given by

$$\tilde{C}^l_{\rm hyb}(k_l) = \left\{ (f_1^{(l)}, f_1^{\prime(l)}, \tau_1^{(l)}, \tau_1^{\prime(l)}), (f_2^{(l)}, f_2^{\prime(l)}, \tau_2^{(l)}, \tau_2^{\prime(l)}), \ldots, (f_{k_l}^{(l)}, f_{k_l}^{\prime(l)}, \tau_{k_l}^{(l)}, \tau_{k_l}^{\prime(l)}) \right\}. \tag{2.240}$$

Here, $f_i^{(l)}$'s and $f_i^{\prime(l)}$'s are "flavors" which specify the orientations of the spins and the types of bath-site operators (creation or annihilation), i.e., $f_i^{(l)}$ $\left[f_i^{\prime(l)}\right]$ is a composite index $f_i^{(l)} = (\sigma_i^{(l)}, t_i^{(l)})$ $\left[f_i^{\prime(l)} = (\sigma_i^{\prime(l)}, t_i^{\prime(l)})\right]$ with the spin index $\sigma_i^{(l)}$ $\left[\sigma_i^{\prime(l)}\right]$ and the type (creation or annihilation) index $t_i^{(l)}$ $\left[t_i^{\prime(l)}\right]$. Note that the type index specifies the operator type of *bath-site* degrees of freedom and that if the type is "creation" ("annihilation"), the corresponding type of the impurity-site operators is "annihilation" ("creation"). Remember that the hybridization vertices are composed of the pair of the creation bath-site operator and the annihilation impurity-site operator, or the annihilation bath-site operator and the creation impurity-site operator. Then, we introduce a $k_l \times k_l$ matrix $A^{(l)}\left[\tilde{C}^l_{\rm hyb}(k_l)\right]$ whose elements are given by

$$A^{(l)}\left[\tilde{C}^{l}_{\mathrm{hyb}}(k_l)\right] = \begin{pmatrix} \tilde{\Gamma}_{\tilde{f}_1^{(l)}\tilde{f}_1'^{(l)}}(\tau_1^{(l)} - \tau_1'^{(l)}) & \tilde{\Gamma}_{\tilde{f}_1^{(l)}\tilde{f}_2'^{(l)}}(\tau_1^{(l)} - \tau_2'^{(l)}) & \cdots & \tilde{\Gamma}_{\tilde{f}_1^{(l)}\tilde{f}_{k_l}'^{(l)}}(\tau_1^{(l)} - \tau_{k_l}'^{(l)}) \\ \tilde{\Gamma}_{\tilde{f}_2^{(l)}\tilde{f}_1'^{(l)}}(\tau_2^{(l)} - \tau_1'^{(l)}) & \tilde{\Gamma}_{\tilde{f}_2^{(l)}\tilde{f}_2'^{(l)}}(\tau_2^{(l)} - \tau_2'^{(l)}) & \cdots & \tilde{\Gamma}_{\tilde{f}_2^{(l)}\tilde{f}_{k_l}'^{(l)}}(\tau_2^{(l)} - \tau_{k_l}'^{(l)}) \\ \vdots & \vdots & \ddots & \vdots \\ \tilde{\Gamma}_{\tilde{f}_{k_l}^{(l)}\tilde{f}_1'^{(l)}}(\tau_{k_l}^{(l)} - \tau_1'^{(l)}) & \tilde{\Gamma}_{\tilde{f}_{k_l}^{(l)}\tilde{f}_2'^{(l)}}(\tau_{k_l}^{(l)} - \tau_2'^{(l)}) & \cdots & \tilde{\Gamma}_{\tilde{f}_{k_l}^{(l)}\tilde{f}_{k_l}'^{(l)}}(\tau_{k_l}^{(l)} - \tau_{k_l}'^{(l)}) \end{pmatrix}, \tag{2.241}$$

where $\tilde{f}_i^{(l)}$ $\left[\tilde{f}_i'^{(l)}\right]$ is the spinor-component index corresponding to the orbital index l and the composite index $f_i^{(l)}$ $\left[f_i'^{(l)}\right]$. For example, in the case where $l = 1$ and $\left\{f_i^{(l)}, f_i'^{(l)}\right\} = \left\{(\uparrow, \text{annihilation}), (\downarrow, \text{annihilation})\right\}$, the corresponding $\tilde{f}_i^{(l)}$ and $\tilde{f}_i'^{(l)}$ are $\left\{\tilde{f}_i^{(l)}, \tilde{f}_i'^{(l)}\right\} = \{1, N_{\mathrm{orb}} + 1\}$. The weight for the $\tilde{C}\left(\{k_l\}, k_s, k_p\right)$ configuration is given by

$$\mathcal{W}_{\mathrm{tot}}\left[\tilde{C}\left(\{k_l\}, k_s, k_p\right)\right] = \left\{\prod_l \det A^{(l)}\left[\tilde{C}^{l}_{\mathrm{hyb}}(k_l)\right] \prod_{i=1}^{k_l} d\tau_i^{(l)} d\tau_i'^{(l)}\right\} \times \mathcal{W}_b\left[\tilde{C}\left(\{k_l\}, k_s, k_p\right)\right] \mathcal{W}_c'\left[\tilde{C}\left(\{k_l\}, k_s, k_p\right)\right] \prod_{i''}^{k_s} d\tau_{i''}'' \prod_{i'''}^{k_p} d\tau_{i'''}''', \tag{2.242}$$

where the methods to compute $\mathcal{W}_b$ and $\mathcal{W}_c'$ are the same as the ones in the normal state simulations [Eqs. (2.202) and (2.211), respectively]. Then the partition function in the superconducting phase is written as

$$\frac{Z(\mathrm{SC})}{Z_{\mathrm{bath}}} = {\sum_{\text{configurations}}}' \mathcal{W}_{\mathrm{tot}}\left[\tilde{C}\left(\{k_l\}, k_s, k_p\right)\right]. \tag{2.243}$$

In the simulation of the superconducting phase, in order to ensure the ergodicity, we need the following updates on top of the updates 1, 2, 5, and 6 described in Sect. 2.3.3.2.

8. Add four hybridization vertices at random times in $[0, \beta)$. They are composed of the $(l\uparrow)$ and $(l\downarrow)$ components of $\hat{\mathcal{H}}_{\mathrm{hyb}}'^{\dagger}$, and the $(m\downarrow)$ and $(m\uparrow)$ components $(m \neq l)$ of $\hat{\mathcal{H}}_{\mathrm{hyb}}'$. It corresponds to the increase of the expansion orders of the lth and mth channels, $k_l \to k_l + 1$ and $k_m \to k_m + 1$.
9. Remove four hybridization vertices from the existing hybridization vertices in the range $[0, \beta)$. They are composed of the $(l\uparrow)$ and $(l\downarrow)$ components of $\hat{\mathcal{H}}_{\mathrm{hyb}}'^{\dagger}$, and the $(m\downarrow)$ and $(m\uparrow)$ components $(m \neq l)$ of $\hat{\mathcal{H}}_{\mathrm{hyb}}'$. The vertices are randomly-chosen with satisfying the above condition. It corresponds to the decrease of the expansion orders of the lth and mth channels, i.e., $k_l \to k_l - 1$ and $k_m \to k_m - 1$.

The updates 8 and 9 have to be performed for all possible combinations of the l and m indices ($l \neq m$). The necessity of these updates can be understood by considering e.g., a following case. Let us assume that a configuration has the following expansion orders, $k_1 = 1, k_2 = 1, k_{l\neq 1,2} = 0, k_s = 0$, and $k_p = 1$. In the first hybridization channel ($l = 1$), the flavors $f_1^{(l=1)}$ and $f_1^{\prime(l=1)}$ are ($\uparrow$, annihilation) and ($\downarrow$, annihilation), respectively. In the second hybridization channel ($l = 2$), the flavors $f_1^{(l=2)}$ and $f_1^{\prime(l=2)}$ are ($\downarrow$, creation) and ($\uparrow$, creation), respectively. Then if the pair-hopping vertex is of ($l'' = 2, m'' = 1$) channel, the configuration can have non-zero weight only in the superconducting state: In this case, the elements of the $A^{(l=1)}$ and $A^{(l=2)}$ matrices become anomalous parts of the hybridization function, thus, the determinants of $A^{(l=1)}$ and $A^{(l=2)}$ matrices are zero in the normal state. While this configuration can appear by e.g., the combination of the updates 5 and 8 starting from zero vertices, it is never realized by the seven types of updates for the normal state calculations.

Let us define the number of bath-site operators in the lth channel with (σ, creation) and (σ, annihilation) flavors as $k^{(l)}_{(\sigma,\mathrm{c})}$ and $k^{(l)}_{(\sigma,\mathrm{a})}$, respectively. They should satisfy the equality

$$k_l = k^{(l)}_{(\uparrow,\mathrm{a})} + k^{(l)}_{(\downarrow,\mathrm{c})} = k^{(l)}_{(\uparrow,\mathrm{c})} + k^{(l)}_{(\downarrow,\mathrm{a})}. \tag{2.244}$$

Note that, in the normal-state simulations, the equalities $k^{(l)}_{(\uparrow,\mathrm{a})} = k^{(l)}_{(\uparrow,\mathrm{c})}$ and $k^{(l)}_{(\downarrow,\mathrm{c})} = k^{(l)}_{(\downarrow,\mathrm{a})}$ always hold. However, in the superconducting-state simulations, it is not the case due to the presence of the updates 8 and 9. Then, the R ratios in Eq. (2.214) for the updates 8 and 9 are given by

$$\begin{aligned}\text{update 8}: R(\tilde{C}_{\mathrm{old}}, \tilde{C}_{\mathrm{new}}) = {} & \frac{\beta^4}{\left(k^{(l)}_{(\uparrow,\mathrm{a})}+1\right)\left(k^{(l)}_{(\downarrow,\mathrm{a})}+1\right)\left(k^{(m)}_{(\downarrow,\mathrm{c})}+1\right)\left(k^{(m)}_{(\uparrow,\mathrm{c})}+1\right)} \\ & \times \frac{\mathcal{W}_b(\tilde{C}_{\mathrm{new}})\mathcal{W}_c(\tilde{C}_{\mathrm{new}})\det A^{(l)}(\tilde{C}_{\mathrm{new}})\det A^{(m)}(\tilde{C}_{\mathrm{new}})}{\mathcal{W}_b(\tilde{C}_{\mathrm{old}})\mathcal{W}_c(\tilde{C}_{\mathrm{old}})\det A^{(l)}(\tilde{C}_{\mathrm{old}})\det A^{(m)}(\tilde{C}_{\mathrm{old}})},\end{aligned} \tag{2.245}$$

and

$$\begin{aligned}\text{update 9}: R(\tilde{C}_{\mathrm{old}}, \tilde{C}_{\mathrm{new}}) = {} & \frac{k^{(l)}_{(\uparrow,\mathrm{a})}k^{(l)}_{(\downarrow,\mathrm{a})}k^{(m)}_{(\downarrow,\mathrm{c})}k^{(m)}_{(\uparrow,\mathrm{c})}}{\beta^4} \\ & \times \frac{\mathcal{W}_b(\tilde{C}_{\mathrm{new}})\mathcal{W}_c(\tilde{C}_{\mathrm{new}})\det A^{(l)}(\tilde{C}_{\mathrm{new}})\det A^{(m)}(\tilde{C}_{\mathrm{new}})}{\mathcal{W}_b(\tilde{C}_{\mathrm{old}})\mathcal{W}_c(\tilde{C}_{\mathrm{old}})\det A^{(l)}(\tilde{C}_{\mathrm{old}})\det A^{(m)}(\tilde{C}_{\mathrm{old}})},\end{aligned} \tag{2.246}$$

respectively. We can further introduce updates, in which four vertices are added or removed within a limited imaginary-time range. The introduction helps to increase the acceptance rate and to improve the efficiency of the QMC simulation. The formulae to compute R ratios for these updates can be derived in a similar way as in the

case of updates 3 and 4. Furthermore, the exchange of time indices of the neighboring vertices on the imaginary-time axis, which is employed in Ref. [93], also improves the efficiency.

In the simulation of the superconducting phase, the expressions of the ratios for the updates 1–7 are slightly modified from those for the normal state. Below, we just list them:

$$\text{update 1}: R(\tilde{C}_{\text{old}}, \tilde{C}_{\text{new}}) = \frac{\beta^2}{\left(k^{(l)}_{(\sigma,\text{c})}+1\right)\left(k^{(l)}_{(\sigma,\text{a})}+1\right)} \frac{\mathcal{W}_b(\tilde{C}_{\text{new}})\mathcal{W}'_c(\tilde{C}_{\text{new}})\det A^{(l)}(\tilde{C}_{\text{new}})}{\mathcal{W}_b(\tilde{C}_{\text{old}})\mathcal{W}'_c(\tilde{C}_{\text{old}})\det A^{(l)}(\tilde{C}_{\text{old}})}, \tag{2.247}$$

$$\text{update 2}: R(\tilde{C}_{\text{old}}, \tilde{C}_{\text{new}}) = \frac{k^{(l)}_{(\sigma,\text{c})}k^{(l)}_{(\sigma,\text{a})}}{\beta^2} \frac{\mathcal{W}_b(\tilde{C}_{\text{new}})\mathcal{W}'_c(\tilde{C}_{\text{new}})\det A^{(l)}(\tilde{C}_{\text{new}})}{\mathcal{W}_b(\tilde{C}_{\text{old}})\mathcal{W}'_c(\tilde{C}_{\text{old}})\det A^{(l)}(\tilde{C}_{\text{old}})}, \tag{2.248}$$

$$\text{update 3}: R(\tilde{C}_{\text{old}}, \tilde{C}_{\text{new}}) = \frac{(\Delta\tau)^2}{\left(k'^{(l)}_{(\sigma,\text{c})}+1\right)\left(k'^{(l)}_{(\sigma,\text{a})}+1\right)} \frac{\mathcal{W}_b(\tilde{C}_{\text{new}})\mathcal{W}'_c(\tilde{C}_{\text{new}})\det A^{(l)}(\tilde{C}_{\text{new}})}{\mathcal{W}_b(\tilde{C}_{\text{old}})\mathcal{W}'_c(\tilde{C}_{\text{old}})\det A^{(l)}(\tilde{C}_{\text{old}})}, \tag{2.249}$$

$$\text{update 4}: R(\tilde{C}_{\text{old}}, \tilde{C}_{\text{new}}) = \frac{k'^{(l)}_{(\sigma,\text{c})}k'^{(l)}_{(\sigma,\text{a})}}{(\Delta\tau)^2} \frac{\mathcal{W}_b(\tilde{C}_{\text{new}})\mathcal{W}'_c(\tilde{C}_{\text{new}})\det A^{(l)}(\tilde{C}_{\text{new}})}{\mathcal{W}_b(\tilde{C}_{\text{old}})\mathcal{W}'_c(\tilde{C}_{\text{old}})\det A^{(l)}(\tilde{C}_{\text{old}})}, \tag{2.250}$$

$$\text{update 5}: R(\tilde{C}_{\text{old}}, \tilde{C}_{\text{new}}) = \frac{4N_{\text{orb}}(N_{\text{orb}}-1)\beta}{k_s+k_p+1} \frac{\mathcal{W}_b(\tilde{C}_{\text{new}})\mathcal{W}_c(\tilde{C}_{\text{new}})}{\mathcal{W}_b(\tilde{C}_{\text{old}})\mathcal{W}'_c(\tilde{C}_{\text{old}})}, \tag{2.251}$$

$$\text{update 6}: R(\tilde{C}_{\text{old}}, \tilde{C}_{\text{new}}) = \frac{k_s+k_p}{4N_{\text{orb}}(N_{\text{orb}}-1)\beta} \frac{\mathcal{W}_b(\tilde{C}_{\text{new}})\mathcal{W}'_c(\tilde{C}_{\text{new}})}{\mathcal{W}_b(\tilde{C}_{\text{old}})\mathcal{W}'_c(\tilde{C}_{\text{old}})}, \tag{2.252}$$

$$\text{update 7}: R(\tilde{C}_{\text{old}}, \tilde{C}_{\text{new}}) = \frac{\mathcal{W}_b(\tilde{C}_{\text{new}})\mathcal{W}'_c(\tilde{C}_{\text{new}})\det A^{(l)}(\tilde{C}_{\text{new}})}{\mathcal{W}_b(\tilde{C}_{\text{old}})\mathcal{W}'_c(\tilde{C}_{\text{old}})\det A^{(l)}(\tilde{C}_{\text{old}})}. \tag{2.253}$$

The method to measure the impurity-site Green's function is also slightly modified as

$$\left[\tilde{\mathbf{G}}_{\text{imp}}(\tau)\right]_{pq} = \frac{1}{\beta}\left\langle \sum_{l=1}^{N_{\text{orb}}} \sum_{i,j=1}^{k_l} \left[B^{(l)}\right]_{ji} \tilde{\delta}(\tau, \tau'^{(l)}_j - \tau^{(l)}_i)\, \delta_{q,\tilde{f}^{(l)}_i}\, \delta_{p,\tilde{f}'^{(l)}_j} \right\rangle_{\text{MC}}, \tag{2.254}$$

where $B^{(l)}$ is the inverse matrix of the $A^{(l)}$ matrix. Then, the s-wave superconducting order parameter $P_{\text{SC}} = \sum_{l=1}^{N_{\text{orb}}} \langle c_{l\downarrow} c_{l\uparrow} \rangle$ is given by $P_{\text{SC}} = \sum_{l=1}^{N_{\text{orb}}} \left[\tilde{\mathbf{G}}_{\text{imp}}(\tau = 0^+)\right]_{l,l+N_{\text{orb}}}$.

2.4 Combining Model Derivation and Model Analysis

2.4.1 Interfaces

Here, we describe interfaces to smoothly connect the downfolding part described in Sect. 2.2 and the low-energy solver described in Sect. 2.3.

2.4.1.1 Preparation of $\mathcal{H}_0(\mathbf{k})$ in Eq. (2.155)

One possible form of the double counting correction $\Delta\varepsilon_l$ in Eq. (2.30) is the Hartree contribution of the local Coulomb interaction calculated with the DFT occupations of the orbitals n_l^{DFT}'s

$$\Delta\varepsilon_l = U_{ll} n_l^{\mathrm{DFT}}/2 + \sum_m (2U_{lm} - J_{lm}) n_m^{\mathrm{DFT}}/2 \tag{2.255}$$

where we explicitly show the orbital indices in the Coulomb interaction parameters. In the case where all the orbitals are degenerate ($n_1^{\mathrm{DFT}} = n_2^{\mathrm{DFT}} = \cdots = n_{N_{\mathrm{orb}}}^{\mathrm{DFT}}$) and there is no orbital dependence in the interaction, the orbital dependence of $\Delta\varepsilon_l$ vanishes, i.e., $\Delta\varepsilon_1 = \Delta\varepsilon_1 = \cdots = \Delta\varepsilon_{N_{\mathrm{orb}}}$. This equality also holds in the case of other definition of the double counting correction (see e.g., Refs. [5–7, 95] for the definitions). Then, the double counting correction gives only a constant shift, which can be absorbed in the chemical potential.

Considering the above arguments, we ignore the double counting correction term from Eq. (2.30) and we calculate $\boldsymbol{\mathcal{H}}_0(\mathbf{k})$ by

$$\boldsymbol{\mathcal{H}}_0(\mathbf{k}) = \sum_{\mathbf{R}\neq\mathbf{0}} \boldsymbol{\mathcal{H}}_0^{(w)}(\mathbf{R}) e^{-i\mathbf{k}\cdot\mathbf{R}}, \tag{2.256}$$

where we exclude $\mathbf{R} = \mathbf{0}$ term from the sum because the degenerate onsite levels $\left[\boldsymbol{\mathcal{H}}_0^{(w)}(\mathbf{R}=\mathbf{0})\right]_{lm} = \varepsilon\delta_{lm}$ again can be absorbed in the chemical potential. Note that, because of the time-reversal symmetry and the space-inversion symmetry, $\boldsymbol{\mathcal{H}}_0(\mathbf{k})$ has no spin dependence, and the matrix elements of $\boldsymbol{\mathcal{H}}_0(\mathbf{k})$ take real numbers [$\because \boldsymbol{\mathcal{H}}_0^{(w)}(\mathbf{R}) = \boldsymbol{\mathcal{H}}_0^{(w)}(-\mathbf{R})$]. Note also that, the $\mathbf{k}$-meshes for the calculation of $\boldsymbol{\mathcal{H}}_0(\mathbf{k})$ can be taken to be much finer than those of the original DFT.

2.4.1.2 Evaluation of Effective Coulomb Interaction Parameters

The partially screened Coulomb interaction $W^{(p)}$ [Eq. (2.33)] calculated by the cRPA is regarded as an effective interaction between the low-energy electrons (t_{1u} electrons in the case of the fullerides). In this thesis, we use the static part of $W^{(p)}$ to calculate the interaction parameters in the low-energy Hamiltonian. Namely, the frequency dependence of $W^{(p)}$ is neglected.[14] However, in the present case, we consider that the usage of the static interaction is a good approximation because of weak frequency dependence of the partially screened Coulomb interaction up to a frequency larger

[14]The calculations of the frequency dependence of the partially screened interactions are highly expensive in the case of the alkali-doped fullerides, which have a large unit cell. In Appendix in Chap. 3, in order to check the validity of using the static interaction, we calculate the frequency dependence in a limited frequency region for a representative material (Cs_3C_{60} with $V_{C_{60}^{3-}} = 762$ Å^3).

than the bandwidth (see Appendix in Chap. 3). A possible (small) effect of the frequency dependence on the quantitative issues such as the calculation of T_c will be discussed in Sect. 5.2.

The onsite Coulomb repulsion U_{lm} and the exchange interaction J_{lm} are evaluated as

$$\begin{aligned} U_{lm} &= \int\int d\mathbf{r}d\mathbf{r}' \left|\phi_{l\mathbf{0}}(\mathbf{r})\right|^2 W^{(p)}(\mathbf{r},\mathbf{r}') \left|\phi_{m\mathbf{0}}(\mathbf{r}')\right|^2 \\ &= \frac{4\pi e^2}{N\Omega} \sum_{\mathbf{q}} \sum_{\mathbf{G}\mathbf{G}'} \rho_{ll}(\mathbf{q}+\mathbf{G}) W^{(p)}_{\mathbf{G},\mathbf{G}'}(\mathbf{q}) \rho^*_{mm}(\mathbf{q}+\mathbf{G}') \end{aligned} \tag{2.257}$$

and

$$\begin{aligned} J_{lm} &= \int\int d\mathbf{r}d\mathbf{r}' \phi^*_{l\mathbf{0}}(\mathbf{r})\phi_{m\mathbf{0}}(\mathbf{r}) W^{(p)}(\mathbf{r},\mathbf{r}')\phi^*_{m\mathbf{0}}(\mathbf{r}')\phi_{l\mathbf{0}}(\mathbf{r}') \\ &= \frac{4\pi e^2}{N\Omega} \sum_{\mathbf{q}} \sum_{\mathbf{G}\mathbf{G}'} \rho_{lm}(\mathbf{q}+\mathbf{G}) W^{(p)}_{\mathbf{G},\mathbf{G}'}(\mathbf{q}) \rho^*_{lm}(\mathbf{q}+\mathbf{G}'), \end{aligned} \tag{2.258}$$

respectively, where Ω is the volume of the unit cell, and $\rho_{lm}(\mathbf{q}+\mathbf{G})$ is given, with the Wannier-gauge Bloch functions $\psi^{(w)}_{l\mathbf{k}}$'s, by

$$\rho_{lm}(\mathbf{q}+\mathbf{G}) = \frac{1}{N} \sum_{\mathbf{k}} \left\langle \psi^{(w)}_{l\mathbf{k}+\mathbf{q}} \middle| e^{i(\mathbf{q}+\mathbf{G})\cdot\mathbf{r}} \middle| \psi^{(w)}_{m\mathbf{k}} \right\rangle. \tag{2.259}$$

Note that the magnitude of the pair-hopping interaction J'_{lm}, which is computed as

$$J'_{lm} = \int\int d\mathbf{r}d\mathbf{r}' \phi^*_{l\mathbf{0}}(\mathbf{r})\phi_{m\mathbf{0}}(\mathbf{r}) W^{(p)}(\mathbf{r},\mathbf{r}')\phi^*_{l\mathbf{0}}(\mathbf{r}')\phi_{m\mathbf{0}}(\mathbf{r}') \tag{2.260}$$

is equal to that of the exchange interaction, i.e., $J'_{lm} = J_{lm}$, because the Wannier functions are real $[\phi^*_{l\mathbf{R}}(\mathbf{r}) = \phi_{l\mathbf{R}}(\mathbf{r})]$.

If there is no orbital dependence in U_{lm}'s and J_{lm}'s, the onsite Coulomb interaction parameters are parametrized as

$$U = U_{ll}, \quad U' = U_{lm}, \quad J_{\mathrm{H}} = J_{lm} = J'_{lm} \qquad (l \neq m). \tag{2.261}$$

The Fourier transform of the off-site Coulomb interaction $V_{\mathbf{q}}$ in Eq. (2.156) can be computed by taking the average over orbital indices (the orbital dependence of the off-site Coulomb interaction is generally very small) as

$$V_{\mathbf{q}} = \frac{1}{N^2_{\mathrm{orb}}} \sum_{lm} \left[V_{lm}(\mathbf{q}) - U_{lm} \right] = \frac{1}{N^2_{\mathrm{orb}}} \sum_{lm} V_{lm}(\mathbf{q}) - \frac{U + (N_{\mathrm{orb}} - 1)U'}{N_{\mathrm{orb}}} \tag{2.262}$$

with

$$V_{lm}(\mathbf{q}) = \frac{4\pi e^2}{\Omega} \sum_{\mathbf{G}\mathbf{G}'} \rho_{ll}(\mathbf{q}+\mathbf{G}) W^{(p)}_{\mathbf{G},\mathbf{G}'}(\mathbf{q}) \rho^*_{mm}(\mathbf{q}+\mathbf{G}'). \tag{2.263}$$

2.4.1.3 Calculation of Phonon-Related Input Parameters

To compute $\mathcal{W}'_c$ in Eq. (2.211), we need the information of $U_{\text{eff}} = U + U_{\text{“ph”}}$, $U'_{\text{eff}} = U' + U'_{\text{“ph”}}$, $\mu_{\text{eff}} = \mu + U_{\text{“ph”}}/2 + (N_{\text{orb}} - 1)U'_{\text{“ph”}}$, and $J_{\text{eff}} = J_{\text{H}} + J_{\text{ph}}$. Since the methods to calculate the Coulomb parameters, U, U', and J_{H}, are described above, we here show how to compute the "phonon" parameters $U_{\text{“ph”}}$, $U'_{\text{“ph”}}$, and J_{ph}. Within the extended DMFT formalism, $U_{\text{“ph”}}$ and $U'_{\text{“ph”}}$ consist of the contribution from the real phonons (U_{ph} and U'_{ph}) and the one from the auxiliary bosons to decompose the non-local Coulomb interactions (U_V and U'_V), i.e., $U_{\text{“ph”}} = U_{\text{ph}} + U_V$, and $U'_{\text{“ph”}} = U'_{\text{ph}} + U'_V$. On the other hand, J_{ph} purely originates from the real phonons, because we consider only the density-type off-site Coulomb interaction and thus off-site Coulomb interactions contribute only to the density-density channels (U_{eff} and U'_{eff}).

Here, we first consider the real-phonon contributions U_{ph}, U'_{ph} and J_{ph}. The partially screened electron-phonon coupling is given by [c.f. Eq. (2.104)][15]

$$g^{(p)\nu}_{lm}(\mathbf{k},\mathbf{q}) = \sum_{\kappa\alpha} \sqrt{\frac{\hbar}{2M_\kappa \omega^{(p)}_{\mathbf{q}\nu}}}\, e^{(p)\alpha}_{\kappa}(\mathbf{q}\nu) \left\langle \psi^{(w)}_{l\mathbf{k}+\mathbf{q}} \left| \frac{\partial V^{(p)}_{\text{SCF}}(\mathbf{r})}{\partial u^{\alpha}_{\kappa}(\mathbf{q})} \right| \psi^{(w)}_{m\mathbf{k}} \right\rangle, \tag{2.264}$$

where we employ the Wannier-gauge for the electrons, and the superscript (p) indicates the partially renormalized quantities. Then, U_{ph}, U'_{ph} and J_{ph} are given by

$$U_{\text{ph}} = -\frac{1}{N_{\mathbf{q}}} \sum_{\mathbf{q}\nu} \frac{2\left|\tilde{g}^{(p)}_{ll}(\mathbf{q},\nu)\right|^2}{\omega^{(p)}_{\mathbf{q}\nu}}, \tag{2.265}$$

$$U'_{\text{ph}} = -\frac{1}{N_{\mathbf{q}}} \sum_{\mathbf{q}\nu} \frac{2\tilde{g}^{(p)}_{ll}(\mathbf{q},\nu)\tilde{g}^{(p)*}_{mm}(\mathbf{q},\nu)}{\omega^{(p)}_{\mathbf{q}\nu}}, \tag{2.266}$$

$$J_{\text{ph}} = -\frac{1}{N_{\mathbf{q}}} \sum_{\mathbf{q}\nu} \frac{2\tilde{g}^{(p)}_{lm}(\mathbf{q},\nu)\tilde{g}^{(p)*}_{lm}(\mathbf{q},\nu)}{\omega^{(p)}_{\mathbf{q}\nu}} = -\frac{1}{N_{\mathbf{q}}} \sum_{\mathbf{q}\nu} \frac{2\tilde{g}^{(p)}_{lm}(\mathbf{q},\nu)\tilde{g}^{(p)*}_{ml}(\mathbf{q},\nu)}{\omega^{(p)}_{\mathbf{q}\nu}}, \tag{2.267}$$

[15] In this thesis, we do not consider the frequency dependence of the partially screened electron-phonon coupling $g^{(p)}$ for the same reason as the partially screened Coulomb interactions $W^{(p)}$. Since the expressions for $g^{(p)}$ Eq. (2.119) and $W^{(p)}$ Eq. (2.114) are similar, we also expect that $g^{(p)}$ has little structure in a frequency region up to a frequency larger than the bandwidth. Then the static approximation is a reasonable assumption in the fulleride problem.

respectively, where we assume that the orbital dependences of $U_{\rm ph}$, $U'_{\rm ph}$ and $J_{\rm ph}$ do not exist, and $\tilde{g}^{(p)}_{lm}(\mathbf{q}, \nu)$ is calculated as

$$\tilde{g}^{(p)}_{lm}(\mathbf{q}, \nu) = \frac{1}{N_{\mathbf{k}}} \sum_{\mathbf{k}} g^{(p)\nu}_{lm}(\mathbf{k}, \mathbf{q}). \tag{2.268}$$

The non-local Coulomb interaction contributions, U_V and U'_V, are identified with the static part of the bosonic Weiss function $\mathcal{D}_0(i\nu_n = 0)$ in Eq. (2.158), i.e., $U_V = U'_V = \mathcal{D}_0(i\nu_n = 0)$. Since we neglect the orbital dependence of the off-site Coulomb interaction, the amounts of the dynamical screening are the same for the intraorbital channel and the interorbital channel ($U_V = U'_V$). Therefore, $U_{\rm eff}$, $U'_{\rm eff}$, and $\mu_{\rm eff}$ are given by

$$U_{\rm eff} = U + U_{\rm ph} + \mathcal{D}_0(i\nu_n = 0), \tag{2.269}$$

$$U'_{\rm eff} = U' + U'_{\rm ph} + \mathcal{D}_0(i\nu_n = 0), \tag{2.270}$$

$$\mu_{\rm eff} = \mu + \big[U_{\rm ph} + \mathcal{D}_0(i\nu_n = 0)\big]/2 + (N_{\rm orb} - 1)\big[U'_{\rm ph} + \mathcal{D}_0(i\nu_n = 0)\big], \tag{2.271}$$

respectively.

Another important quantity related with the "phonons" is the $K_{ll'}(\tau)$ function defined in the interval $[0, \beta]$ [Eq. (2.203)], which is used to calculate $\mathcal{W}_b$ in Eq. (2.202). As for the contributions from the real phonons $K^{\rm ph}_{ll'}(\tau)$, we follow the recipe of Eqs. (2.203) and (2.204):

$$\begin{cases} K^{\rm ph}_{ll'}(\tau) = K'^{\rm ph}_{ll'}(\tau) - K'^{\rm ph}_{ll}(\tau) & (2.272) \\ K'^{\rm ph}_{ll'}(\tau) = -\dfrac{1}{N_{\mathbf{q}}} \displaystyle\sum_{\mathbf{q}\nu} \frac{\tilde{g}^{(p)}_{ll}(\mathbf{q}, \nu)\, \tilde{g}^{(p)*}_{l'l'}(\mathbf{q}, \nu)}{\big(\omega^{(p)}_{\mathbf{q}\nu}\big)^2} \frac{\cosh\big[(\tau - \beta/2)\omega^{(p)}_{\mathbf{q}\nu}\big]}{\sinh\big[\beta\omega^{(p)}_{\mathbf{q}\nu}/2\big]} & (2.273) \end{cases}$$

Note that, although we explicitly show the orbital indices here, in the case of the alkali-doped fullerides, $K^{\rm ph}_{ll'}(\tau)$'s take only two types of values: the intraorbital and interorbital values. On the other hand, as for the non-local Coulomb interaction contributions $K^V(\tau)$ (we omit the orbital indices because there is no orbital dependence), while we treat the propagator on the imaginary axis $\mathcal{D}_0(i\nu_n)$, we do not explicitly know the frequencies of the fictitious "phonons". In this case, $K^V(\tau)$ can be calculated by [69]

$$K^V(\tau) = \frac{1}{\beta} \sum_{n \neq 0} \frac{\mathcal{D}_0(i\nu_n) - \mathcal{D}_0(0)}{(i\nu_n)^2} \big(e^{i\nu_n \tau} - 1\big) \tag{2.274}$$

$$= -\frac{2}{\beta} \sum_{n > 0} \frac{\mathcal{D}_0(i\nu_n) - \mathcal{D}_0(0)}{\nu_n^2} \big[\cos(\nu_n \tau) - 1\big], \tag{2.275}$$

where, we have employed the equality $\mathcal{D}_0(i\nu_n) = \mathcal{D}_0(-i\nu_n) = \mathcal{D}_0(i\nu_{-n})$ in the last equality. With $K^{\mathrm{ph}}_{ll'}(\tau)$ and $K^V(\tau)$, $K_{ll'}(\tau)$ is given by the simple sum of them as

$$K_{ll'}(\tau) = K^{\mathrm{ph}}_{ll'}(\tau) + K^V(\tau). \tag{2.276}$$

2.4.2 *Overview of Whole Scheme*

Here, we briefly overview the whole calculation procedure. See Fig. 2.4 for more details.

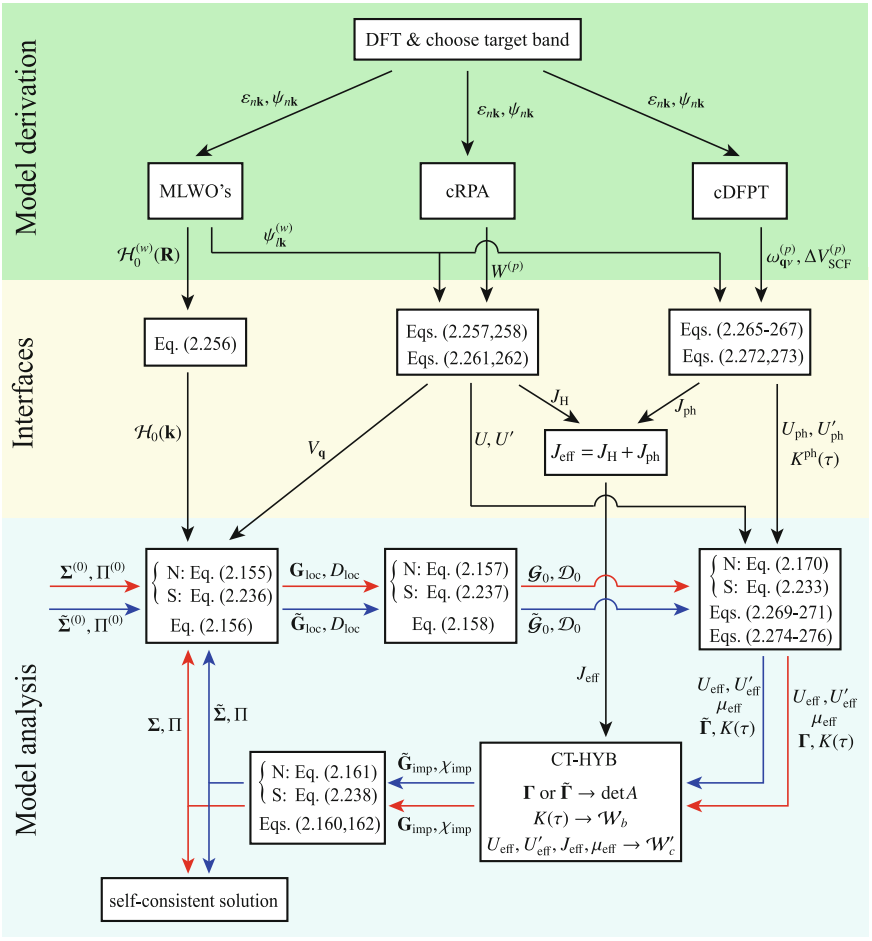

Fig. 2.4 Schematic picture of whole scheme. In the model analysis part, *arrows* in *red* (*blue*) indicate the flow of the normal (superconducting) state simulation. Correspondingly, "N" and "S" in the figure are the abbreviations for the normal and superconducting states, respectively

1. Calculate a global band structure using the DFT and choose the target band.
2. Construct MLWO's within the t-subspace.
3. Perform the cRPA and cDFPT calculations.
4. Perform the interface calculations.
5. Analyze the derived model by the extended DMFT.

Appendix: Supplemental Information for DFPT

A. Expression for Interatomic Force Constants with Non-local Pseudopotential

In Sect. 2.2.4, the expression of the interatomic force constants is based on the locality of the ionic potential. However, in the actual DFPT calculations with the plane-wave basis, the true ionic potential, which is local, is replaced by the pseudopotential. When the pseudopotential has non-local components, i.e., depends on two coordinates $\mathbf{r}$ and $\mathbf{r}'$,[16] we need some modifications in the equations. The generalized expression for the second derivative of the energy with respect to parameters $\{\lambda_i\}$ reads

$$\frac{\partial^2 E_\lambda}{\partial\lambda_i\partial\lambda_j} = \sum_{\mathbf{k}}\sum_{n}^{\text{occ.}}\left[\left\langle\frac{\psi_{n\mathbf{k}}}{\partial\lambda_i}\middle|\frac{\partial V_\lambda}{\partial\lambda_j}\middle|\psi_{n\mathbf{k}}\right\rangle + \left\langle\psi_{n\mathbf{k}}\middle|\frac{\partial V_\lambda}{\partial\lambda_j}\middle|\frac{\psi_{n\mathbf{k}}}{\partial\lambda_i}\right\rangle + \left\langle\psi_{n\mathbf{k}}\middle|\frac{\partial^2 V_\lambda}{\partial\lambda_i\partial\lambda_j}\middle|\psi_{n\mathbf{k}}\right\rangle\right] \tag{2.277}$$

with $\psi_{n\mathbf{k}}$ being the one-particle wave function with the band n and the wave vector $\mathbf{k}$. Then, the electronic contribution to the interatomic force constant ${}^{el}C^{\alpha\alpha'}_{\kappa\kappa'}(\mathbf{q})$, i.e., the contribution other than the ionic contribution $\partial E_{\mathrm{N}}(\{\mathbf{R}\})/\partial\mathbf{u}^{*\alpha}_{\kappa}(\mathbf{q})\partial\mathbf{u}^{\alpha'}_{\kappa'}(\mathbf{q})$, is given by

$$\begin{aligned}
{}^{el}C^{\alpha\alpha'}_{\kappa\kappa'}(\mathbf{q}) &= \left[\sum_{\mathbf{k}}\sum_{n}^{\text{occ.}}\left(\frac{4}{N}\left\langle\frac{\psi_{n\mathbf{k}}}{\partial u^{\alpha}_{\kappa}(\mathbf{q})}\middle|\frac{\partial V_{\text{ion}}}{\partial u^{\alpha'}_{\kappa'}(\mathbf{q})}\middle|\psi_{n\mathbf{k}}\right\rangle + \frac{2}{N}\left\langle\psi_{n\mathbf{k}}\middle|\frac{\partial^2 V_{\text{ion}}}{\partial u^{*\alpha}_{\kappa}(\mathbf{q})\partial u^{\alpha'}_{\kappa'}(\mathbf{q})}\middle|\psi_{n\mathbf{k}}\right\rangle\right)\right]_{u=0} \\
&= \left[\sum_{\mathbf{k}}\sum_{n}^{\text{occ.}}\left(\frac{4}{N}\left\langle\frac{\psi_{n\mathbf{k}}}{\partial u^{\alpha}_{\kappa}(\mathbf{q})}\middle|\frac{\partial V_{\text{ion}}}{\partial u^{\alpha'}_{\kappa'}(\mathbf{q})}\middle|\psi_{n\mathbf{k}}\right\rangle\right.\right. \\
&\quad \left.\left. + \delta_{\kappa\kappa'}\frac{2}{N}\left\langle\psi_{n\mathbf{k}}\middle|\frac{\partial^2 V_{\text{ion}}}{\partial u^{\alpha}_{\kappa}(\mathbf{q}=0)\partial u^{\alpha'}_{\kappa'}(\mathbf{q}=0)}\middle|\psi_{n\mathbf{k}}\right\rangle\right)\right]_{u=0}
\end{aligned} \tag{2.278}$$

[16] The pseudopotential is composed of the local part $V_{\text{loc}}(\mathbf{r})$ and the non-local part $V_{\text{NL}}(\mathbf{r},\mathbf{r}')$.

B. Confirmation of the Equality $\Sigma = \Sigma_t + \Sigma_r$ in Sect. 2.2.5.2

Here, we show that the equality $\Sigma = \Sigma_t + \Sigma_r$ in Sect. 2.2.5.2 indeed holds. In principle, the self-energy Σ, the electron-phonon coupling g, the polarization function χ^0, and so on, are expressed as matrices. In this section, for the sake of simplicity, we treat them as if they were scalar quantities. One can easily extend the proof to the case where they are matrices. $\Sigma_t = |g^{(p)}|^2 \chi^t_{\mathrm{LDA}}$ is rewritten as

$$\begin{aligned}
\Sigma_t &= |g^{(p)}|^2 \frac{\chi_t^0}{1 - \tilde{W}^{(p)} \chi_t^0} \\
&= |g^{(b)}|^2 \frac{1}{1 - \tilde{v}\chi_r^0} \frac{\chi_t^0}{1 - \tilde{W}^{(p)} \chi_t^0} \frac{1}{1 - \tilde{v}\chi_r^0} \\
&= |g^{(b)}|^2 \left(1 + \frac{\tilde{v}\chi_r^0}{1 - \tilde{v}\chi_r^0}\right) \frac{\chi_t^0}{1 - \tilde{W}^{(p)} \chi_t^0} \left(1 + \frac{\tilde{v}\chi_r^0}{1 - \tilde{v}\chi_r^0}\right) \\
&= |g^{(b)}|^2 \left(1 + \chi_r^0 \tilde{W}^{(p)}\right) \frac{\chi_t^0}{1 - \tilde{W}^{(p)} \chi_t^0} \left(1 + \tilde{W}^{(p)} \chi_r^0\right) \\
&= |g^{(b)}|^2 \Bigg[\frac{\chi_t^0}{1 - \tilde{W}^{(p)} \chi_t^0} + \chi_r^0 \frac{\tilde{W}^{(p)}}{1 - \tilde{W}^{(p)} \chi_t^0} \chi_t^0 \\
&\quad + \chi_t^0 \frac{\tilde{W}^{(p)}}{1 - \tilde{W}^{(p)} \chi_t^0} \chi_r^0 + \chi_r^0 \tilde{W}^{(p)} \frac{\chi_t^0}{1 - \tilde{W}^{(p)} \chi_t^0} \tilde{W}^{(p)} \chi_r^0 \Bigg] \\
&= |g^{(b)}|^2 \Bigg[\chi_t^0 + \chi_t^0 \tilde{W}^{(f)} \chi_t^0 + \chi_r^0 \tilde{W}^{(f)} \chi_t^0 + \chi_t^0 \tilde{W}^{(f)} \chi_r^0 + \chi_r^0 \tilde{W}^{(p)} \frac{\chi_t^0}{1 - \tilde{W}^{(p)} \chi_t^0} \tilde{W}^{(p)} \chi_r^0 \Bigg].
\end{aligned} \tag{2.279}$$

Similarly, $\Sigma_r = |g^{(b)}|^2 \chi^r_{\mathrm{LDA}}$ is rewritten as

$$\Sigma_r = |g^{(b)}|^2 \frac{\chi_r^0}{1 - \tilde{v}\chi_r^0} = |g^{(b)}|^2 \Big[\chi_r^0 + \chi_r^0 \tilde{W}^{(p)} \chi_r^0 \Big]. \tag{2.280}$$

Using the equality

$$\tilde{W}^{(p)} + \tilde{W}^{(p)} \frac{\chi_t^0}{1 - \tilde{W}^{(p)} \chi_t^0} \tilde{W}^{(p)} = \frac{\tilde{W}^{(p)}}{1 - \tilde{W}^{(p)} \chi_t^0} = \tilde{W}^{(f)}, \tag{2.281}$$

one can show that $\Sigma_t + \Sigma_r$ is expressed as

$$\begin{aligned}\Sigma_t + \Sigma_r &= |g^{(b)}|^2 \Big[\chi_t^0 + \chi_r^0 + \big(\chi_t^0 + \chi_r^0\big) \tilde{W}^{(f)} \big(\chi_t^0 + \chi_r^0\big) \Big] \\ &= |g^{(b)}|^2 \Big[\chi^0 + \chi^0 \tilde{W}^{(f)} \chi^0 \Big] \\ &= |g^{(b)}|^2 \chi_{\mathrm{LDA}}, \end{aligned} \tag{2.282}$$

which agrees with the expression for Σ in Eq. (2.122).

References

1. M. Born, J.R. Oppenheimer, Ann. Phys. (Leipzig) **84**, 457 (1927)
2. P. Hohenberg, W. Kohn, Phys. Rev. **136**, B864 (1964)
3. W. Kohn, L.J. Sham, Phys. Rev. **140**, A1133 (1965)
4. N.F. Mott, Proc. Phys. Soc. Lond. Sect. A **62**, 416 (1949)
5. G. Kotliar, S.Y. Savrasov, K. Haule, V.S. Oudovenko, O. Parcollet, C.A. Marianetti, Rev. Mod. Phys. **78**, 865 (2006)
6. K. Held, Adv. Phys. **56**(6), 829 (2007)
7. M. Imada, T. Miyake, J. Phys. Soc. Jpn. **79**(11), 112001 (2010)
8. J.W. Negele, H. Orland, *Quantum Many-Particle Systems* (Westview Press, Boulder, 1988)
9. K.G. Wilson, Rev. Mod. Phys. **55**, 583 (1983)
10. P. Werner, M. Casula, T. Miyake, F. Aryasetiawan, A.J. Millis, S. Biermann, Nat. Phys. **8**, 331 (2012)
11. N. Marzari, D. Vanderbilt, Phys. Rev. B **56**, 12847 (1997)
12. I. Souza, N. Marzari, D. Vanderbilt, Phys. Rev. B **65**, 035109 (2001)
13. N. Marzari, A.A. Mostofi, J.R. Yates, I. Souza, D. Vanderbilt, Rev. Mod. Phys. **84**, 1419 (2012)
14. M. Hirayama, T. Miyake, M. Imada, Phys. Rev. B **87**, 195144 (2013)
15. F. Aryasetiawan, M. Imada, A. Georges, G. Kotliar, S. Biermann, A.I. Lichtenstein, Phys. Rev. B **70**, 195104 (2004)
16. Y. Nomura, K. Nakamura, R. Arita, Phys. Rev. Lett. **112**, 027002 (2014)
17. R.G. Parr, W. Yang, *Density-Functional Theory of Atoms and Molecules* (Oxford University Press USA, New York, 1994)
18. W. Kohn, *Highlights of Condensed Matter Theory* (North-Holland, Amsterdam, 1985)
19. M. Levy, Proc. Nat. Acad. Sci. **76**(12), 6062 (1979)
20. M. Levy, Phys. Rev. A **26**, 1200 (1982)
21. D.M. Ceperley, B.J. Alder, Phys. Rev. Lett. **45**, 566 (1980)
22. J.P. Perdew, A. Zunger, Phys. Rev. B **23**, 5048 (1981)
23. J.P. Perdew, K. Burke, M. Ernzerhof, Phys. Rev. Lett. **77**, 3865 (1996)
24. J.P. Perdew, K. Burke, M. Ernzerhof, Phys. Rev. Lett. **78**, 1396 (1997)
25. M.S. Hybertsen, S.G. Louie, Phys. Rev. B **35**, 5585 (1987)
26. P. Giannozzi, S. de Gironcoli, P. Pavone, S. Baroni, Phys. Rev. B **43**, 7231 (1991)
27. S. de Gironcoli, Phys. Rev. B **51**, 6773 (1995)
28. F. Favot, A. Dal, Corso. Phys. Rev. B **60**, 11427 (1999)
29. S. Baroni, S. de Gironcoli, A. Dal, Corso, P. Giannozzi, Rev. Mod. Phys. **73**, 515 (2001)
30. J.M. Ziman, *Principles of the Theory of Solids* (Cambridge University Press, Cambridge, 1972)
31. H. Hellmann, *Einführung in die Quantenchemie* (Franz Deuticke, Leipzig, 1937)
32. R.P. Feynman, Phys. Rev. **56**, 340 (1939)

33. P.P. Ewald, Ann. der Phys. **369**(3), 253 (1921)
34. A. Georges, G. Kotliar, W. Krauth, M.J. Rozenberg, Rev. Mod. Phys. **68**, 13 (1996)
35. A.M. Sengupta, A. Georges, Phys. Rev. B **52**, 10295 (1995)
36. Q. Si, J.L. Smith, Phys. Rev. Lett. **77**, 3391 (1996)
37. T. Maier, M. Jarrell, T. Pruschke, M.H. Hettler, Rev. Mod. Phys. **77**, 1027 (2005)
38. R. Blankenbecler, D.J. Scalapino, R.L. Sugar, Phys. Rev. D **24**, 2278 (1981)
39. M. Imada, Y. Hatsugai, J. Phys. Soc. Jpn. **58**(10), 3752 (1989)
40. W.L. McMillan, Phys. Rev. **138**, A442 (1965)
41. D. Ceperley, G.V. Chester, M.H. Kalos, Phys. Rev. B **16**, 3081 (1977)
42. H. Yokoyama, H. Shiba, J. Phys. Soc. Jpn. **56**(10), 3582 (1987)
43. H. Yokoyama, H. Shiba, J. Phys. Soc. Jpn. **56**(4), 1490 (1987)
44. D. Tahara, M. Imada, J. Phys. Soc. Jpn. **77**(11), 114701 (2008)
45. N.E. Bickers, D.J. Scalapino, S.R. White, Phys. Rev. Lett. **62**, 961 (1989)
46. N.E. Bickers, S.R. White, Phys. Rev. B **43**, 8044 (1991)
47. S.R. White, Phys. Rev. Lett. **69**, 2863 (1992)
48. S.R. White, Phys. Rev. B **48**, 10345 (1993)
49. W. Metzner, M. Salmhofer, C. Honerkamp, V. Meden, K. Schönhammer, Rev. Mod. Phys. **84**, 299 (2012)
50. M. Imada, T. Kashima, J. Phys. Soc. Jpn. **69**(9), 2723 (2000)
51. S. Sugiura, A. Shimizu, Phys. Rev. Lett. **108**, 240401 (2012)
52. S. Sugiura, A. Shimizu, Phys. Rev. Lett. **111**, 010401 (2013)
53. Y. Kuramoto, T. Watanabe, Phys. B+C **148**(1–3), 80 (1987)
54. W. Metzner, D. Vollhardt, Phys. Rev. Lett. **62**, 324 (1989)
55. E. Müller-Hartmann, Z. Phys. B **74**, 507 (1989)
56. A. Georges, G. Kotliar, Phys. Rev. B **45**, 6479 (1992)
57. F.J. Ohkawa, J. Phys. Soc. Jpn. **60**(10), 3218 (1991)
58. F.J. Ohkawa, Prog. Theoret. Phys. Suppl. **106**, 95 (1991)
59. M. Jarrell, Phys. Rev. Lett. **69**, 168 (1992)
60. R. Bulla, Phys. Rev. Lett. **83**, 136 (1999)
61. G. Moeller, Q. Si, G. Kotliar, M. Rozenberg, D. Fisher, Phys. Rev. Lett. **74**, 2082 (1995)
62. R. Bulla, T.A. Costi, D. Vollhardt, Phys. Rev. B **64**, 045103 (2001)
63. N.H. Tong, S.Q. Shen, F.C. Pu, Phys. Rev. B **64**, 235109 (2001)
64. M. Imada, A. Fujimori, Y. Tokura, Rev. Mod. Phys. **70**, 1039 (1998)
65. J. Hubbard, Proc. R. Soc. Lond. Ser. A. Math. Phys. Sci. **281**(1386), 401 (1964)
66. W.F. Brinkman, T.M. Rice, Phys. Rev. B **2**, 4302 (1970)
67. P. Sun, G. Kotliar, Phys. Rev. B **66**, 085120 (2002)
68. P. Sun, G. Kotliar, Phys. Rev. Lett. **92**, 196402 (2004)
69. T. Ayral, S. Biermann, P. Werner, Phys. Rev. B **87**, 125149 (2013)
70. L. Huang, T. Ayral, S. Biermann, P. Werner, Phys. Rev. B **90**, 195114 (2014)
71. R.L. Stratonovich, Sov. Phys. Dokl. **2**, 416 (1957)
72. J. Hubbard, Phys. Rev. Lett. **3**, 77 (1959)
73. E. Gull, A.J. Millis, A.I. Lichtenstein, A.N. Rubtsov, M. Troyer, P. Werner, Rev. Mod. Phys. **83**, 349 (2011)
74. J.E. Hirsch, R.M. Fye, Phys. Rev. Lett. **56**, 2521 (1986)
75. A. Rubtsov, A. Lichtenstein, J. Exp. Theoret. Phys. Lett. **80**(1), 61 (2004)
76. A.N. Rubtsov, V.V. Savkin, A.I. Lichtenstein, Phys. Rev. B **72**, 035122 (2005)
77. E. Gull, P. Werner, O. Parcollet, M. Troyer, EPL (Europhys. Lett.) **82**(5), 57003 (2008)
78. P. Werner, A. Comanac, L. de' Medici, M. Troyer, A.J. Millis, Phys. Rev. Lett. **97**, 076405 (2006)
79. P. Werner, A.J. Millis, Phys. Rev. Lett. **99**, 146404 (2007)
80. P. Werner, A.J. Millis, Phys. Rev. Lett. **104**, 146401 (2010)
81. I.G. Lang, Y.A. Firsov, Sov. Phys. JETP **16**, 1301 (1963)
82. K. Steiner, Y. Nomura, P. Werner, Phys. Rev. B **92**, 115123 (2015)

83. N. Metropolis, A.W. Rosenbluth, M.N. Rosenbluth, A.H. Teller, E. Teller, J. Chem. Phys. **21**(6), 1087 (1953)
84. W.K. Hastings, Biometrika **57**, 97 (1970)
85. P. Werner, A.J. Millis, Phys. Rev. B **74**, 155107 (2006)
86. K. Haule, Phys. Rev. B **75**, 155113 (2007)
87. N. Parragh, A. Toschi, K. Held, G. Sangiovanni, Phys. Rev. B **86**, 155158 (2012)
88. H. Shinaoka, M. Dolfi, M. Troyer, P. Werner, J. Stat. Mech. Theory Exp. **2014**(6), P06012 (2014)
89. M. Matsumoto, T. Nishimura, A.C.M. Trans, Model. Comput. Simul. **8**(1), 3 (1998)
90. J. Sherman, W.J. Morrison, Ann. Math. Stat. **20**(4), 620 (1949)
91. J. Sherman, W.J. Morrison, Ann. Math. Stat. **21**(1), 124 (1950)
92. A. Georges, G. Kotliar, W. Krauth, Zeitschrift für Phys. B Condens. Matter **92**(3), 313 (1993)
93. A. Koga, P. Werner, Phys. Rev. A **84**, 023638 (2011)
94. Y. Murakami, P. Werner, N. Tsuji, H. Aoki, Phys. Rev. B **88**, 125126 (2013)
95. V.I. Anisimov, F. Aryasetiawan, A.I. Lichtenstein, J. Phys.: Condens. Matter **9**(4), 767 (1997)

http://www.springer.com/978-981-10-1441-3

Ab Initio Studies on Superconductivity in Alkali-Doped Fullerides

Nomura, Y.

2016, XX, 143 p. 27 illus., 18 illus. in color., Hardcover
ISBN: 978-981-10-1441-3